REPORT DOCUMENTATION PAGE

Form Approved
OMB No. 0704-0188

1. REPORT DATE *(DD-MM-YYYY)*	2. REPORT DATE	3. DATES COVERED *(From - To)*
11/15/2001	November 2001	1996 - 2001

4. TITLE AND SUBTITLE
Effects of Pollutants and Micro-Organisms on the Absorption of Electrolytic Hydrogen in Iron

5a. CONTRACT NUMBER
N00014-96-1-0913

5b. GRANT NUMBER

5c. PROGRAM ELEMENT NUMBER

6. AUTHOR(S)
H. W. Pickering

5d. PROJECT NUMBER

5e. TASK NUMBER

5f. WORK UNIT NUMBER

7. PERFORMING ORGANIZATION NAME(S) AND ADDRESS(ES)
The Pennsylvania State University
Materials Science & Engineering Dept.
326 Steidle Bldg.
University Park, PA 16802

8. PERFORMING ORGANIZATION REPORT NUMBER

9. SPONSORING/MONITORING AGENCY NAME(S) AND ADDRESS(ES)
Office of Naval Research
John A. Sedriks, Program Officer ONR 332
800 N. Quincy St., Ballston Centre Tower One
Arlington, VA 22217

10. SPONSOR/MONITOR'S ACRONYM(S)

11. SPONSORING/MONITORING AGENCY REPORT NUMBER

12. DISTRIBUTION AVAILABILITY STATEMENT
Approved for public release; distribution is unlimited.

13. SUPPLEMENTARY NOTES

14. ABSTRACT
See attached

15. SUBJECT TERMS

16. SECURITY CLASSIFICATION OF:			17. LIMITATION OF ABSTRACT	18. NUMBER OF PAGES	19a. NAME OF RESPONSIBLE PERSON
a. REPORT	b. ABSTRACT	c. THIS PAGE			Dr. Howard W. Pickering
					19b. TELEPONE NUMBER *(Include area code)* 814-863-2640

FINAL REPORT

TO

OFFICE OF NAVAL RESEARCH

Contract USN 00014-96-1-0913

November 2001

EFFECTS OF POLLUTANTS AND MICRO-ORGANISMS ON THE ABSORPTION OF ELECTROLYTIC HYDROGEN IN IRON

H. W. Pickering

Department of Materials Science and Engineering
The Pennsylvania State University
University Park, PA 16802

PENNSTATE

Abstract:

The objective of this research was to define the conditions under which pollutants, in particular, those produced by bacteria such as sulfide end products of the SRB, affect the amount of hydrogen absorption by iron/steel. The research focused on thiosulfate and H_2S as promoters of hydrogen absorption, as well as some potential inhibitor species, and included both modeling and hydrogen permeation experiments. For improved understanding of how these species affect the absorption of hydrogen into steel, the Iyer-Pickering-Zamenzadeh (IPZ) analysis method was first generalized to include Frumkin adsorption of the hydrogen on the steel's surface and then used to analyze the measured steady state hydrogen permeation data. The results are described in the six publications to date and one review paper that is in preparation.

Overview

The absorption of electrolytic hydrogen into the steels used in the marine industry leads to their degradation due to hydrogen embrittlement. It is such a serious problem that the hydrogen embrittlement of steels has been a major focus of researchers for several decades. It is generally accepted that once hydrogen is absorbed, the steel will be susceptable to one form or another of hydrogen degradation. The best known examples are those encountered in environments where hydrogen sulfide is present such as in the presence of micro-organisms, e.g., sulfate reducing bacteria (SRB) which produce hydrogen sulfide in the cycle of their metabolism.

Hydrogen absorption into metals occurs as a side reaction of the hydrogen evolution reaction (HER) on metals. The HER occurs as a viable cathodic reaction during corrosion, cathodic protection, pickling and electroplating of metals. It is because of the multi-step nature of the HER that hydrogen absorption occurs.

The detailed results of this investigation are described in the following published research papers and one review paper that is in preparation.

"Effect of Thiosulfate and Sulfite on the Permeation Rate of Hydrogen Through Iron", *Corrosion*, **57**, 428 (2001): M.H. Abd Elhamid, B.G. Ateya, K.G. Weil, and H.W. Pickering

"An Analysis Procedure for Hydrogen Absorption under Frumkin Adsorption Conditions", *J. Electrochemical Soc.*, **148**, E248 (2001): F.M. Al-Faqeer and H.W. Pickering

"Determination of the Rate Constants of Hydrogen Absorption into Metals", *J. Electrochemical Soc.*, **147**, 2959 (2000): M.H. Abd Elhamid, B.G. Ateya and H.W. Pickering

"Calculation of the Hydrogen Surface Coverage and Rate Constants of the Hydrogen Evolution Reaction from Polarization Data", *J. Electrochemical Soc.*, **147**, 2148 (2000): M.H. Abd Elhamid, B.G. Ateya, K.G. Weil and H.W. Pickering

"Effect of Benzotriazole on the Hydrogen Absorption by Iron", *J. Electrochemical Soc.* **144**, L58 (1997): M.H. Abd Elhamid, B.G. Ateya and H.W. Pickering

"The Effect of Iodide Ions on the Kinetics of Hydrogen Absorption by Iron", *J. Electrochemical Soc.*, **147**, 2258 (2000): M.H. Abd Elhamid, B.G. Ateya and H.W. Pickering

"Kinetics of Electrochemical Hydrogen Degradation in Metals" in preparation: F.M. Al-Faqeer and H.W. Pickering

KINETICS OF ELECTROCHEMICAL HYDROGEN DEGRADATION IN METALS

F. M. Al-Faqeer and H. W. Pickering
Department of Materials Science and Engineering
The Pennsylvania State University
University Park, PA 16802

Abstract

This paper will review the recent developments regarding the kinetics of hydrogen entry into metals. Mechanistic analyses have been developed which evaluate the kinetics of the hydrogen evolution and absorption reactions on metals. These analyses can determine the individual rate constants of the hydrogen evolution reaction, k_1 and k_2, (from the steady state permeation data or the polarization curve) and the kinetic-diffusion rate constant, k, the hydrogen surface coverage, θ_H, and the hydrogen concentration in the charging side of the membrane, C^o, (from permeation data). The original IPZ analysis has been used extensively in the literature. An example is given in this review illustrating the application of the newer generalized IPZ analysis for characterizing the effect of hydrogen sulfide on the hydrogen evolution and absorption reactions.

Introduction

The hydrogen absorption and evolution reactions on metals have been studied extensively in the literature after the development of the hydrogen electrochemical permeation cell[1-10]. Progress in combining the hydrogen absorption reaction with the hydrogen evolution reaction was made in different studies[2,8,10-13,14]. Different analyses have been used in attempts to evaluate the kinetics of the electrochemically charged hydrogen permeation through metals. This paper will focus on the IPZ analyses, the first of which was developed by Iyer et. al., in 1989 to evaluate the hydrogen permeation data and to describe the kinetics of the hydrogen evolution and absorption reactions[11].

The Original IPZ Analysis

The original IPZ analysis developed a set of equations which relate the charging, recombination and steady state hydrogen permeation current densities and the charging electrode potential. The analysis has been used widely to analyze the hydrogen permeation data on iron in the presence of different solution additives, inhibitors and promoters[11-13,15]. The analysis has also been used to analyze the permeation data for different metals[11,16,17].

The hydrogen evolution reaction (HER) is not a single step reaction. The reaction proceeds in two main steps, one of which is the discharge of protons on the metal surface to form adsorbed hydrogen atoms. The discharge step is represented by reaction (1).

$$H^+ + e^- + M \rightarrow M\text{-}H_{ads} \qquad (1)$$

In a corrosive environment, the majority of the adsorbed atomic hydrogen ($M\text{-}H_{ads}$) combines to form molecular hydrogen which bubbles off the surface. This can occur by either of two reactions, but the IPZ analysis only applies when it occurs by chemical recombination as shown in reaction (2).

$$M\text{-}H_{ads} + M\text{-}H_{ads} \rightarrow 2M + H_2 \qquad (2)$$

A side reaction of the HER is the hydrogen absorption reaction (HAR) which takes place according to reaction (3).

$$M\text{-}H_{ads} = M + H_{abs} \qquad (3)$$

where H_{abs} refers to a hydrogen atom absorbed in the metal.

The IPZ analysis assumes that the HER proceeds according to a coupled discharge-recombination (Volmer-Tafel) mechanism. In the original IPZ analysis Langmuir conditions were assumed for the hydrogen surface coverage. Thus, the analysis ignores the adsorption of

other species on the surface. The analysis also assumes that the charging current is the sum of the recombination and steady state permeation current densities ($i_c = i_r + i_\infty$)[11].

The original IPZ analysis expresses the current density of the first step of the HER (reaction 1) using the Langmuir adsorption isotherm as follows[11]

$$i_c = Fk_1 C_{H+} (1-\theta_H) \exp(-a\alpha\eta) \qquad (4)$$

where i_c is the cathodic current density, C_{H+} is the hydrogen ion concentration, a = F/RT, α is the transfer coefficient and η is the hydrogen overpotential.

Equation (4) was rearranged in the analysis to

$$i_c \exp(a\alpha\eta) = i_o' (1-\theta_H) \qquad (5)$$

$$i_o' = Fk_1 C_{H+} = i_o/(1-\theta_H^e) \qquad (6)$$

where $i_c\exp(a\alpha\eta)$ is referred to as the charging function, i_o is the exchange current density of the hydrogen evolution reaction and θ_H^e is the equilibrium hydrogen surface coverage.

The rate of the recombination step of the hydrogen evolution reaction (reaction 2) was given by the analysis as[11,13]

$$i_r = Fk_2\theta^2_H \qquad (7)$$

The flux of the hydrogen atoms passing through the membrane using Fick's first law is shown in equation (8).[2]

$$J = -D\frac{dC}{dx} \qquad (8)$$

Using equations (9) and (10) as the boundary conditions,

$$C(x=0) = C_H^o \qquad (9)$$

$$C(x=L) = C_H^L = 0 \qquad (10)$$

the steady state hydrogen permeation flux is[1-4]

$$J = D\frac{C_H^o}{L} \qquad (11)$$

where D is the hydrogen diffusion coefficient within the metal and L is the thickness of the membrane.

From the flux in equation (11), the steady state hydrogen permeation current density is given by[1,2]

$$i_\infty = FD\frac{C_H^o}{L} \qquad (12)$$

Equation (12) can be used to estimate the absorbed hydrogen concentration at the charging side of the membrane, C_H^o, if the hydrogen diffusivity in the membrane is known. The diffusion coefficient of hydrogen through the membrane can be found using the permeation transient from the breakthrough time, t_b. The breakthrough time is the time it takes the hydrogen atom to diffuse through the membrane from the charging to the exit side. It can be calculated using equation (13).[18]

$$t_b = \frac{L^2}{15.3^* D} \qquad (13)$$

Kim and Wilde[8], showed that the steady state hydrogen permeation current, i_∞, is given by equation (14). The IPZ analysis uses this relation in the development of its main relations[11].

$$i_\infty = Fk_{abs}\theta_H - Fk_{des}C_H^o \qquad (14)$$

Substituting C_H^o from equation (12) into equation (14) gives

$$i_\infty = Fk_{abs}\theta_H - Fk_{des}\frac{L\,i_\infty}{FD} \qquad (15)$$

Rearranging equation (15)[11]

$$i_\infty = \mathrm{F}\frac{k_{abs}}{1+\frac{L\,k_{des}}{D}}\,\theta_H \qquad (16)$$

The kinetic-diffusion constant, k, is expressed in terms of the adsorption and absorption rate constants as shown in equation (17)[11,14,20].

$$k = \frac{k_{abs}}{1+k_{des}\frac{L}{D}} \qquad (17)$$

Equation (16) can be simplified using the kinetic-diffusion constant, k, to equation (18).

$$i_\infty = \mathrm{F}\ k\ \theta_H \qquad (18)$$

Equation (18) relates the steady state hydrogen permeation current density to the hydrogen surface coverage. Equations (17) and (18) are two major relations in the IPZ analysis.

Substituting the hydrogen surface coverage from equation (7) into equation (18) and rearranging gives[11,19]

$$i_\infty = k\sqrt{\frac{\mathrm{F}}{k_2}}\sqrt{i_r} \qquad (19)$$

Equation (19) shows the relation between the steady state hydrogen permeation current density, i_∞, and the square root of the hydrogen recombination current density, $\sqrt{i_r}$. This relation should be a straight line passing through the origin with a slope of $k\sqrt{\frac{\mathrm{F}}{k_2}}$ for the application of the IPZ analysis. This limitation on the application of the original IPZ analysis will be discussed in more detail below.

Similarly, substituting the hydrogen coverage, θ_H, from equation (18) into equation (5) and rearranging gives[11].

$$i_c\exp(a\alpha\eta) = i_o'\left(1-\frac{1}{\mathrm{F}k}\,i_\infty\right) \qquad (20)$$

Equation (20) shows the relation between the charging function, $i_c\exp(a\alpha\eta)$ and the steady state hydrogen permeation current density, i_∞. This relation should be a straight line with a slope of $-\frac{i_o'}{Fk}$ and an intercept of i_o'.

The original IPZ analysis developed the major relations, (17), (18), (19) and (20), between the various variables in the hydrogen permeation system[11,13,14,19,20]. The kinetic-diffusion constant, k, and i_o' can be found from the slope and intercept of equation (20). The recombination rate constant, k_2, can be evaluated using the estimated kinetic-diffusion constant, k, and the slope of equation (19). The value of the exchange current density, i_o, can be estimated using the value of i_o'. The discharge rate constant, k_1, can be found from the exchange current density using the formula $i_o' = Fk_1C_H$. The hydrogen surface coverage, θ_H, can be evaluated using the kinetic-diffusion constant, k, and equation (18). Therefore, these kinetic and thermodynamic parameters of both the hydrogen evolution and absorption reactions can be determined using the IPZ analysis when the experimental data satisfies the requirements of equations (19) and (20).

Membrane Thickness Effect

The IPZ analysis can be used to evaluate the absorption and desorption rate constants , k_{abs} and k_{des}. Rearranging equation (17) can give a relation between the kinetic-diffusion constant, k, and the membrane thickness, L.[20]

$$\frac{1}{k} = \frac{1}{k_{abs}} + \frac{L}{D}\frac{k_{des}}{k_{abs}} \qquad (21)$$

Permeation experiments need to be done at different metal membrane thicknesses, L, in order to use equation (21). Once the kinetic-diffusion constants are obtained at different membrane thicknesses, equation (21) can be used to obtain k_{abs} and k_{des}. Equation (21) shows a straight line between the reciprocal of the kinetic-diffusion constant, k, and the membrane thickness, L. The slope of this relation will give the value of the desorption constant, k_{des}. The intercept will give the absorption rate constant, k_{abs}.

Calculation of θ_H and rate constants of the HER from Polarization Data

Elhamid et al. (21), showed that the polarization curve of the HER can be analyzed to calculate the hydrogen surface coverage and the rate constants of the hydrogen discharge and recombination reactions for metals with very low hydrogen permeability. They assumed in their study that the permeation current density is very low for some metals such as copper and therefore, the charging current density, i_c, will be equal to the recombination current density, i_r. They developed and used Equation 22 to calculate the exchange current density, i_o, and k_2. Then, k_1 was calculated from the exchange current density using $i_o = Fk_1C_H+$. The hydrogen

surface coverage was calculated from Equation 7. More details about this kind of calculation can be found in Ref. 21.

$$i_c \exp(a\alpha\eta) = i_o' \left(1 - \frac{\sqrt{i_c}}{\sqrt{Fk_2}}\right) \qquad (22)$$

Frumkin Modification of the Original IPZ Analysis

The Frumkin adsorption isotherm assumes that the free energy of adsorption of a species decreases with coverage according to the following equation[22-25].

$$\Delta G_\theta^\circ = \Delta G_0^\circ + f\, RT\, \theta \qquad (23)$$

where f is a dimensionless factor that describes the deviation from the ideal Langmuir behavior. The f RT quantity is sometimes called the rate of change of the standard free energy of adsorption, ΔG_θ° and ΔG_0° are the standard free energy of adsorption at a certain coverage, θ, and at zero coverage, $\theta = 0$, respectively, R is the gas constant and T is the absolute temperature.

The Langmuir adsorption isotherm assumes that the standard free energy of adsorption is independent of coverage ($f = 0$). This isotherm is usually applicable at low values of coverage ($\theta < 0.1$) and at coverages close to unity ($\theta > 0.9$)[24,25]. In some instances it has been found to be applicable also for intermediate coverages of hydrogen on iron surfaces.[15,20,27]

Writing the rate equations in view of the Frumkin adsorption conditions, one has for the rate of proton discharge and hydrogen evolution.[13,23,28-30]

$$i_c = i_o'(1-\theta_H)\exp(-a\alpha\eta)\exp(-\alpha f \theta_H) \qquad (24)$$

$$i_r = Fk_2\theta_H^2 \exp(2\alpha f \theta_H) \qquad (25)$$

Inserting θ_H from equation (18) into equation (25)

$$i_r = Fk_2\left(\frac{i_\infty}{Fk}\right)^2 \exp\left(2\alpha f \frac{i_\infty}{Fk}\right) \qquad (26)$$

Taking the square root of equation (26)

$$\sqrt{i_r} = \sqrt{\frac{k_2}{F}} * \frac{i_\infty}{k} * \exp(\alpha f \frac{i_\infty}{Fk}) \qquad (27)$$

Dividing both sides of equation (27) by i_∞ and taking the natural logarithm (ln)[29,30]

$$\ln(\frac{\sqrt{i_r}}{i_\infty}) = \ln(\sqrt{\frac{k_2}{F}} * \frac{1}{k}) + \frac{\alpha f}{Fk} i_\infty \qquad (28)$$

This relation, which was also derived by Iyer, et. al.[13,28], in a similar form, but with different slope and intercept, can be used for determining the rate constants when the value of f is known or can otherwise be estimated.[13,28,31] Recently, Al-Faqeer and Pickering (29) arrived at another relationship which, when applied to the steady state permeation data, can yield the rate constants without a prior knowledge of the value of f. In fact, the value of f is a result of the analysis. This derivation follows:

Rearranging equation (24) and solving for $\exp(\alpha f \theta_H)$

$$\exp(\alpha f \theta_H) = \frac{i_o^{'}(1-\theta_H)}{i_c \exp(a \alpha \eta)} \qquad (29)$$

Taking the square root of equation (25)

$$\sqrt{i_r} = \sqrt{Fk_2} * \theta_H * \exp(\alpha f \theta_H) \qquad (30)$$

Substituting $\exp(\alpha f \theta_H)$ from equation (28) into equation (30)

$$\sqrt{i_r} = \sqrt{Fk_2} * \theta_H * \frac{i_o^{'}(1-\theta_H)}{i_c \exp(a \alpha \eta)} \qquad (31)$$

Rearranging and inserting for θ_H from equation (18) into equation (31)

$$\sqrt{i_r}\ i_c \exp(a \alpha \eta) = \sqrt{Fk_2} * \frac{i_\infty}{Fk} * i_o^{'}(1-\frac{i_\infty}{Fk}) \qquad (32)$$

Dividing both sides of equation (32) by i_∞

$$\frac{\sqrt{i_r}}{i_\infty} i_c \exp(a\,\alpha\,\eta) = \sqrt{\frac{k_2}{F}} * \frac{i_o'}{k} (1 - \frac{1}{Fk} i_\infty) \qquad (33)$$

Equations (28) and (33) can be simplified to equations (19) and (20) if the Langmuir adsorption conditions are assumed instead of the Frumkin adsorption conditions. In other words, the generalized IPZ analysis[29] reduces to the original Langmuir IPZ analysis[11] if the standard free energy of adsorption is assumed to be independent of the hydrogen coverage, i.e., $f = 0$. Thus, the original IPZ analysis is a special case of the generalized IPZ analysis, in the same way the Langmuir isotherm is a special case of the Frumkin isotherm.

Plots of both $\ln(\frac{\sqrt{i_r}}{i_\infty})$ and $\frac{\sqrt{i_r}}{i_\infty} i_c \exp(a\alpha\,\eta)$ vs. i_∞ should give straight lines according to equations (28) and (33), respectively.

The procedure of calculating the unknowns in the system is[29]:

- From the slope and intercept of equation (33), k can be calculated.
- From the slope of equation (28) and knowing k from step 1, f can be calculated, after using the charging (Tafel) data to obtain the value of α.
- From the intercept of equation (28) and knowing k from step 1, k_2 can be calculated.
- From the intercept of equation (33) and knowing k from step 1 and k_2 from step 3, i_o' can be calculated.
- From equation (18) and knowing k from step 1, the hydrogen surface coverage (θ_H) can be calculated.

Application of the Generalized IPZ analysis

The original IPZ analysis has been used extensively in the literature. Details about using the original IPZ analysis to evaluate the experimental data can be found elsewhere[11,19,20,28]. In what follows, we give an example where the Frumkin modification of the IPZ analysis was used to evaluate the experimental data on the effect of hydrogen sulfide on the hydrogen evolution and absorption reactions on an iron membrane. The electrochemical hydrogen permeation technique was used to carry out the experimental part of the research.

The effect of hydrogen sulfide concentrations on the relation between the measured steady state hydrogen permeation current density, i_∞, and the cathodic potential, E, in the charging compartment of the cell is presented in Figure 1. The figure shows that hydrogen sulfide strongly enhances hydrogen absorption into iron since the steady state hydrogen permeation current density increases by more than an order of magnitude with increasing H_2S concentration at the same cathodic potential.

Figure 2 shows the effect of hydrogen sulfide concentrations on the relation between the rate of the hydrogen charging reaction, i_c, and the cathodic potential, E. The figure reveals that hydrogen sulfide enhances the HER since the hydrogen overpotential is less (E is more positive) at the same value of the applied cathodic charging current.

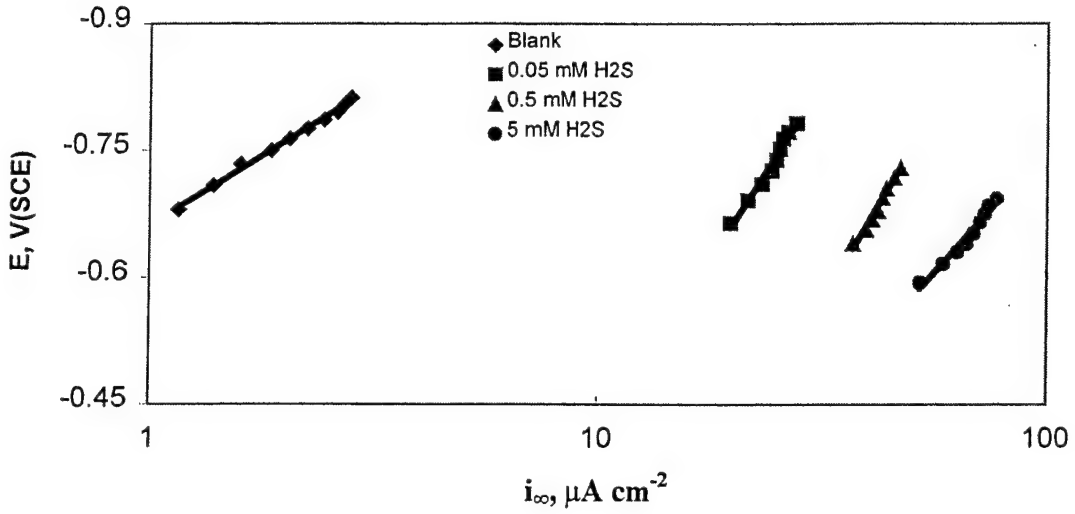

Figure 1: The relation between i_∞ and E obtained at different hydrogen sulfide concentrations at pH 2

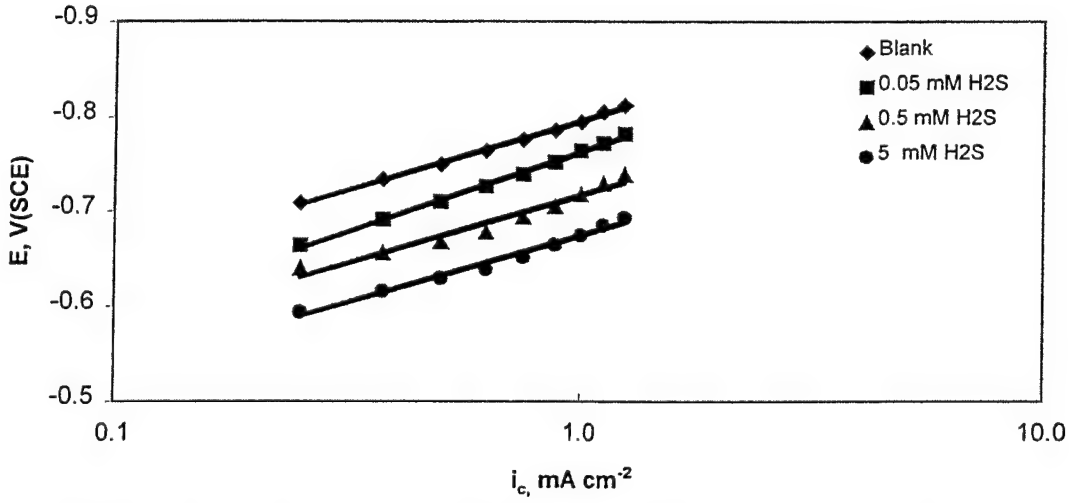

Figure 2: The relation between i_c and E obtained at different hydrogen sulfide concentrations at pH 2

Figure 3 shows the effect of hydrogen sulfide on the hydrogen concentration inside the membrane. This figure reveals that the hydrogen concentration inside the membrane increases as the hydrogen sulfide concentration increases in the charging solution.

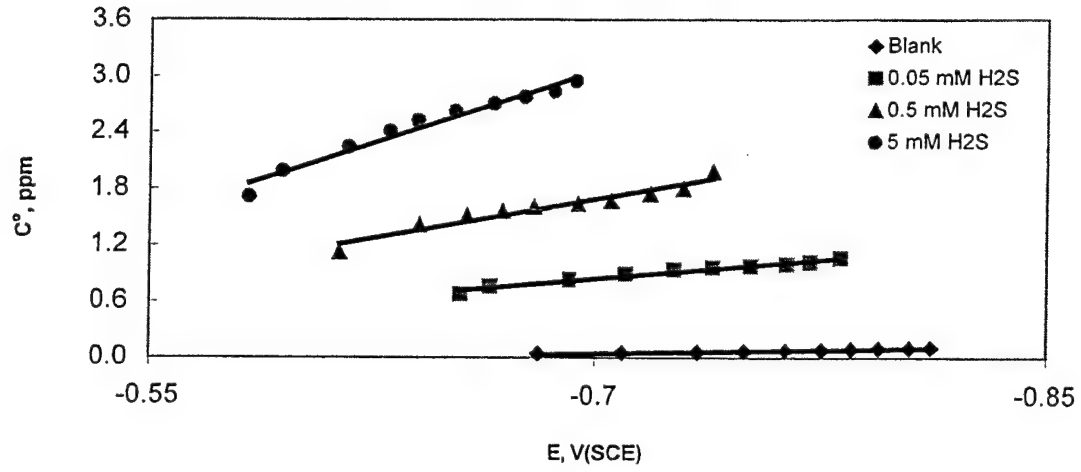

Figure 3: The relation between C^{o} and E obtained at different hydrogen sulfide concentrations at pH 2

Figure 4 shows the relation between the measured steady state permeation current density, i_{∞}, and the square root of the recombination current density, $\sqrt{i_r}$, obtained at different hydrogen sulfide concentrations. This Figure shows straight lines but only the blank solution line passes by the origin in accord with equation (19). In the presence of hydrogen sulfide, the lines do not pass through the origin and have a finite intercept with the y-axis. This indicates that the original IPZ analysis cannot be used to evaluate the data in the presence of hydrogen sulfide.

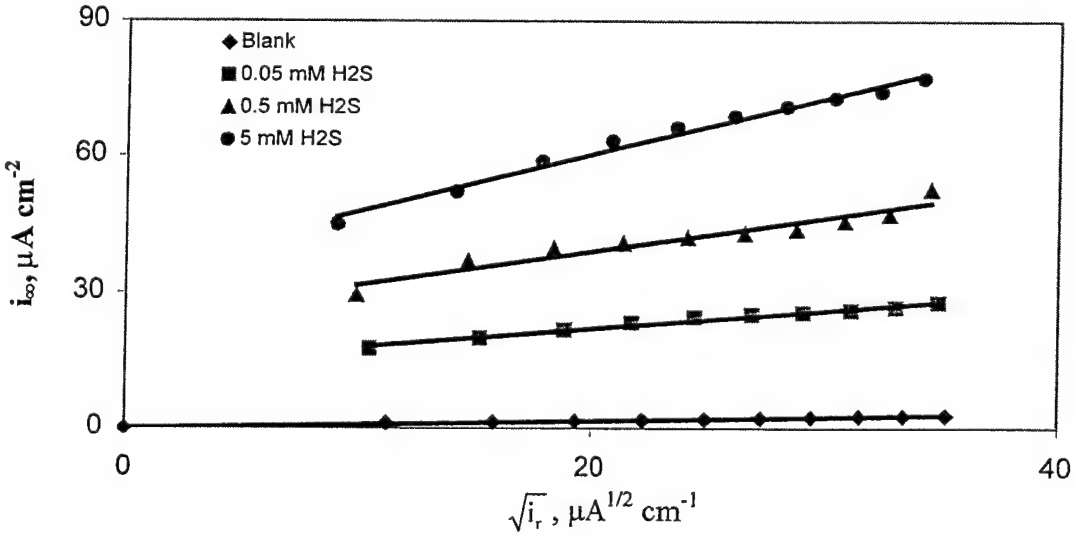

Figure 4: The relation between i_{∞} and $\sqrt{i_r}$ obtained at different hydrogen sulfide concentrations at pH 2.

Figure 5 shows the relation between $\ln(\frac{\sqrt{i_r}}{i_\infty})$ and the measured steady state hydrogen permeation current density, i_∞. The figure shows straight lines in accord with equation (27). Figure 6 shows linear relations between $\frac{\sqrt{i_r}}{i_\infty} i_c \exp(a\alpha\eta)$ and the measured steady state hydrogen permeation current density, i_∞, in accord with equation (32). This indicates the generalized IPZ analysis can be used to analyze the data.

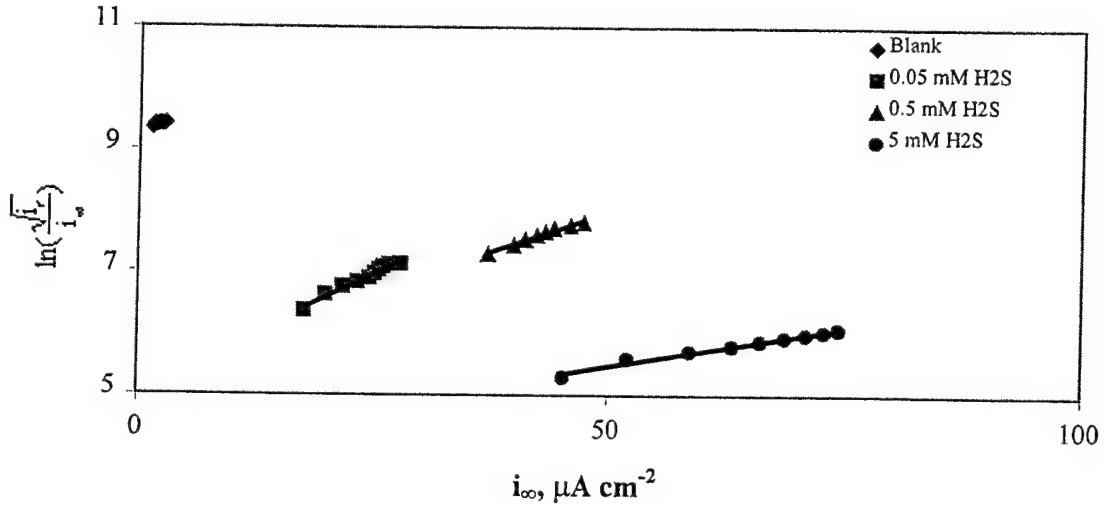

Figure 5 The relation between $\ln(\frac{\sqrt{i_r}}{i_\infty})$ and i_∞ obtained at different hydrogen sulfide concentrations at pH 2

The slopes of the lines in Figure 6 were used along with the intercepts for the values of the kinetic-diffusion constant, k, according to Equation (32). The values of k at different hydrogen sulfide concentrations were used to estimate the hydrogen recombination rate constant, k_2, and f, from the intercepts and slopes of the lines in Figure 6 respectively, in accord with Equation (27). Values of k and k_2 were used to calculate the hydrogen exchange current density at different hydrogen sulfide concentrations, $i_0 = \frac{i_o'}{(1-\theta_H^e)} = i_o'$ when $\theta_H^e << 1$, from the intercepts of Figure 6, in accord with equation (32). The calculated values of the exchange current density were used to estimate the discharge rate constant, k_1, at different hydrogen sulfide concentration using the relation $i_0' = F k_1 C_{H+}$.

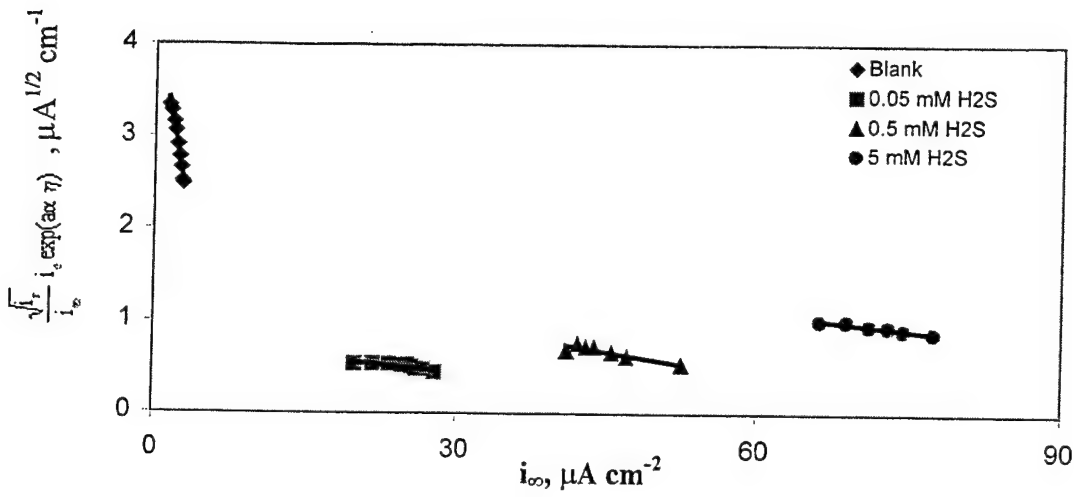

Figure 6: The relation between $\frac{\sqrt{i_r}}{i_\infty} i_c \exp(a\alpha\eta)$ and i_∞ obtained at different hydrogen sulfide concentrations at pH 2

Table I shows values for i_o, k_1, k_2, k and f at different hydrogen sulfide concentrations. These results show that hydrogen sulfide increases the proton discharge rate constant, k_1, and decreases the recombination rate constant of the HER, k_2. This could lead to an increase in the hydrogen surface coverage, θ_H. The values of k were used to estimate the hydrogen surface coverage, θ_H, using Equation (18) at different potentials and hydrogen sulfide concentrations. Figure 7 shows the relations between the hydrogen surface coverage, θ_H, and cathodic potential, E. It reveals that the hydrogen coverage increases with the increase in both hydrogen sulfide concentration and the potential in the cathodic direction.

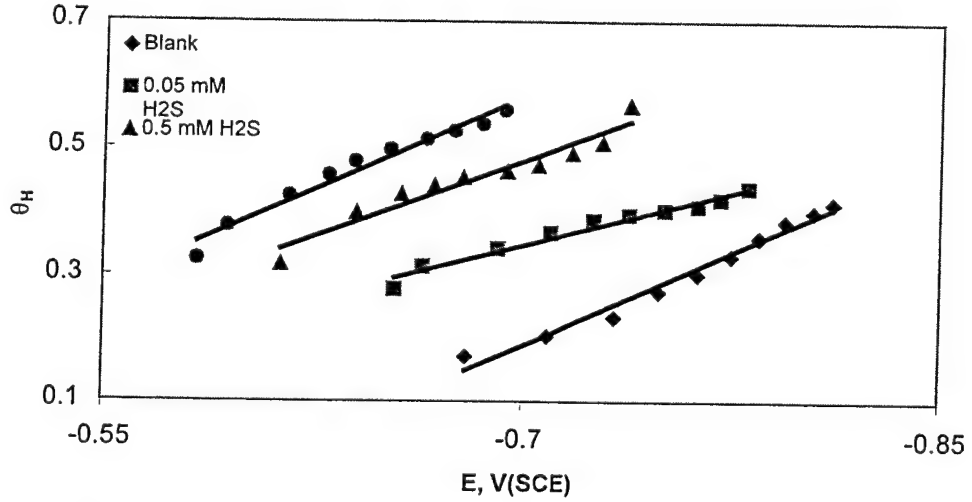

Figure 7: The relations between θ_H and E obtained at different hydrogen sulfide concentrations at pH 2

Table I also shows that hydrogen sulfide affects f. The value of f increased from almost zero (0.49) in the absence of hydrogen sulfide to nearly 8.7 in the presence of hydrogen sulfide. This indicates that the standard free energy of adsorption is coverage dependent, and that the Frumkin adsorption isotherm was correctly applied.

The increase in θ_H and f, dominate over the decrease in the hydrogen recombination rate constant of the HER, k_2, which leads to an increase in the hydrogen evolution reaction rate. However, the increase in the hydrogen absorption reaction rate is attributed to increases in the hydrogen surface coverage, θ_H, and the kinetic-diffusion constant, k.

Table I: Values of k, k_2, i_o, k_1 and f obtained on iron membrane at different hydrogen sulfide concentrations at pH 2.

H_2S Content	k mol cm^{-2} s^{-1}	k_2 mol cm^{-2} s^{-1}	i_o μA cm^{-2}	k_1 cm s^{-1}	f
Blank	7.02×10^{-11}	4.96×10^{-8}	0.421	4.36×10^{-7}	0.49
50 μM (1.7 ppm)	6.61×10^{-10}	2.82×10^{-9}	2.78	2.89×10^{-6}	8.94
500 μM (17 ppm)	9.62×10^{-10}	$2.66 \times ^{-9}$	9.22	9.56×10^{-6}	8.87
5 mM (170 ppm)	1.43×10^{-9}	9.24×10^{-10}	26.1	2.70×10^{-5}	8.26

Conclusion

The kinetics of hydrogen entry in metals has been studied using different analyses. The original IPZ analysis has been applied to steady state permeation data to yeild the individual rate constants of the hydrogen evolution reaction, k_1 and k_2, the kinetic-diffusion constant, k, the hydrogen surface coverage, θ_H, and the hydrogen concentration in the charging side, C^o. It was also shown how θ_H, k_1 and k_2 could be determined from the measured HER polarization curve. The analysis was modified assuming the validity of the Frumkin adsorption isotherm where a general analysis was developed. The experimental data in the presence of hydrogen sulfide fits the relations derived in the case of the generalized IPZ analysis. However, there is no independent evidence that the Frumkin approach is a better description than the Langmuir approach for hydrogen adsorption under these conditions. Furthermore, the adsorption of the sulfur species was ignored; therefore, any effect that they may have had on the available hydrogen adsorption sites on the surface was ignored too, for the sake of an approximation.

Acknowledgment

The authors gratefully acknowledge financial support by the U. S. Steel Corporation, Saudi Aramco and the Office of Naval Research.

List of Symbols

a	a constant, F/RT, V^{-1}
C_H^+	hydrogen ion concentration in the electrolyte, mol L^{-1}
C^o	hydrogen concentration in the metal at the charging surface, ppm
D	hydrogen diffusion coefficient, cm^2 s^{-1}
F	Faraday constant, 96484.6 C mol^{-1}
f	a factor that describes the deviation from the ideal Langmuir behavior, dimensionless
ΔG_θ°	standard free energy of adsorption at certain coverage, J mol^{-1}
ΔG_0°	standard free energy of adsorption at zero coverage, J mol^{-1}
i_c	charging current density, A cm^{-2}
i_∞	steady state hydrogen permeation current density, A cm^{-2}
i_o	exchange current density, A cm^{-2}
i_o'	$i_o/(1-\theta_H^e)$, A cm^{-2}
i_r	hydrogen recombination current density, A cm^{-2}
k_{abs}	absorption rate constant, mol $(cm^2\ s)^{-1}$
k_{des}	desorption rate constant, cm s^{-1}
k	kinetic-diffusion constant, mol cm^{-2} s^{-1}
k_1	discharge rate constant, cm s^{-1}
k_2	recombination rate constant, mol $(cm^2\ s)^{-1}$
L	membrane thickness, cm
R	gas constant, 8.314 J $(mol\ K)^{-1}$
T	absolute temperature, K

Greek Symbols

α	transfer coefficient, dimensionless
η	overpotential of the HER, V
θ_H	hydrogen surface coverage, dimensionless
θ_H^e	hydrogen surface coverage at equilibrium, dimensionless

REFERENCES

1. M. A. Devanathan and Z. Stachurski, Proc. Roy. Soc.Chem. A270, 90 (1962).

2. M. A. Devanathan and Z. Stachurski, J. Electrochem. Soc., 111, 619 (1964).

3. J. McBreen, L. Nanis and W. Beck, J. Electrochem. Soc., 113, 1219 (1966).

4. J. O'M Bockris, J. McBreen and L. Nanis, Electrochem. Soc., 112, 1025 (1965).

5. L. Nanis and T. K. Namboodhiri, J. Electrochem. Soc., 119, 691 (1972).

6. W. Beck, A. L. Glass and E. Taylor, J. Electrochem. Soc., 112, 53 (1965).

7. M. A. Devanathan, Z. Stakurski and W. Beck, J. Electrochem. Soc., 110, 880 (1963).

8. C. D. Kim and B. E. Wilde, J. Electrochem. Soc., 118, 202 (1971).

9. J. O'M. Bockris, J. L. Carbajal, B. R. Scharifker and K. Chandrasekaran, J. Electrochem. Soc., 134, 1957 (1987).

10. J. O'M. Bockris and P. K. Subramanyan, Electrochem. Acta, 16, 2169 (1971).

11. R. N. Iyer, H. W. Pickering and M. Zamanzadeh, J. Electrochem. Soc., 136, 2463 (1989).

12. M. H. Abd Elhamid, B. G. Ateya and H. W. Pickering, J. Electrochem. Soc., 144, L58 (1997).

13. R. N. Iyer, I. Takeuchi, M. Zamanzadeh and H. W. Pickering, Corrosion, 46, 360 (1990).

14. M.Ramasubramanian, B. N. Popov and R. E. White, J. Electrochem. Soc., 145, 1907 (1998).

15. H. A. Durtee, D. M. See, B. N. Popov and R. E. White, J. Electrochem. Soc., 144, 2313 (1997).

16. M. Manohar and B. E. Wilde, Corros. Sci., 37,607(1995).

17. D. H. Coleman, G. Zheng, B. N. Popov and R. E. White, J. Electrochem. Soc., 143, 1871 (1995).

18. J. Flis, Corrosion of Metals and Hydrogen Related Phenomena (Elsevier, Amsterdam, 1991), 25-280

19. M. H. Abd Elhamid, B. G. Ateya and H. W. Pickering, J. Electrochem. Soc., 147, 2258 (2000).

20. M. H. Abd Elhamid, B. G. Ateya and H. W. Pickering, J. Electrochem. Soc., 147, 2959 (2000).

21. M. H. Abd Elhamid, B. G. Ateya, K. G. Weil and H. W. Pickering, J. Electrochem. Soc., 147, 2148 (2000).

22. M. Temkin and V. Pyzhev, *Acta Physicochimica*, 12, 327 (1940).

23. A. Frumkin and N. Aladjalova, *Acta Physicochimica*, 19, 1 (1944).

24. E. Gileadi and B. E. Conway; "The Behavior of Intermediate in Electrical Catalysis" in Modern Aspects of Electrochemistry No.3; J. O'M. Bockris and B. E. Conway, editors, Butterworths, Washington, 1964, pp 347-442.

25. E. Gileadi, Electrode Kinetics for Chemists, Chemical Engineers, and Materials Scientists, Wiley-VCH, New York, 1993. 261-279.

26. R. N. Iyer and H. W. Pickering, J. Electrochem. Soc., 137, 3512 (1990).

27. D Tromans, Acta Metall. Mate., 42, 2043 (1994).

28. R.N. Iyer and H. W. Pickering, "Mechanism and Kinetics of Electrochemical Hydrogen Entry and Degradation of Metallic Systems," Annual Review of Materials Science, Vol. 20, Annual Reviews, Inc., Palo Alto, CA., (1990).

29. F. M. Al-Faqeer and H. W. Pickering, J. Electrochem. Soc., 148, E248 (2001).

30. Faisal M. Al-Faqeer, "Effect of Sulfur Containing Compounds on Hydrogen Absorption by Iron" (Master Thesis, The Pennsylvania State University, University Park, 1999), 27-45.

31. A. Durairajan, A Krishnyier, B. S. Haran, R. E. White and B. N. Popov, Corrosion, 56, 283 (1998).

Effect of Benzotriazole on the Hydrogen Absorption by Iron

M. H. Abd Elhamid,*,a B. G. Ateya,b and H. W. Pickering***,a**

[a]*Department of Materials Science and Engineering, Pennsylvania State University, Univeristy Park, Pennsylvania 16802, USA*
[b]*Department of Chemistry, Faculty of Science, Cairo University, Cairo, Egypt*

ABSTRACT

The results presented show that benzotriazole (BTA) inhibits the absorption of hydrogen into iron which is cathodically polarized in an acid (pH ≅ 1.7) sulfate solution. Analysis of the results indicates that BTA inhibits also the hydrogen evolution reaction, although it does not change its mechanism, which is shown to be proton discharge-Tafel recombination. However, BTA shifts the position of the equilibrium, $H_{ads} \rightleftharpoons H_{abs}$, toward the left side and hence leads to a decrease in the concentration of H_{abs} within the lattice. The extent of this decrease depends on the BTA concentration, *e.g.*, about fivefold at 1 m*M* and tenfold at 10 m*M* BTA. This effect is opposite to that reported for inhibitors such as thiourea which inhibits the hydrogen evolution reaction and yet promotes hydrogen permeation.

Introduction

The absorption of hydrogen in metals and alloys is a precursor to hydrogen embrittlement, the deterioration of the materials mechanical properties, and failure by crack propagation.[1,2] The problem is hardly avoidable since hydrogen enters metals and alloys from many sources, *e.g.*, corrosion, acid pickling, electroplating, welding, cathodic protection. In aqueous environments, the introduction of hydrogen within the metal or the alloy occurs during the hydrogen evolution reaction (HER).[3-6] There are two generally accepted mechanisms for this reaction[3,6,7]: the discharge-Tafel recombination

$$H^+ + e \rightarrow M\text{-}H_{ads} \quad [1]$$

$$M\text{-}H_{ads} + M\text{-}H_{ads} \rightarrow H_2 \quad [2]$$

and the discharge-electrochemical desorption which begins with reaction 1 followed by

$$M\text{-}H_{ads} + H^+ + e \rightarrow H_2 \quad [3]$$

where $M\text{-}H_{ads}$ refers to a nascent hydrogen atom adsorbed on the metal surface. The major part of this adsorbed hydrogen reacts to give hydrogen molecules through reactions 2 or 3. A fraction of this adsorbed hydrogen is adsorbed into the metallic lattice, $M(H_{abs})$

$$M\text{-}H_{ads} \underset{k_{des}}{\overset{k_{abs}}{\rightleftharpoons}} M(H_{abs}) \quad [4]$$

This adsorbed hydrogen diffuses within the metal and eventually causes embrittlement. Many theories have been proposed to explain the phenomenon, *e.g.*, the pressure theory, the adsorption theory, the decohesion theory, and the hydride theory.[1,2]

Different approaches have been proposed to mitigate the problem, either by the use of inhibitors,[8-15] by coating the surface,[16-18] or alloying with elements which have lower diffusivities for hydrogen.[19,20] Among the inhibitors, BTA has been tested on iron[6] and steel[10] in strongly acidic media. None of these referenced works dealt with the mechanism involved in the inhibition of the hydrogen absorption process. Further, both sets of results produced different conclusions. For instance, Dull and Nobe[6] found that the efficiency of BTA as an inhibitor for hydrogen absorption increases significantly with the rate of hydrogen evolution, whereas Subramanyan *et al.*[10] found that the efficiency to be independent of the extent of cathodic polarization and hence of the rate of hydrogen evolution. These measurements were obtained in unbuffered and strongly acidic media where BTA is known to be less efficient as a general corrosion inhibitor.[21]

Our objective here is to explore the effect of BTA on the kinetics of the hydrogen absorption within iron. The experimental results were obtained in a buffered acidic medium of a pH at which BTA has a high efficiency as a general corrosion inhibitor. BTA is widely used as a general corrosion inhibitor for copper and its alloys[22-25] and to lesser extent for iron base alloys.[21,26-28]

* Electrochemical Society Student Member.
** Electrochemical Society Active Member.
*** Electrochemical Society Fellow.

Experimental

A hydrogen permeation cell[29,30] was used to measure the permeability of hydrogen through iron membranes. The cell consists of two identical parts separated by the metal membrane, Fig. 1. One side and its associated circuitry were used to generate the hydrogen charging current and to measure the potential of the charging side of the membrane while the other side was used to monitor the diffusion flux of hydrogen through the membrane by measuring the hydrogen oxidation current at the exit surface of the membrane. The charging side had a saturated calomel reference electrode whereas the exit side had a Hg/HgO reference electrode. Both sides had Pt counterelectrodes, which were separated from the solution using glass frits. The exposed surface area of the sample was 0.8 cm^2.

The iron membranes (0.025 cm thick) were obtained from Goodfellow with the following composition: Mn, 0.3% Si, 0.1%; C, <0.08%; S, <0.05%; and the balance is iron. They were polished successively down to 600 emery paper, degreased ultrasonically in acetone, annealed at 900°C for 2 h in pure hydrogen, and furnace cooled in the same atmosphere.

The charging solution was 0.1 *N* H_2SO_4 + 0.9 *N* Na_2SO_4, pH ≅ 1.7. The solutions were prepared from analytical grade chemicals and double-distilled water. They were pre-electrolyzed at 3 mA for 24 h in external cells. All solutions were continuously deaerated with pure hydrogen.

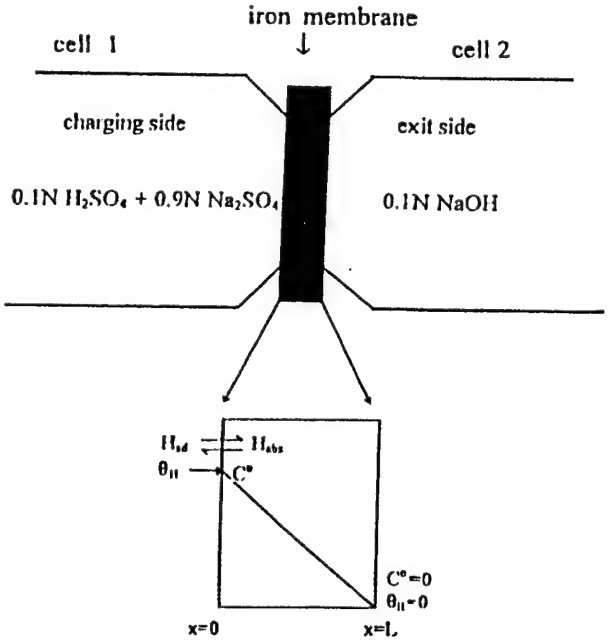

Fig. 1. Schematic illustration showing (a, top) the position of the iron membrane between the two electrolytic cells and (b, bottom) the boundary conditions imposed on the membrane by the two cells.

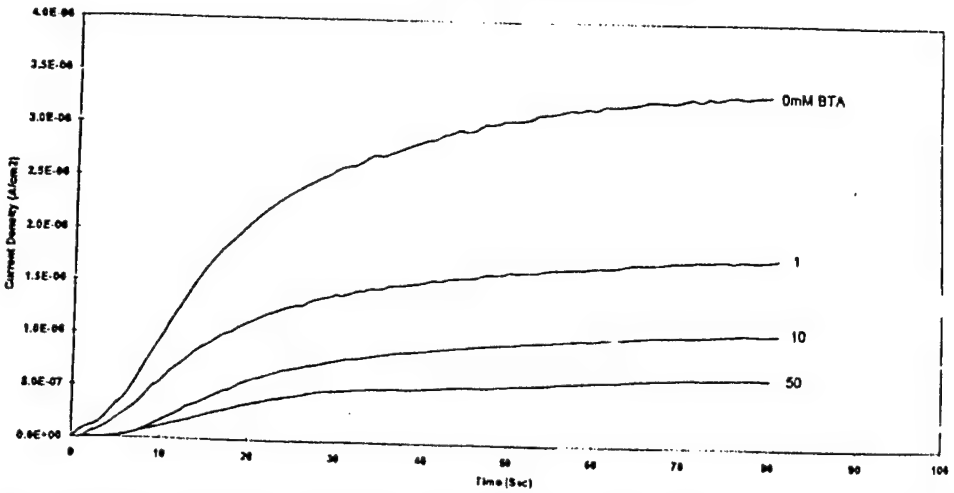

Fig. 2. Hydrogen permeation transients obtained at different BTA concentrations, at a cathodic charging current of 1.25 mA cm^{-2}.

The exit side of the membrane was coated with a thin layer of Pd using a commercial electroless plating bath, Pallamerse. This Pd layer protects the exit side of the membrane and provides a catalytic surface for the oxidation of hydrogen. The exit side of the membrane was polarized anodically to + 150 mV (Hg/HgO). The current was recorded until it decayed to a constant value, normally below 0.2 μA cm $^{-2}$. The solution was introduced into the charging side of the cell under conditions of cathodic protection to protect the sample from corrosion if left at the open-circuit potential. The permeation current (anodic current at the exit surface) was recorded *vs.* time until a steady-state permeation current was obtained. The cathodic current at the charging surface was then increased in a stepwise fashion after reaching a steady permeation rate at each value. Other sets of experiments were conducted with charging electrolytes containing different BTA concentrations.

Results and Discussion

Figure 2 shows typical permeation transients obtained at a charging current density of 1.25 mA cm $^{-2}$ for charging electrolytes containing different BTA concentrations. The permeation current increases with time toward a limiting steady-state value, i_∞. The figure reveals that the permeability of hydrogen through iron decreases with increase of BTA concentration. Further, BTA shifts the potential at the charging side of the membrane toward more cathodic values to an extent which also depends on the BTA concentration, as shown below. Several permeation transients were obtained at different charging currents and were repeated at different BTA concentrations.

The rate of proton discharge (reaction 1) i_c is given by

$$i_c = Fk_1C_{H^+}(1 - \theta_H)\exp\left(-\frac{\alpha F\eta}{RT}\right) \quad [5]$$

where k_1 is the rate constant of reaction 1, C_{H^+} is the hydrogen ion concentration, θ_H is the degree of surface coverage of the membrane with adsorbed hydrogen, α is the transfer coefficient of the discharge reaction (Eq. 1), η is the cathodic polarization, F is the Faraday constant, R is the universal gas constant, and T is the absolute temperature. The rate of the (Tafel) recombination reaction (Eq. 2) is given by

$$i_r = Fk_r\theta_H^2 \quad [6]$$

For a mechanism of the HER involving coupled proton discharge (Eq. 1)-Tafel recombination (Eq. 2), various theoretical treatments[12,31-35] relate the steady-state permeation (i_∞) and recombination (i_r) currents by

$$i_\infty = \frac{FD}{L}\frac{k_{abs}}{k_{des}}\sqrt{\frac{i_r}{Fk_r}} \quad [7a]$$

where D is the diffusivity of hydrogen in the membrane and L is its thickness. In view of Eq. 6, the above equation also can be expressed as

$$i_\infty = \frac{FD}{L}\frac{k_{abs}}{k_{des}}\theta_H \quad [7b]$$

Equation 7a predicts a straight line relation between i_∞ and $\sqrt{i_r}$ where $i_r = i_c - i_\infty$. Figure 3 shows several such plots at different BTA concentrations. The plots show satisfactory straight lines passing through the origin which confirm that the reaction proceeds via the Tafel recombination and that the permeation rate is controlled by hydrogen diffusion through the membrane and not by slow kinetics at the surface, *i.e.*, Eq. 4 is in local equilibrium. Further, the slopes of the straight lines decrease, indicating lower permeation currents as the BTA concentration increases. According to the above equations, a decrease in the permeation current may be brought about by a decrease in θ_H and/or in the ratio k_{abs}/k_{des} which is the equilibrium constant of reaction 4. This indicates that BTA either decreases the coverage of the iron surface with adsorbed hydrogen and/or diminishes the rate constant of the forward step of reaction 4. In principle, a similar effect may be observed if BTA were to increase k_{des}, *i.e.*, to favor the reverse step of reaction 4.

Figure 4 shows the E-log(i) relations of the HER obtained on iron in the presence of various concentrations of BTA. Clearly, BTA decreases the HER rate at a given potential. It also increases the Tafel slope (2.3 $RT/\alpha F$) from 120 mV per current decade for the blank electrolyte to 146, 169, and 169 mV for the electrolytes containing 1, 10, and 50 mM BTA, respectively. These plots indicate that the rate-determining step of the HER is a charge-transfer reaction (*i.e.*, proton discharge, reaction 1) with a transfer coefficient α equal to 0.5 for the blank electrolyte and α equal to 0.35 in the presence of 10 mM BTA. Reaction 2 is excluded as a possible rate-determining step, as this requires a Tafel slope of only 30 mV

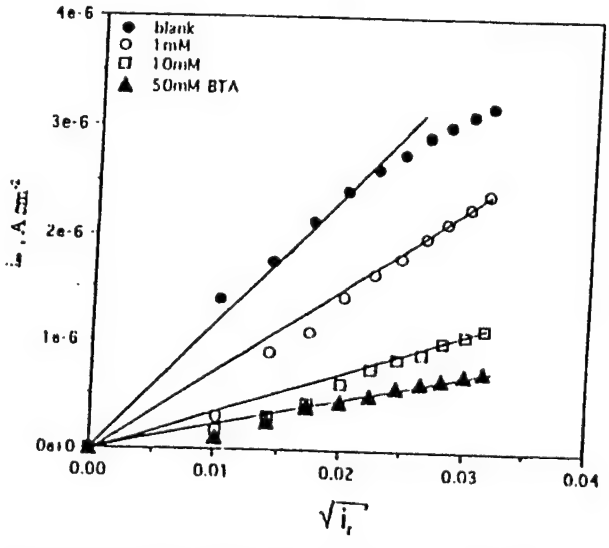

Fig. 3. Plots of the steady-state hydrogen permeation current (i_∞) *vs.* square root of the recombination current (i_r) at different BTA concentrations.

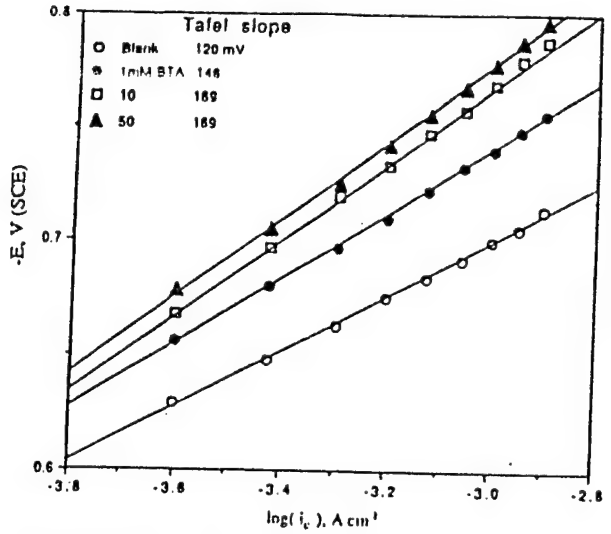

Fig. 4. Tafel plots of the hydrogen evolution reaction at different BTA concentrations.

per current decade,[7] which was not observed here. This analysis of Fig. 4 indicates that BTA also inhibits the HER by decreasing the rate constant of proton discharge (k_1, see Eq. 5), or the fraction of uncovered electrode area, which becomes $(1 - \theta_H - \theta_{BTA})$. In principle, a similar effect may be observed on a decrease in the rate of recombination (Eq. 2). If the mechanism of the HER is coupled proton discharge-Tafel recombination (Eq. 1 and 2) with both steps proceeding at comparable rates. The increase in the Tafel slope is determined solely by a decrease in α (Eq. 5).

Figure 5 shows the relation between the steady-state permeation current and the cathodic potential at different BTA concentrations. It reveals that the permeation current increases at more negative (cathodic) potentials and decreases with increasing BTA concentration. This indicates that BTA inhibits the hydrogen absorption process (reaction 4) in addition to its effect of inhibiting the HER (see Fig. 4). This effect of BTA is different than that of thiourea[8,35,36] which inhibits the HER and promotes hydrogen absorption and that of H_2S[36] which promotes hydrogen absorption and only mildly affects the HER. The mechanism by which such additives (poisons) promote hydrogen absorption was discussed recently[37] in terms of electronic interactions between the adsorbed promoters and the adsorbed hydrogen atoms on the metal surface. More work must be done to unravel the mechanism of this dual inhibitive action of BTA on the simultaneous hydrogen evolution and hydrogen absorption reactions.

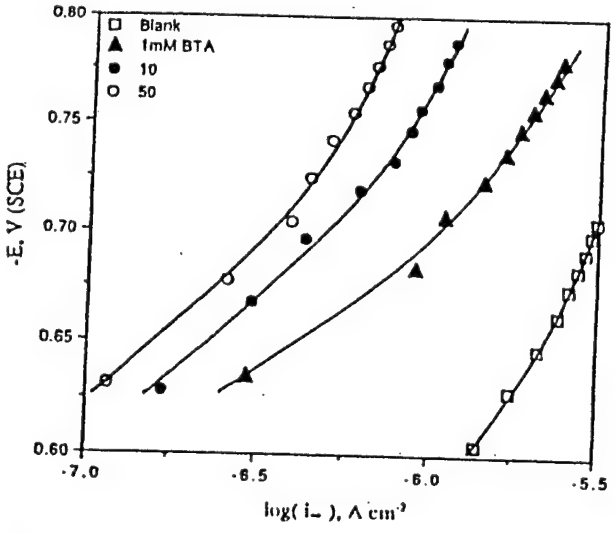

Fig. 5. Steady-state permeation current (i_∞) *vs.* cathodic potential ($-E$) at different BTA concentrations.

Table I. Values of the steady-state permeation current, i_∞, ar the concentration of hydrogen in iron at the input surface C^o, at different concentrations of the BTA at a potential of −0.65 V (SCE).

[BTA], m*M*	i_∞ (μA cm^{-2})	C^o (mol cm^{-3})
0	2.17	4.7×10^{-7}
1	0.46	1.0×10^{-7}
10	0.24	5.0×10^{-8}
50	0.16	3.5×10^{-8}

The steady-state permeation current is related to the concentration C^o by

$$i_\infty = FDC^o/L \quad [$$

where D is the diffusivity of hydrogen in the membrane of thickness L. Equation 8 reveals that the decrease in the steady-state permeation current is brought about by a decrease in C^o. This can be caused by either a decrease in θ_H or by a shift of the equilibrium position of reaction 4 toward the left, *i.e.*, away from $M(H_{abs})$ toward $M\text{-}H_{ads}$. This conclusion is consistent with that obtained from analyzing the data in Fig. 3, in the light of Eq. 7a and b.

Equation 8 can be used to calculate the values of C^o under various conditions provided the value of D is known. We measured diffusivity of 1.2×10^{-5} cm^2 s^{-1} for hydrogen in iron using the equation of breakthrough time given by Devanathan and Stachurski.[1] Table I lists the values of C^o so obtained at − 650 mV [saturated calomel electrode (SCE)] as a function of BTA concentration. As the BTA concentration increases, C^o decreases. A 10 m*M* BTA solution decreases C^o by about one order of magnitude.

Conclusion

The present work shows that BTA is an efficient inhibitor for the absorption of H into iron and also for the hydrogen evolution reaction. The increase of the BTA concentration causes an increase in the cathodic polarization and in the cathodic Tafel slope on iron. It also causes a decrease in the steady-state permeation current and hence in the concentration of hydrogen in the metallic lattice. The adsorption of BTA on the iron surface leads to a marked decrease in the rate of proton discharge and a shift of the surface equilibrium $M - H_{ads} \rightleftharpoons H_{abs}$) toward the left side which results in a decrease in the concentration of absorbed hydrogen within the metal. This effect is opposite to that reported for some other inhibitors such as thiourea which inhibits the hydrogen evolution reaction and yet promotes hydrogen permeation. The specific effect of BTA may yet be sorted out from additional measurements and analysis.

Acknowledgment

The authors gratefully acknowledge the encouragement and the financial assistance by the Office of Naval Research (Dr. A. J. Sedriks), Grant No. N00014-94-1-0086.

Manuscript submitted Nov. 23, 1996; revised manuscript received Jan. 31, 1997.

The Pennsylvania State University assisted in meeting the publication costs of this article.

REFERENCES

1. H. K. Birnbaum, in *Atomistics of Fracture*, R. M. Latanision and R. M. Pickens, Editors, Plenum Press, New York (1981).
2. R. Oriani, *Corrosion*, **43**, 390 (1987).
3. M. Enyo, in *Modern Aspects of Electrochemistry*, Vol. 11, J. O'M. Bockris and B. E. Conway, Editors, p. 251, Plenum Press, New York (1975).
4. B. G. Pound, in *Modern Aspects of Electrochemistry*, Vol. 25, J. O'M. Bockris, B. E. Conway, and R. W. White, Editors, p. 63, Plenum Press, New York (1993).
5. B. K. Subramanyan, in *Comprehensive Treatise of Electrochemistry*, Vol. 4, J. O'M. Bockris, B. E. Conway, E. Yeager, and R. E. White, Editors, p. 411, Plenum Press, New York (1981).
6. J. O'M. Bockris and S. U. M. Khan, *Surface Electrochemistry*, p. 833, Plenum Press, New York (1993).
7. K. J. Vetter, *Electrochemical Kinetics*, pp. 525-535, Academic Press, New York (1967).
8. D. L. Dull and K. Nobe, *Corrosion*, 35, 535 (1979).

9. Y. Saito and K. Nobe, *ibid.*, **36,** 178 (1980).
10. N. Subramanyan, K. Balakrishnan, and B. Sathianan, in *Proceedings of the Third European Symposium on Corrosion Inhibitors,* 5, pp. 591-616 (1970).
11. S. M. Wilhelm and D. Abayarathna, *Corrosion,* **50,** 152 (1994).
12. J. O'M. Bockris, J. McBreen, and L. Nanis, *This Journal,* **112,** 1025 (1965).
13. K. Kobayashi, K. Shimizu, and M. Iida, *Corros. Sci.,* **35,** 1431 (1993).
14. R. M. Hudson and C. J. Waring, *ibid.,* **10,** 121 (1970).
15. Y. T. Al-Janabi and A. L. Lewis, *This Journal,* **142,** 2865 (1995).
16. S. S. Chatterjee, B. G. Ateya, and H. W. Pickering, *Met. Trans.,* **A9,** 389 (1978).
17. M. Zamanzadeh, A. Allam, C. Kato, B. G. Ateya, and H. W. Pickering, *This Journal,* **129,** 284 (1982).
18. D. R. Cole, G. Zheng, B. N. Popov, and R. E. White, *ibid.,* **143,** 1871 (1996).
19. J. O'M. Bockris, M. A. Genshaw, and M. Fullenwider, *Electrochim. Acta.,* **15,** 47 (1970).
20. E. Riecke, B. Johnen, and H. J. Grabke, *Werkst. Korros.,* 36, 435 (1985).
21. R. Chin and K. Nobe, *This Journal,* **118,** 545 (1971).
22. D. Tromans and J. C. Silva, *ibid.,* **143,** 458 (1996).
23. V. Brusic, M. A. Frisch, B. N. Eldridge, F. P. Novak, F. Kaufman, B. M. Rush, and G. S. Frankel, *ibid.,* **138,** 2253 (1991).
24. C. Clerc and R. Alkire, *ibid.,* **138,** 25 (1991).
25. K. I. Kuznetsov, in *Organic Inhibitors of Corrosion of Metals,* J. G. N. Thomas, Editor, Plenum Press, New York (1996).
26. B. Sathianandhan, K. Balakrishnan, and N. Subramanyan, *Br. Corros. J.,* **5,** 271 (1970).
27. N. Eldakar and K. Nobe, *Corrosion,* **36,** 271 (1981).
28. R. Alkire and A. Cangellari, *This Journal,* **135,** 2441 (1988).
29. A. N. Frumkin and N. Aladyalova, *Acta Physicochim. (USSR),* **19,** 1 (1944).
30. M. A. Devanathan and Z. Stachurski, *Proc. R. Soc.,* **A270,** 90 (1962).
31. M. A. Devanathan and Z. Stachurski, *This Journal,* **111,** 619 (1964).
32. C. D. Kim and B. E. Wilde, *ibid.,* **118,** 202 (1971).
33. C. Kato, H. J. Grabke, B. Egert, and G. Panzer, *Corros. Sci.,* **24,** 591 (1984).
34. R. N. Iyer, H. W. Pickering, and M. Zamanzadeh, *This Journal,* **136,** 2463 (1989).
35. B. G. Ateya and H. E. Abd Elal, in *Corrosion-Industrial Problems, Treatment and Control Techniques,* V. Ashworth, Editor, p. 201, Conf. Proc., KFAS Proc. Series, Pergamon Press, New york (1987).
36. Y. Saito and K. Nobe, *Br. Corros. J.,* **119,** 30 (1995).
37. G. Jerkiewicz, J. Borodzinski, W. Chrzanowski, and B. E. Conway, *This Journal,* **142,** 3755 (1995).

Journal of The Electrochemical Society, **147** (6) 2258-2262 (2000)
S0013-4651(99)07-049-4 CCC: $7.00

The Effect of Iodide Ions on the Kinetics of Hydrogen Absorption by Iron

M. H. Abd Elhamid,*,[a] B. G. Ateya,,[b] and H. W. Pickering***,[z]**

Department of Materials Science and Engineering, The Pennsylvania State University, University Park, Pennsylvania 16802, USA

The effect of iodide ions on the kinetics of both the hydrogen evolution reaction, HER, and the hydrogen absorption reaction, HAR, on iron (steel) membranes was investigated using an electrochemical hydrogen permeation cell. Iodide ions inhibit the HER by decreasing the rate constant of proton discharge. Iodide enhances the HAR, and in turn increases the concentration of hydrogen inside the metal, although it decreases the hydrogen surface coverage. The increased HAR rate is due to an increase in the composite rate constant of the hydrogen absorption step at the metal surface.

Manuscript submitted July 12, 1999; revised manuscript received February 10, 2000.

The presence of some additives in the environment affects the kinetics of the hydrogen evolution reaction (HER) on the surface (see Eq. 1 and 2) and, consequently, the hydrogen absorption reaction (HAR) within metals (Eq. 3). While some compounds inhibit both reactions, for example, benzonitrile, benzotriazole, and pyrroles,[1-7] others inhibit the HER while promoting the HAR, [8-28] *e.g.*, iodide ions, thiourea, and aminotriazole.[1,2,8,15,18-21] The mechanism of action of these additives is attracting considerable attention.[1-3,8-34] Inhibitors of both the HER and HAR are compounds which adsorb preferentially on the metal surface and hence decrease the hydrogen surface coverage, which in turn decreases the rate of both the HER and HAR.[1,2,7,33,34] By similar argument, others[8,9,11,35] attributed the effect of promoters of the HAR (Eq. 3) to inhibition of the recombination reaction (Eq. 2). This leads to a decrease in the rate of the HER (Eq. 2) but to an increase in the hydrogen surface coverage and hence to an increase in the hydrogen absorption. It has also been suggested that the adsorbed species, including iodide in acid sulfate solution, weaken the metal hydrogen bond[1,10,15,17] and hence facilitate the entry of hydrogen into the metal. Another group of authors attributed the accelerating affect of these additives on the HAR to an electronic interaction between the adsorbed hydrogen atoms and the adsorbed additive.[24,26,36] While additives with electron donating nature, such as iodide,[37] are reasoned to accelerate hydrogen absorption, those with electron withdrawing nature have the opposite effect.[24,26,36]

Recently, Qian *et al.*[38,39] investigated the effect of arsenic oxide and hydrogen sulfide in promoting hydrogen absorption into iron and steel in alkaline solutions. Their results revealed that arsenic oxide enhances hydrogen absorption through its reduction to arsenic hydride (AsH_3). These authors concluded that AsH_3 is desorbed from the metal surface, thereby increasing the number of adsorption sites for hydrogen. Thus, the hydrogen surface coverage and, consequently, the hydrogen absorption rate are increased[38] as reported earlier.[8] In the case of hydrogen sulfide in alkaline solution, they concluded that HS^- adsorbs on the surface, thereby, decreasing both the hydrogen surface coverage and the hydrogen desorption rate, although enhancing hydrogen absorption.[39] In a prior study of the Fe/H_2S–acid system, Iyer *et al.*[40] concluded that H_2S caused an increase in the hydrogen surface coverage and, in turn, accounted for the increase in the hydrogen absorption rate.

The aim of the present study is to analyze the effects of iodide ions on the kinetics of both the HER and HAR on iron in a more in-depth manner than in the past. Of particular importance is the effect of iodide ions on the hydrogen coverage of the iron surface and the rate constant of the hydrogen absorption step which affects the rate of hydrogen permeation within iron. The analysis of the results makes use of models that have been extensively tested in the literature.[1,8,9,17,21,30,40-46]

Model

Consider a coupled (Volmer) discharge-(Tafel) recombination mechanism for the HER, taking place on the left side of the membrane shown in Fig. 1, *i.e.*

$$H^+ + e^- + M \xrightarrow{k_1} M\text{-}H_{ads} \quad [1]$$

$$M\text{-}H_{ads} + M\text{-}H_{ads} \xrightarrow{k_2} 2M + H_2 \quad [2]$$

where $M\text{-}H_{ads}$ refers to an adsorbed hydrogen atom on the metal surface and k_1 and k_2 are the rate constants of the discharge and recom-

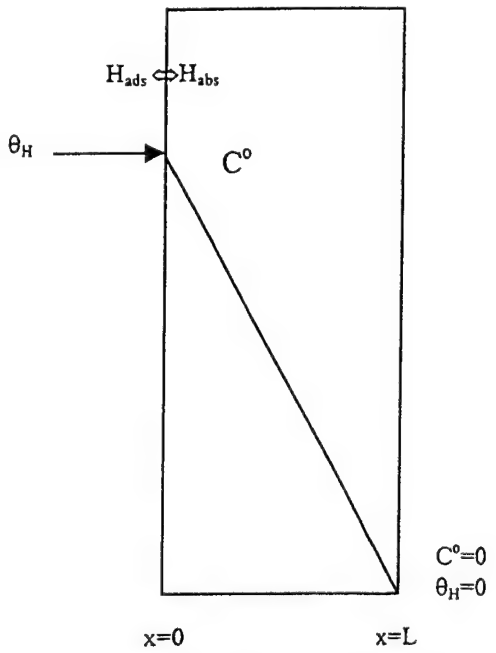

Figure 1. Schematic illustration showing the boundary conditions imposed on the metal.

* Electrochemical Society Student Member.
** Electrochemical Society Active Member.
*** Electrochemical Society Fellow.
[a] Present address: Global Alternative Propulsion Center, General Motors, Warren Michigan 48090, USA.
[b] Present address: Department of Chemistry, Faculty of Science, Kuwait University, Kuwait.
[z] E-mail: pick@ems.psu.edu

S0013-4651(99)07-049-4 CCC: $7.00 © The Electrochemical Society, Inc.

bination steps of the HER. This adsorbed hydrogen, M-H_{ads}, is also involved in the hydrogen absorption reaction, *i.e.*

$$\text{M-H}_{ads} \underset{k_{des}}{\overset{k_{abs}}{\rightleftharpoons}} \text{H}_{abs} + \text{M} \qquad [3]$$

where H_{abs} refers to the absorbed hydrogen atom within the metal lattice and k_{abs} and k_{des} refer to the rate constants of the forward and backward directions of Reaction 3, respectively (see Fig. 1). In addition to the assumption of a coupled Volmer-Tafel mechanism for the HER, we also assume the following: (*i*) that Reaction 1 (Volmer reaction) proceeds irreversibly, (*ii*) a Langmuirian adsorption for hydrogen, and (*iii*) hydrogen diffuses as atomic hydrogen within the iron membrane. These assumptions have been widely adopted in the literature.[1,8,9,17,30,40-46] As shown below, the results of this work appear compatible with the above assumptions. The questions of Langmuirian adsorption is addressed in the Conclusion. According to Eq. 1 the rate (current density) of the HER is given by

$$i_c = Fk_1C_{H^+}(1 - \theta_H)\exp\left(-\frac{F}{RT}\alpha\eta\right) \qquad [4]$$

where C_{H+} is the hydrogen ion concentration, α is the transfer coefficient of the HER, and η is the hydrogen overpotential. According to the IPZ analysis,[43,44] Eq. 4 gives

$$i_c \exp\left(\frac{F}{RT}\alpha\eta\right) = i_o'(1 - \theta_H) \qquad [5]$$

where the left side of Eq. 5 is referred to as the charging function and $i_o' = Fk_1C_{H+} = i_o/(1 - \theta_H^e)$ where i_o is the exchange current density of the HER and θ_H^e is the hydrogen surface coverage at equilibrium. The rate of the recombination reaction, Eq. 2, is given by

$$i_r = Fk_2\theta_H^2 \qquad [6]$$

The recombination current density, i_r, is the difference between the cathodic current density i_c, and the steady state hydrogen permeation current density, i_∞. The steady state hydrogen permeation current density, i_∞, is given by

$$i_\infty = \frac{FDC^o}{L} \qquad [7]$$

where D is the diffusion coefficient of atomic hydrogen within the metal, C^o is the concentration of the absorbed hydrogen just beneath its surface, and L is the thickness of the membrane. This current is given by the difference between the rates of the partial reactions involved in Eq. 3,[1,9,21,40,41-43] *i.e.*

$$i_\infty = Fk_{abs}\theta_H - Fk_{des}C^o \qquad [8]$$

Combining Eq. 7 and 8 gives

$$i_\infty = Fk\theta_H \qquad [9]$$

where k is the kinetic-diffusion constant and is defined as

$$k = \frac{k_{abs}}{1 + k_{des}\dfrac{L}{D}} \qquad [10]$$

This composite rate constant, k, in Eq. 10 is an improved version of that (k') in the original paper where $k' = kL/D$.[43] Equation 10 was also recently derived by Ramasubramanian *et al.*[46] Combining Eq. 6 and 9 gives

$$i_\infty = k\sqrt{\frac{F}{k_2}}\sqrt{i_r} \qquad [11]$$

This relationship has been experimentally observed by Dafft *et al.*[8] and others in various systems. Equation 11 predicts a straight line relation passing by the origin between i_∞ and $\sqrt{i_r}$ with a slope of $k\sqrt{F/k_2}$.

Combining Eq. 5 and 9 gives a relation between the charging function and the steady state hydrogen permeation current

$$i_c \exp\left(\frac{F}{RT}\alpha\eta\right) = i_o' - \frac{i_o'}{Fk}i_\infty \qquad [12]$$

Equation 12 relates the charging function, $i_c \exp(F/RT\,\alpha\eta)$, which includes the charge transfer kinetics at the charging surface of the membrane, and the steady state hydrogen permeation current density (i_∞) which is dependant on the transport properties of the membrane. It predicts a straight line relation between the charging function and i_∞, the slope of which equals $-i_o'/Fk$ and the intercept is i_o'. Consequently, values of k and i_o' can be evaluated graphically from such plots. The value of i_o' can be used to obtain $k_1 = (i_o'/FC_{H^+})$ and $i_o \approx i_o'$, while k can be used to evaluate the hydrogen surface coverage, θ_H, from Eq. 9. The value of k can also be used to evaluate the recombination rate constant, k_2, from the slope of the results plotted according to Eq. 11. Substituting for i_∞ from Eq. 7 and Eq. 8 and rearranging, one obtains[21,43]

$$C^o = k\theta_H L/D \qquad [13]$$

It follows that once k and θ_H are known, the concentration of hydrogen inside the metal at the charging side, C^o, can be obtained from Eq. 13, as well as from Eq. 7 using the measured i_∞ and D values.

Experimental

The electrochemical hydrogen permeation apparatus consisted of two matching three-electrode cells, similar to that used by Frumkin[47] and by Devanathan and Stachurski.[48] It was used to collect data on both the HER and HAR on iron membranes in an acidic solution of 0.1 N H_2SO_4 + 0.9 N Na_2SO_4 of pH 1.8. The iron (steel) samples, 0.25 mm thick, were obtained from Goodfellow with the following composition: Mn 0.3%; Si 0.1%; C <0.08%; S <0.05%; and the balance is iron. They were polished down to 0.5 μm alumina and then degreased in acetone and washed with double-distilled water. They were subsequently annealed in pure hydrogen at 900°C for 2 h in a tube furnace and furnace cooled in the same atmosphere. All solutions were prepared from analytical grade chemicals and double-distilled water. Before admitting the solutions to the cell, they were pre-electrolyzed at 3 mA for 2 h to remove impurities that could otherwise affect the quality of the data. The solutions were subsequently deaerated with hydrogen. The exit surface of the membrane was coated with electrolessly deposited palladium using Pallamerse solution before the membrane was mounted between the two cells. The exit cell contained 0.1 N NaOH and the potential of the Pd coated exit side was set at 0.150 mV (Hg/HgO) using a potentiostat to ensure complete oxidation of the dissolved hydrogen diffusing through the membrane. In order to minimize the production of traps in the membrane during the measurements, the cathodic current, i_c, at the charging surface was set at the highest value and then decreased in a setpwise fashion after reaching within minutes the steady-state permeation current at each value of i_c. Similarly, the polarization curve measurements in the same cell, the cathodic current, i_c, was decreased in a stepwise fashion after reaching in seconds the stationary electrode potential of the charging surface at each value of i_c. Further details about the experimental setup are reported elsewhere.[31,49]

Results and Discussion

Figure 2 shows the effect of iodide ion concentration on the relation between the steady-state hydrogen permeation current density, i_∞, and the overpotential, η, of the HER at the charging side of the membrane ($\eta = E - E^{eq}$ where $E^{eq} = -0.349$ V (standard calomel electrode) for the experimental system in this paper). Iodide ions enhance hydrogen absorption, *i.e.*, the steady-state hydrogen permeation current density increases for increasing iodide concentration at a given overpotential of the HER. Alternatively, at a certain concentration of iodide ions, larger negative overpotentials produce larger steady-state permeation currents, in agreement with the results of

S0013-4651(99)07-049-4 CCC: $7.00 © The Electrochemical Society, Inc.

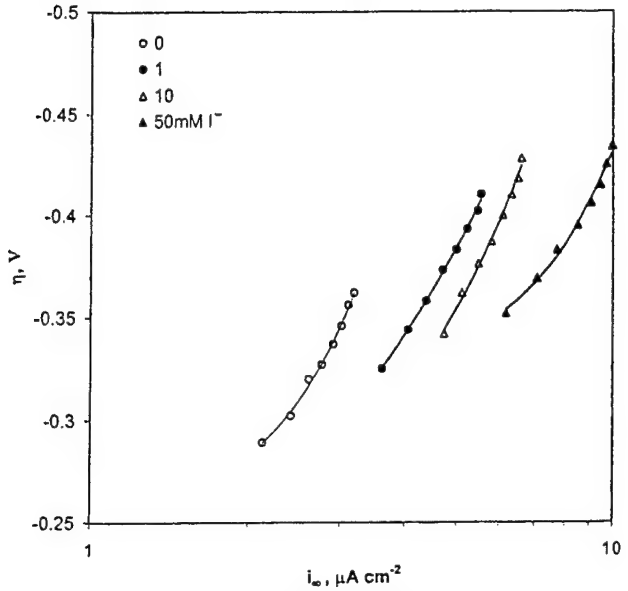

Figure 2. The relation between the steady-state hydrogen permeation current and the overpotential of the HER obtained on an iron membrane 0.25 mm thick in 0.1 N H_2SO_4 + 0.9 N Na_2SO_4, at different iodide ion concentrations.

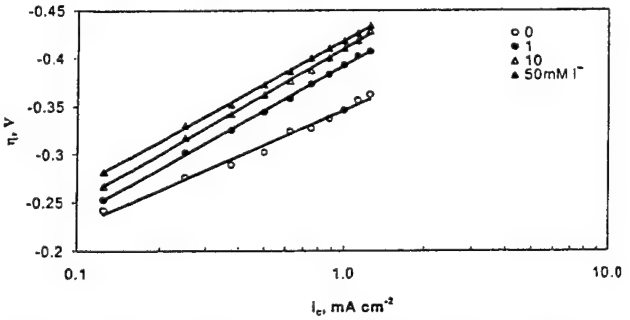

Figure 3. Tafel plots obtained on an iron membrane 0.25 mm thick in 0.1 N H_2SO_4 + 0.9 N Na_2SO_4 at different iodide ion concentrations.

other authors.[1,8] The diffusivity of hydrogen within the iron membrane was estimated using the breakthrough time method.[48] A value of 1.2×10^{-5} cm^2 s^{-1} was obtained which is in good agreement with the values reported in the literature for the diffusivity of hydrogen in iron.[26] The increase in the steady-state hydrogen permeation current density is accompanied by a decrease in the rate of the HER, as shown by Fig. 3 which indicates that the iodide ions inhibit the HER.

Figure 4 shows the relation between the steady-state hydrogen permeation current density and the square root of the hydrogen recombination current density. This figure shows data which lie fairly well on the straight lines drawn through the point of origin, in accord with the coupled discharge-recombination mechanism of the

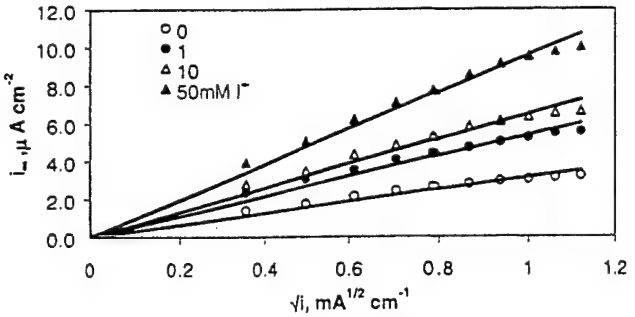

Figure 4. Relationship between the steady-state hydrogen permeation current, i_∞, and the square root of the hydrogen recombination current, $\sqrt{i_r}$, obtained on an iron membrane in 0.1 N H_2SO_4 + 0.9 N Na_2SO_4, at different iodide ion concentrations.

HER,[43] in the absence and in the presence of iodide ions. The slopes of the lines in Fig. 4, $k\sqrt{F/k_2}$ (from Eq. 11), increase as the iodide ion concentration increases, see Table I. Thus, an increase in the slopes of these straight lines results from an increase in the ratio of $k/\sqrt{k_2}$. This may be caused by an increase in k (*i.e.*, enhancement of the HAR, Eq. 3). It may also result from a greater increase in k than in $\sqrt{k_2}$, and/or a decrease in k_2 (*i.e.*, retardation of the recombination step, Eq. 2).

The Tafel slope for the blank solution (Fig. 3) was 120 mV corresponding to a transfer coefficient $\alpha = 0.5$. This value was used to calculate the charging function, $i_c \exp(\alpha\eta F/RT)$ under various conditions. Figure 5 shows the relation between the charging function and the steady-state permeation current at different iodide concentrations. The relations are satisfactory straight lines with negative slopes, $-i'_o/Fk$, in agreement with the prediction of Eq. 12. The magnitude of the slope decreases sharply with the iodide ion concentration, see Table I. The decrease in the slopes of the lines can be brought about by an increase in k, a decrease in i'_o, and/or a greater increase in k than in i'_o. The intercepts of the lines in Fig. 5 with the y-axis give the values of the exchange current density of the HER, $i'_o = i_o(1 - \theta^e_H) \approx i_o$ for cases of $\theta^e_H << 1$. The discharge rate constant was then calculated from the relation $i'_o = Fk_1C_{H^+}$. The slopes of the lines in Fig. 5 were solved with the intercepts for the values of the kinetic-diffusion constant, k (according to Eq. 12). The values of k at different iodide ion concentrations were then used to estimate the recombination rate constant of the HER, k_2, from the slopes of the lines in Fig. 4, in accord with Eq. 11. Table I shows values for i_o, k_1, k_2, and k at different iodide ion concentrations. The results show that iodide ions inhibit the HER by decreasing the discharge rate constant, k_1. Similar results were found in the literature for the effect of organic inhibitors on the discharge rate constant of the HER.[30,50] On the other hand, iodide promotes the HAR by increasing the kinetic-diffusion constant, k (Eq. 9) with in turn increases the concentration of hydrogen, C^o, just inside the metal (Eq. 13 and Fig. 6) and the rate of hydrogen permeation (Eq. 7)

The results in Table I also show that the iodide ions slightly increase the recombination rate constant of the HER, k_2. The values of k_2 in Table I differ by much more than the standard deviation of

Table I. Values of i_o, k_1, i'_o/Fk, $k\sqrt{F/k_2}$, k_2, and k obtained on a iron membrane in 0.1 N H_2SO_4 + 0.9 N Na_2SO_4 at different iodide ion concentrations.

[I$^-$], mM	i_o, A cm^{-2}	k_1, cm s^{-1}	i'_o/Fk	$k\sqrt{\frac{F}{k_2}}$, A$^{1/2}$ cm^{-1}	k, mol cm^{-2} s^{-1}	k_2, mol cm^{-2} s^{-1}
0	2.0×10^{-6}	1.3×10^{-6}	0.40	1.0×10^{-4}	5.2×10^{-11}	2.6×10^{-8}
1	1.2×10^{-6}	7.3×10^{-7}	0.13	1.8×10^{-4}	9.3×10^{-11}	2.7×10^{-8}
10	9.0×10^{-7}	5.6×10^{-7}	0.08	2.1×10^{-4}	1.1×10^{-10}	2.8×10^{-8}
50	6.0×10^{-7}	3.8×10^{-7}	0.03	3.1×10^{-4}	2.0×10^{-10}	3.8×10^{-8}

S0013-4651(99)07-049-4 CCC: $7.00 © The Electrochemical Society, Inc.

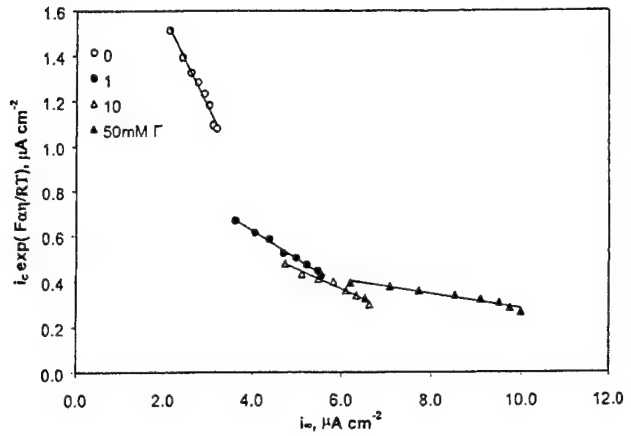

Figure 5. Relationship between the charging function, $i_c \exp(\alpha F\eta/RT)$, and the steady-state hydrogen permeation current, i_∞, for an iron membrane 0.25 mm thick in 0.1 N H_2SO_4 + 0.9 N Na_2SO_4, at different iodide ion concentrations.

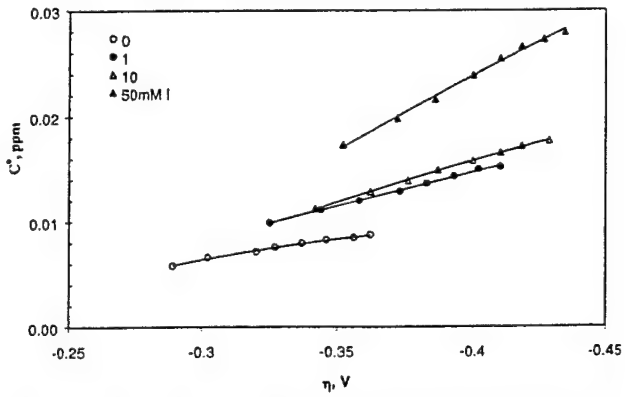

Figure 6. Variation of the concentration of hydrogen in iron at the input surface, C^o, with the overpotential of the HER obtained on an iron membrane 0.25 mm thick, in 0.1 N H_2SO_4 + 0.9 N Na_2SO_4, at different iodide ion concentrations.

the measured i_∞ values in three or four duplicate runs at all I^- concentrations. The mean values of i_∞ were used to determine the k, k_1, and k_2 values in Table I. These changes in k_1 and k_2 could lead to a decrease in the hydrogen surface coverage. The values of k were used to estimate the hydrogen surface coverage using Eq. 9 at different values of the hydrogen overvoltage and iodide concentrations. Figure 7 gives the relations between the hydrogen surface coverage and hydrogen overpotential. It reveals that the hydrogen coverage increases with the increase in the overpotential, which confirms results obtained by other authors.[20,26,30,42-46,51,52] Figure 7 also reveals that the hydrogen surface coverage decreases with increasing concentration of iodide ions in the charging solution, in contrast to the increase in concentration of hydrogen in the metal (Fig. 6).

Conclusions

In acidic solutions, iodide ions inhibit the HER on iron while enhancing the HAR. Using the IPZ analysis of the experimental results, we show that iodide ions lead to the following effects.

1. A decrease in the hydrogen surface coverage, θ_H;
2. An increase in the concentration of hydrogen in the iron, C^o;
3. A decrease in the discharge rate constant of the HER, k_1, and hence in the exchange current density, i_o;
4. An increase in the value of the kinetic-diffusion constant of the HAR, k, which causes an increase in the rate of hydrogen absorption within the metal (Eq. 3) and in C^o (Eq. 13).

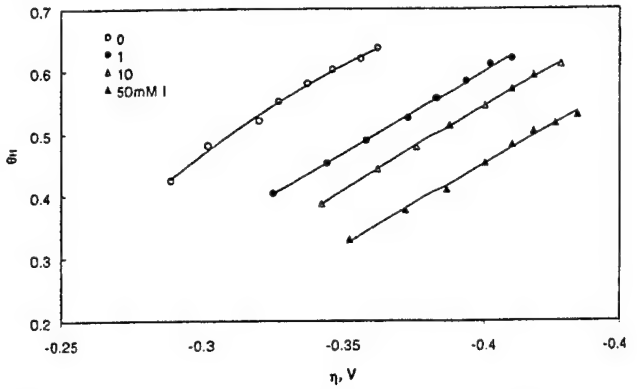

Figure 7. Variation of the hydrogen surface coverage, θ_H, with the overpotential of the HER obtained on an iron membrane 0.25 mm thick in 0.1 N H_2SO_4 + 0.9 N Na_2SO_4, at different iodide ion concentrations.

5. A slight increase in the recombination rate constant of the HER, k_2.

Accordingly, the above data and IPZ analysis reveal that the increase in the hydrogen absorption rate in the presence of iodide ions is caused by an increase in the kinetic-diffusion constant, k. This increase in k dominates over the decrease in surface coverage that is also caused by the iodide ion. Note that k is a composite quantity (Eq. 10) which includes the rate constants of both the absorption and desorption steps (forward and reverse directions of Reaction 3), the diffusivity of hydrogen within the membrane and the membrane thickness. Thus, an increase in k is caused by increases in k_{abs} and k_{des} within the thermodynamic constraint that their ratio remains unchanged. The extent of the contributions of the changes in k_{abs} and k_{des} to the measured increase in k, can be assessed based upon the measurements of i_∞ for membranes of different thickness.[43,44,49,53] These experiments have yet to be done for iodide ions.

This effect of iodide ions may result from its interaction with the metal surface and/or with the adsorbed hydrogen atoms. Further measurements are needed to reveal the nature and extent of this interaction with the metal surface. The interaction between iodide ions and adsorbed hydrogen atoms could also be treated within the context of Frumkin adsorption. However, the above changes in the kinetic parameters are only small (k_2) or moderate (i_o, k_1, and k) and are not associated with any significant deviation from the behavior of the system in the absence of iodide ions. Furthermore, the different sets of data are internally consistent and compatible with the underlying model,[1,9,17,30,40-46] which has been widely adopted in the literature, in the presence or absence of additives. Consequently, one might argue in favor of small, if any, lateral interactive (Frumkin) effects.

Acknowledgment

Professor Konrad G. Weil provided valuable comments. Financial support was provided by the Office of Naval Research, grant no. N00014-96-1-0913 (A. J. Sedriks) and the Division of the International Programs of the National Science Foundation (grant INT-9724698).

Dr. Pickering assisted in meeting the publication costs of this article.

List of Symbols

C_{H^+}	hydrogen ion concentration, mol cm^{-3}
C^o	concentration of the absorbed hydrogen at the input surface, mol cm^{-3}
D	hydrogen diffusion coefficient, cm^2 s^{-1}
F	Faraday's constant, C mol^{-1}
i'_o	$= Fk_1C_{H^+} = i_o/(1 - \theta_H^c)$, A cm^{-2}
i_o	exchange current density, A cm^{-2}
i_r	steady-state recombination current density, A cm^{-2}
i_∞	steady-state hydrogen permeation current density, A cm^{-2}
k_1	discharge rate constant, cm s^{-1}
k_2	recombination rate constant, mol cm^{-2} s^{-1}

S0013-4651(99)07-049-4 CCC: $7.00

k_{abs} absorption rate constant, mol cm^{-2} s^{-1}
k_{des} desorption rate constant, cm s^{-1}
k kinetic-diffusion constant, mol cm^{-2} s^{-1}
R general gas constant, 8.314 J mol^{-1} K^{-1}
T absolute temperature, K

Greek

α transfer coefficient, dimensionless
η cathodic overvoltage, V
θ_H^e hydrogen surface coverage at equilibrium, dimensionless
θ_H hydrogen surface coverage, dimensionless

References

1. J. O'M Bockris, J. McBreen, and L. Nanis, *J. Electrochem. Soc.*, **112**, 1025 (1965).
2. D. L. Dull and K. Nobe, *Corrosion*, **35**, 535 (1979).
3. H. A. Durte, D. M. See, D. M. Popov, and R. E. White, *Corrosion*, **54**, 187 (1998).
4. S. M. Wilhelm and D. Abayarathna, *Corrosion*, **50**, 152 (1994).
5. R. Agrawal and T. K. G. Namboodhiri, *J. Appl. Electrochem.*, **27**, 1265 (1997).
6. G. Schmitt, B. Olbertz, and K. Kurtz, *Werkst. Korros.*, **35**, 107 (1984).
7. Y. T. Al-Janabi, A. L. Lewis, and G. A.Oweimreen, *J. Electrochem. Soc.*, **142**, 2865 (1995).
8. E. G. Dafft, K. Bohnenkamp, and H. J. Engell, *Corros. Sci.*, **19**, 591 (1979).
9. T. P. Radhakrishnan and L. Shreir, *Electrochim. Acta*, **11**, 1007 (1966).
10. Z. A. Foroulis, *J. Electrochem. Soc.*, **128**, 219 (1981).
11. W. Beck, A. L. Glass, and E. Taylor, *J. Electrochem. Soc.*, **53**, 112 (1965).
12. M. A. Devanathan, Z. Stachurski, and W. Beck, *J. Electrochem. Soc.*, **110**, 880 (1963).
13. Z. S. Smialowski and M. Smialowski, *J. Electrochem. Soc.*, **110**, 444 (1963).
14. B. E. Conway, J. H. Barber, L. Gao, and S. Y. Qian, *J. Alloys Compd.*, **253**, 475 (1997).
15. L. Gao and B. E. Conway, *Electrochim. Acta*, **39**, 1681 (1994).
16. G. Jerkiewicz, *Prog. Surf. Sci.*, **57**, 137 (1998).
17. M. A. Devanathan, J. O'M. Bockris, and W. Mehl, *J. Electroanal. Chem.*, **1**, 143 (1959).
18. N. Subramanyan, K. Balakrishnan, and B. Sathianan, in *Corrosion Inhibitors Proceeding of the 3rd European Symposium*, p. 591, Ferrara University, Italy (1970).
19. R. Agrawal and T. K. Namboodhiri, *Corros. Sci.*, **30**, 37 (1990).
20. J. L. Carbajal and R. E. White, in *Electrochemistry in Transition*, O. J. Murphy, S. Srinivasan, and B. E. Conway, Editors, p. 339, Plenum Press, New York (1992).
21. B. G. Ateya and H. E. Abd Elal, in *Corrosion-Industrial Problems, Treatment and Control Techniques*, V. Ashworth, Editor, p. 201, Pergamon Press, New York (1987).
22. C. C. Juang and J. K. Wu, *Corros. Sci.*, **36**, 1727 (1994).
23. Y. Sato and K. Nobe, *Brit. Corros.*, **30**, 119 (1995).
24. B. E. Conway and G. Jerkiewicz, *J. Electroanal. Chem.*, **47**, 357 (1993).
25. E. Protopopoff and P. Marcus, in *Electrochemical and Materials Science of Cathodic Hydrogen Adsorption and Absorption*, B. E. Conway and G. Jerkiewicz, Editors, PV 94-21, p. 374, The Electrochemical Society Proceedings Series, Pennington, NJ (1995).
26. S. Y. Qian, L. Gao, and B. E. Conway, in *Electrochemical Surface Science of Hydrogen Adsorption and Absorption*, G. Jerkiewicz and P. Marcus, Editors, PV 97-16, p. 180, The Electrochemical Society Proceedings Series, Pennington, NJ (1997).
27. J. F. Newman and L. L. Shreir, *Corros. Sci.*, **9**, 631 (1969).
28. T. Zakroczymski, in *Hydrogen Degradation of Ferrous Alloys*, R. Oriani, J. P. Hirth, and M. Smialowski, Editors, p. 239, Noyes Publications, Park Ridge, NJ (1985).
29. H. J. Flitt and J. O'M. Bockris, *Int. J. Hydrogen Energy*, **7**, 411 (1982).
30. H. A. Durtee, D. M. See, B. N. Popov, and R. E. White, *J. Electrochem. Soc.*, **144**, 2313 (1997).
31. M. H. Abd Elhamid, B. G. Ateya, and H. W. Pickering, *J. Electrochem. Soc.*, **144**, L58 (1997).
32. T. Mizuno and M. Enyo, in *Modern Aspects of Electrochemistry*, Vol. 30, R. E. White, B. E. Conway, and J. O. M'Bockris, Editors, p. 451, Plenum Press, New York (1996).
33. M. A. Quraishi, M. A. W. Khan, M. Jamal, S. Muralidharan, and S. V. Iyer, *Brit. Corros.*, **32**, 72 (1997).
34. M. A. Quraishi, J. Rawat, and M. Ajmal, *Corrosion*, **54**, 996 (1998).
35. B. K. Subramanyan, in *Comprehensive Treatise of Electrochemistry*, Vol. 4, J. O'M. Bockris, B. E. Conway, E. Yeager, and R. E. White, Editors, p. 411, Plenum Press, New York (1981).
36. G. Jerkiewicz, J. Borodzinski, W. Chrzanowski, and B. E. Conway, *J. Electrochem. Soc.*, **142**, 3755 (1995).
37. U. Kaoru and S. Masahiro, *J. Electrochem. Soc.*, **146**, 1496 (1999).
38. S. Y. Qian, B. E. Conway, and G. Jerkiewicz, *J. Chem. Soc. Faraday Trans.*, **94**, 2945 (1998).
39. S. Y. Qian, B. E. Conway, and G. Jerkiewicz, *J. Phys. Chem. Chem. Phys.*, **1**, 2805 (1999).
40. R. N. Iyer, I. Takauchi, M. Zamanzadeh, and H. W. Pickering, *Corrosion*, **46**, 360 (1990).
41. C. D. Kim and B. E. Wilde, *J. Electrochem. Soc.*, **118**, 202 (1971).
42. M. A. Devanathan and Z. Stachurski, *J. Electrochem. Soc.*, **111**, 619 (1964).
43. R. N. Iyer, H. W. Pickering, and M. Zamanzadeh, *J. Electrochem. Soc.*, **136**, 2463 (1989).
44. R. N. Iyer and H. W. Pickering, *Annu. Rev. Mater. Sci.*, **20**, 299 (1990).
45. D. H. Coleman, G. Zheng, B. N. Popov, and R. E. White, *J. Electrochem. Soc.*, **143**, 1871 (1995).
46. M. Ramasubramanian, B. N. Popov, and R. E. White, *J. Electrochem. Soc.*, **145**, 1907 (1998).
47. A. N. Frumkin and N. Aladyalova, *Acta Physicochim*, **19**, 1 (1944).
48. M. A. Devanathan and Z. Stachurski, *Proc. Roy. Soc. Chem.*, **A270**, 90 (1962).
49. M. H. Abd Elhamid, B. G. Ateya, and H. W. Pickering, *J. Electrochem. Soc.*, Submited.
50. L. A. Antropov, *Corros. Sci.*, **7**, 607 (1967).
51. J. O'M. Bockris, J. L. Carbajal, B. R. Scharifker, and K. Chandrasekaran, *J. Electrochem. Soc.*, **134**, 1957 (1987).
52. M. A. Devanathan and M. Selvaratnam, *Trans. Faraday Soc.*, **56**, 1820 (1960).
53. R. N. Iyer and H. W. Pickering, *J. Electrochem. Soc.*, **137**, 3512 (1990).

Journal of The Electrochemical Society, **147** (6) 2148-2150 (2000)
S0013-4651(99)10-058-2 CCC: $7.00

Calculation of the Hydrogen Surface Coverage and Rate Constants of the Hydrogen Evolution Reaction from Polarization Data

M. H. Abd Elhamid,*,[b] B. G. Ateya,,[a] K. G. Weil,** and H. W. Pickering*****

Department of Materials Science and Engineering, The Pennsylvania State University, University Park, Pennsylvania 16802, USA

We show in this communication that the polarization data of the hydrogen evolution reaction (HER) can be analyzed to calculate the hydrogen surface coverage and the rate constants of the hydrogen discharge and recombination reactions for metals which have very low permeabilities of hydrogen and on which the HER proceeds through a coupled Volmer discharge-Tafel recombination mechanism. The analysis is applied to the results of the HER on copper and iron. For both metals, this polarization analysis yields exchange current densities that are comparable to the literature values and degrees of surface coverage which vary with potential in a manner that is well documented in the literature. The results on iron yield rate constants that are in a good agreement with those predicted in other studies using the Iyer, Pickering, and Zamanzadeh analysis.

Manuscript submitted October 14, 1999; revised manuscript received February 7, 2000.

The hydrogen evolution reaction (HER) is of particular importance in electrochemistry in view of its relevance to corrosion, electrolytic hydrogen production, electroplating, electrocatalysis, etc.[1-17] Adsorbed hydrogen (H_{ads}) is an important intermediate in the evolution of electrolytic hydrogen on metal surfaces,[1,4,5,7,8,11,14,16] and also because of its absorption within the metals and the subsequent problem of hydrogen embrittlement.[3-5,8,14-17] Proper characterization of the mechanism of the HER requires knowledge of the values of the rate constants of the various steps and the degree of surface coverage of the metal with adsorbed hydrogen. The experimental determination of the degree of coverage of metals with adsorbed hydrogen is a task that is fraught with many difficulties.[5,14,18,19]

In this communication, we show that the polarization curves of the HER can be analyzed to yield the individual rate constants of the two steps of the HER and the degree of coverage of the metal surface with adsorbed hydrogen. The analysis is suitable for metals which have low absorption rates for hydrogen and for which the HER occurs by the coupled volmer discharge-Tafel recombination mechanism. The proposed analysis is applied to the polarization curve of the HER on Cu and Fe. Using iron under conditions of a relatively small rate of hydrogen absorption, a comparison is made between results obtained using the present polarization analysis and those obtained from steady-state hydrogen permeation data using the Iyer, Pickering, and Zamanzadeh (IPZ) analysis.[20,21]

Experimental

Cathodic polarization experiments were carried out on copper samples of purity 99.5% and iron samples of purity 99.5% in 0.1 N H_2SO_4 + 0.9 N Na_2SO_4 (pH 1.8), using an EG&G PAR potentiostat model 276. The samples were polished down to 0.5 μm alumina, rinsed with acetone and double distilled water. The test solutions were prepared from analytical grade chemicals and double distilled water. All solutions were pre-electrolyzed at 3 mA for 2 h before measurements were taken. Before running the experiments the solutions were deaerated using hydrogen to remove the dissolved oxygen from the solution. A conventional three-electrode cell was used with saturated calomel as a reference electrode and two identical graphite rods as the counter electrodes.

Results and Discussion

Theoretical background.—Assume the HER proceeds by a discharge-recombination mechanism, *i.e.*

$$H^+ + e^- + M \xrightarrow{k_1} M\text{-}H_{ads} \quad [1]$$

$$M\text{-}H_{ads} + M\text{-}H_{ads} \xrightarrow{k_2} 2M + H_2 \quad [2]$$

where $M\text{-}H_{ads}$ refers to an adsorbed hydrogen atom on the metal surface and k_1 and k_2 are the rate constants of the discharge and recombination steps of the HER, respectively. This adsorbed hydrogen is also involved in an absorption reaction, *i.e.*

$$M\text{-}H_{ads} \rightleftarrows H_{abs} + M \quad [3]$$

where H_{abs} refers to the hydrogen absorbed within the lattice of the metal. A measure of a metal's tendency for absorbing hydrogen is its steady-state rate of hydrogen permeation, i_∞. However, the i_∞ value could underestimate the absorption rate that occurs prior to steady-state permeation, since the transient rate of hydrogen absorption can be much higher than the steady-state value, especially initially when there can exist a high density of unfilled traps for hydrogen in the metal, *e.g.*, in the case of certain steels or in the case of metals which exhibit high solubilities and/or diffusivities for hydrogen, *e.g.*, palladium. Thus, if i_∞ data are used as a measure of hydrogen absorption, it is advisable that i_∞ is orders of magnitude below i_c in order that the absorption rate is insignificant at all times with respect to the rate of the HER.

At steady state the rate of generation of H_{ads} by Reaction 1 (i_c) equals the sum of the rates of Reactions 2 (i_r) and 3 (i_∞), *i.e.*

$$i_c = i_r + i_\infty \quad [4]$$

For some metals, such as the face-centered cubic metals copper and nickel, the permeabilities of hydrogen are typically very low in view of their low diffusivities for hydrogen in comparison to the rate of the HER, *i.e.*, $i_c = i_r >> i_\infty$. This condition ($i_c \cong i_r$) could also hold for other metals like iron where the value of i_∞, though readily measurable, nevertheless is often some two to three orders of magnitude smaller than i_c. However, for iron in the presence of poisons such as hydrogen sulfide, the measured values of i_∞ are much higher and the assumption $i_c = i_r$ becomes less valid. Accordingly, if i_∞ is insignificant with respect to i_c, i_{abs} may also be insignificant with respect to i_c during measurement of the steady-state polarization curve, in which case the analysis can yield the hydrogen surface coverage and the rate constants of the HER, as is shown below.

The rate of proton discharge (denoted i_c) in the Tafel region of the polarization curve is given by

$$i_c = Fk_1C_{H^+}(1 - \theta_H)\exp\left(-\frac{F}{RT}\alpha\eta\right) = i_o'(1 - \theta_H)\exp\left(-\frac{F}{RT}\alpha\eta\right) \quad [5]$$

* Electrochemical Society Student Member.
** Electrochemical Society Active Member.
*** Electochemical Society Fellow.
[a] Department of Chemistry, Faculty of Science Kuwait University, Kuwait.
[b] General Motors, Global Propulsion Center, Warren, Michigan 48090.

S0013-4651(99)10-058-2 CCC: $7.00 © The Electrochemical Society, Inc.

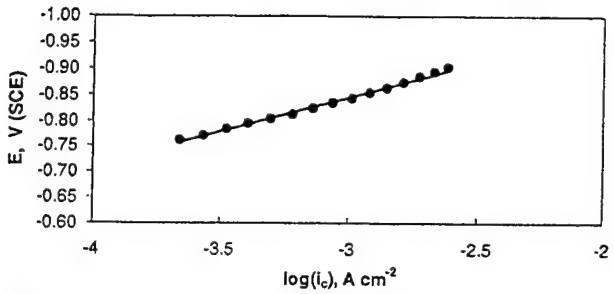

Figure 1. The relation between the cathodic current and the electrode potential obtained on copper in 0.1 N H_2SO_4 + 0.9 N Na_2SO_4.

where $i'_o = Fk_1C_{H^+} = i_o/(1 - \theta^e_H)$, i_o is the exchange current density of the HER at the limit of the equilibrium coverage, $\theta^e_H = 0$, C_{H^+} is the hydrogen ion concentration, α is the transfer coefficient of the HER, and η is the overpotential driving the HER. The rate of the recombination reaction, Eq. 2, is given by

$$i_r = Fk_2\theta^2_H \quad [6]$$

Rearranging Eq. 5 gives[20,21]

$$i_c \exp\left(\frac{F}{RT}\alpha\eta\right) = i'_o(1 - \theta_H) \quad [7]$$

The left side of Eq. 7 is called the charging function which combines the rate and driving force of the HER. Solving Eq. 6 for θ_H gives

$$\theta_H = \frac{\sqrt{i_r}}{\sqrt{Fk_2}} \quad [8a]$$

Inserting Eq. 4 with $i_\infty << i_c$, Eq. 8a becomes

$$\theta_H = \frac{\sqrt{i_c}}{\sqrt{Fk_2}} \quad [8b]$$

Combining Eq. 7 and 8b yields

$$i_c \exp\left(\frac{F}{RT}\alpha\eta\right) = i'_o\left(1 - \frac{\sqrt{i_c}}{\sqrt{Fk_2}}\right) \quad [9]$$

Equation 9 predicts a straight line relation between the charging function, $i_c \exp(F/RT\,\alpha\eta)$, and $\sqrt{i_c}$. From the slope $-i'_o/\sqrt{Fk_2}$ and the intercept (i'_o) of this plot one obtains i'_o and k_2.

From Eq. 5 at the limit of $\theta_H = \theta^e_H$ one has

$$i_o = Fk_1C_{H^+}(1 - \theta^e_H)$$
$$= Fk_1C_{H^+}, \text{ for } \theta^e_H = 0 \quad [10]$$

While i_o can be inserted into Eq. 10 to calculate k_1, k_2 can be used to calculate the hydrogen surface coverage at different potentials, using Eq. 6, assuming $i_c = i_r$.

Data analysis.—Figure 1 shows the Tafel plot obtained for hydrogen evolution on copper in 0.1 N H_2SO_4 + 0.9 N Na_2SO_4 at 25°C. The Tafel line has a slope of 121 mV (*i.e.*, $\alpha \cong 0.5$) which is comparable to the values in the literature.[22-25] Figure 2 is a plot of the charging function, $i_c \exp(F/RT\,\alpha\eta)$, *vs.* $\sqrt{i_c}$. It shows a satisfactory straight line with a negative slope and a positive intercept (see Eq. 9). Table I shows the values of the exchange current density, i_o, discharge rate constant, k_1, and the recombination rate constant, k_2, which were calculated using the slope and the intercept of the line in Fig. 2. The values are $i_o = 8 \times 10^{-8}$ A cm^{-2}, $k_1 = 5 \times 10^{-8}$ cm s^{-1}, and $k_2 = 1.8 \times 10^{-7}$ mol cm^{-2} s^{-1}. The value of the recombination rate constant, k_2, was used to calculate the hydrogen surface coverage θ_H using Eq. 6. Figure 3 shows the relation between θ_H and the electrode potential. This figure shows that the hydrogen surface coverage increases as the potential becomes less noble, *i.e.*, as the overpotential for the HER increases. This trend is well documented in the literature.[21,26-34]

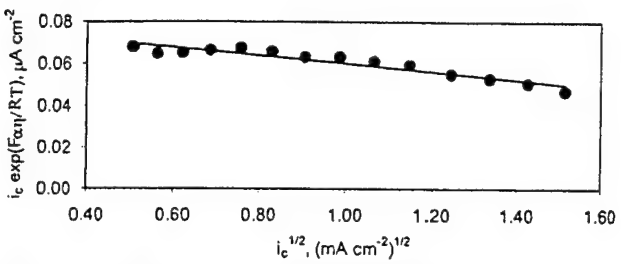

Figure 2. The relation between the charging function and the square root of the cathodic current obtained on copper in 0.1 N H_2SO_4 + 0.9 N Na_2SO_4.

The present polarization analysis was also applied to the polarization curve of hydrogen evolution obtained on iron in deaerated 0.1 N H_2SO_4 + 0.9 N Na_2SO_4. Figure 4 shows the relation between the charging function and the square root of the cathodic charging current obtained on iron. The charging function was calculated using a value of $\alpha = 0.5$ as measured in this work. This figure shows a straight line relation with a negative slope in accord with Eq. 9. A comparison is made in Table I between the values of the exchange current density and the rate constants obtained from this analysis and those obtained for this same system from steady-state hydrogen permeation data using the IPZ analysis.[35,36] The table shows that the present polarization analysis gives the same order-of-magnitude values as the IPZ analysis gives. The values of the hydrogen surface coverage estimated from the IPZ analysis were also compared with those obtained using the present analysis, see Fig. 5. This figure shows a good agreement in particular at the less noble potentials. At the more noble potentials, *e.g.*, −0.63 V, [35,36] the value of θ_H calculated in this work is approximately 15% lower than that obtained from the IPZ analysis.

The results presented herein show how the polarization data can be analyzed for the kinetic parameters (rate constants) and the hydrogen surface coverage of the HER on metals, when the hydrogen absorption rate is negligible with respect to the cathodic hydrogen evolution current density, i_c. Analysis of the results on copper gives a value for the exchange current density of the HER which is similar to those reported in the literature.[22,37,38] It was shown that the hydrogen surface coverage changes with the potential in a trend that is well documented in the literature. Applying the above analysis to the polarization data for iron gives values of the exchange current density, rate constants, and values for the hydrogen surface coverage which are comparable to those obtained by applying the IPZ analysis to hydrogen permeation data.

Table I. Comparison of the exchange current density, discharge and recombination rate constants, and the transfer coefficient for iron in 0.1 N H_2SO_4 + 0.9 N Na_2SO_4 obtained from the IPZ analysis [35,36] and the above polarization data analysis. The same quantities were also obtained for copper using the polarization data analysis.

Analysis	i_o (A cm^{-2})		k_2 (mol cm^{-2} s^{-1})		k_i (cm s^{-1})		α	
	Fe	Cu	Fe	Cu	Fe	Cu	Fe	Cu
IPZ	2.0×10^{-6}	—	2.6×10^{-8}	—	1.3×10^{-6}	—	0.5	—
Polarization data	2.0×10^{-6}	8.0×10^{-8}	3.0×10^{-8}	1.8×10^{-7}	1.3×10^{-6}	5.0×10^{-8}	0.5	0.5

S0013-4651(99)10-058-2 CCC: $7.00 © The Electrochemical Society, Inc.

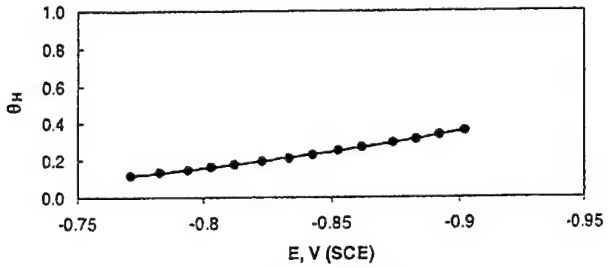

Figure 3. The relation between the hydrogen surface coverage and the electrode potential obtained on copper in 0.1 N H_2SO_4 + 0.9 N Na_2SO_4.

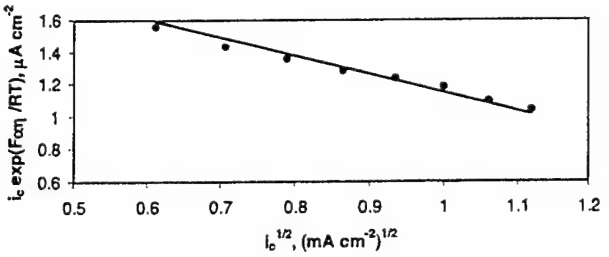

Figure 4. The relation between the charging function and the square root of the cathodic current obtained on iron in 0.1 N H_2SO_4 + 0.9 N Na_2SO_4.

The above described analysis of polarization data is clearly less applicable in cases where hydrogen absorption and permeation are significant with respect to i_c, *e.g.*, in the case of Pd which has a very high permeability for hydrogen, and iron in poisoned solutions where the presence of the poison significantly increases the rate of hydrogen absorption. The above analysis of polarization data invovles a limiting case of the IPZ analysis,[20,21] where i_∞ is very small compared to i_c. A comparison between the results obtained on iron using the IPZ analysis and the above polarization data analysis shows that both analyses give the same order-of-magnitude values of the kinetic parameters (exchange current density and recombination rate constant) and of the hydrogen surface coverage. Being less than the complete IPZ analysis, the above polarization data analysis cannot predict the rate constants of the hydrogen absorption and desorption reactions.

Acknowledgment

The authors acknowledge financial support of this work by the U.S. Steel Corporation, the Office of Naval Research (grant no. N00014-96-1-0913), and the Division of the International Program of the National Science Foundation (grant INT-9724698).

The Pennsylvania State University assisted in meeting the publication costs of this article.

List of Symbols

C_{H^+}	hydrogen ion concentration, mol cm^{-3}
F	Faraday's constant, C mol^{-1}
i'_o	$= Fk_1C_{H^+} = i_o/(1 - \theta^e_H)$, A cm^{-2}
i_o	exchange current density, A cm^{-2}
i_r	steady-state recombination current density, A cm^{-2}
i_p	steady-state hydrogen permeation current density, A cm^{-2}
k_1	discharge rate constant, cm s^{-1}
k_2	recombination rate constant, mol cm^{-2} s^{-1}
R	the general gas constant, 8.314 J mol^{-1} K^{-1}
T	absolute temperature, K

Greek

α	transfer coefficient, dimensionless
η	cathodic overvoltage, V
θ^e_H	hydrogen surface coverage at equilibrium, dimensionless
θ_H	hydrogen surface coverage, dimensionless

References

1. J. O'M. Bockris, *Chem. Rev.*, **43**, 525 (1948).
2. T. N. Veziroglu, H. J. Plass, and F. Barbir, in *Electrochemistry in Transition*, O. J. Murphy, S. Srinivasan, and B. E. Conway, Editors, p. 325, Plenum Press, New York (1992).
3. B. G. Pound, in *Modern Aspects of Electrochemistry*, J. O.'M. Bockris, B. E. Conway, and R. E. White, Editors, Vol. 25, p. 63, Plenum Press, New York (1993).
4. G. Jerkiewicz, *Prog. Surf. Sci.*, **57**, 137 (1998).
5. A. Lasia, *Pol. J. Chem.*, **69**, 639 (1995).
6. J. O'M. Bockris, *Inter. J. Hydrogen Energy*, **24**, 1 (1999).
7. K. J. Vetter, *Electrochemical Kinetics*, p. 525-535, Academic Press, New York (1967).
8. B. K. Subramanyan, in *Comprehensive Treatise of Electrochemistry*, J. O'M. Bockris, B. E. Conway, E. Yeager, and R. E. White, Editors, Vol. 4, p. 411, Plenum Press, New York (1981).
9. S. Trasatti, in *Advances in Electrochemical Science and Engineering*, H. Gerischer and C. W. Tobias, Editors, Vol. 2, p. 1, VCH, New York (1992).
10. R. L. Augustine, in *Catalytic Hydrogenation*, p. 26, Marcel Decker, Inc., New York (1985).
11. *Electrocatalysis*, J. Lipkowski and P. N. Ross, Editors, Wiley-VCH, New York (1998).
12. C. A. McAuliffe, *Hydrogen and Energy*, Gulf Pub., Houston, TX (1980).
13. D. Talbot and J. Talbot, in *Corrosion Science and Technology*, CRC Press, Houston, TX (1998).
14. T. Mizuno and M. Enyo, in *Modern Aspects of Electrochemistry*, R. E. White, B. E. Conway, and J. O'M. Bockris, Editors, Vol. 30, p. 451, Plenum Press, New York (1996).
15. M. A. Fullenweider, in *Hydrogen Entry and Action in Metals*, Pergamon Press, New York (1983).
16. G. B. Nielsen, J. E. T. Andersen, and J. C. Reeve, in *Modern Aspects of Electrochemistry*, R. E. White, B. E. Conway, and J. O'M. Bockris, Editors, Vol. 31, p. 251, Plenum Press, New York (1997).
17. J. W. Dini, in *Electrodeposition, The Materials Science of Coatings and Substrates*, Noyes Publications, Park Ridge, NJ (1993).
18. H. Flitt and J. O'M. Bockris, *Int. J. Hydrogen Energy*, **7**, 51 (1982).
19. J. O'M. Bockris, J. L. Carbajal, B. R. Scharifker, and K. Chandrasekaran, *J. Electrochem. Soc.*, **134**, 1957 (1987).
20. R. N. Iyer, H. W. Pickering, and M. Zamanzadeh, *J. Electrochem. Soc.*, **136**, 2463 (1989).
21. R. N. Iyer and H. W. Pickering, *Annu. Rev. Mater. Sci.*, **20**, 299 (1990).
22. N. Pentland, J. O'M. Bockris, and E. Sheldon, *J. Electrochem. Soc.*, **104**, 182 (1957).
23. J. O'M. Bockris and N. Pentland, *Trans. Faraday Soc.*, **48**, 833 (1952).
24. S. Y. Lanina and Z. A. Iofa, *Sov. Electrochem.*, **5**, 327 (1969).
25. D. Altura and K. Nobe, *Corrosion*, **28**, 345 (1972).
26. M. A. Devanathan, J. O'M. Bockris, and W. Mehl, *J. Electroanal. Chem.*, **1**, 143 (1959).
27. C. D. Kim and B. E. Wilde, *J. Electrochem. Soc.*, **118**, 202 (1971).
28. R. N. Iyer, I. Takauchi, M. Zamanzadeh, and H. W. Pickering, *Corrosion*, **46**, 360 (1990).
29. J. L. Carbajal and R. E. White, in *Electrochemistry in Transition*, O. J. Murphy, S. Srinivasan, and B. E. Conway, Editors, p. 339, Plenum Press, New York (1992).
30. D. H. Coleman, G. Zheng, B. N. Popov, and R. E. White, *J. Electrochem. Soc.*, **143**, 1871 (1995).
31. B. E. Conway, J. H. Barber, L. Gao, and S. Y. Qian, *J. Alloys Compd.*, **253**, 475 (1997).
32. H. A. Durtee, D. M. See, B. N. Popov, and R. E. White, *J. Electrochem. Soc.*, **144**, 2313 (1997).
33. S. Y. Qian, B. E. Conway, and G. Jerkiewicz, *J. Chem. Soc., Faraday Trans.*, **94**, 2945 (1998).
34. M. Ramasubramanian, B. N. Popov, and R. E. White, *J. Electrochem. Soc.*, **145**, 1907 (1998).
35. M. H. Abd Elhamid, B. G. Ateya, and H. W. Pickering, *J. Electrochem. Soc.*, **147**, 2258 (2000).
36. M. H. Abd Elhamid, B. G. Ateya, and H. W. Pickering, *J. Electrochem. Soc.*, To be published.
37. A. J. Appleby, in *Encyclopedia of Electrochemistry of the Elements*, A. J. Bard, Editor, Vol. 4, p. 383, Marcel Decker, New York (1975).
38. A. T. Kuhn and C. J. Mortimer, *J. Electroanal. Chem.*, **34**, 1 (1972).

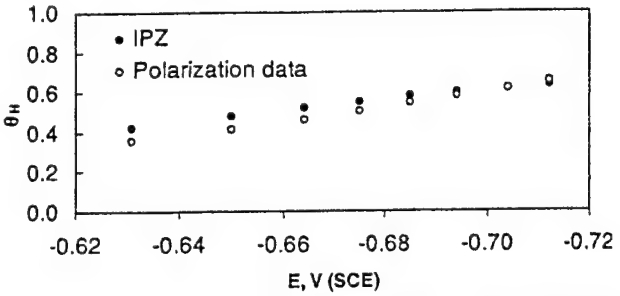

Figure 5. The relation between the hydrogen surface coverage and the electrode potential obtained on iron in 0.1 N H_2SO_4 + 0.9 N Na_2SO_4 using the IPZ analysis and the analysis developled in this paper which uses polarization data.

Journal of The Electrochemical Society, **147** (8) 2959-2963 (2000)
S0013-4651(99)09-067-9 CCC: $7.00 © The Electrochemical Society, Inc.

Determination of the Rate Constants of Hydrogen Absorption into Metals

M. H. Abd Elhamid,*,[a] B. G. Ateya,,[b] and H. W. Pickering***,[z]**

Department of Materials Science and Engineering, The Pennsylvania State University, University Park, Pennsylvania 16802, USA

Hydrogen absorption into iron (steel) membranes was studied using an electrochemical hydrogen permeation technique. The Iyer, Pickering, and Zamanzaden analysis of the measured steady-state hydrogen permeation rates, obtained for different membrane thicknesses, gives the rate constants of hydrogen absorption, k_{abs}, and desorption, k_{des}, in addition to those quantities which can be obtained from data for a single membrane thickness: *i.e.*, the hydrogen surface coverage, θ_H, exchange current density, i_o, rate constants, k_1 and k_2, of the hydrogen evolution reaction, and the important composite quantity called the kinetic-diffusion constant, $k = k_{abs}/(1 + k_{des}\,L/D)$, where L is the membrane thickness and D is the diffusivity of hydrogen within the metal. The product of k and θ_H determines the steady-state permeability of hydrogen within the metal. For large D and/or small L, $k = k_{abs}$, and the hydrogen permeation process is under surface control. From the analysis, we obtained $k_{abs} = 2 \times 10^{-10}$ mol cm^{-2} s^{-1} and $k_{des} = 1.9 \times 10^{-3}$ cm s^{-1} for iron in acidic sulfate solution.

Manuscript submitted September 20, 1999; revised manuscript received May 1, 2000.

The absorption of electrolytic hydrogen into metals is the first and necessary step in the hydrogen embrittlement of metals.[1-12] It is equally important in the permeation and storage of hydrogen within metals.[13-19] The process of hydrogen absorption has long been studied using an electrochemical permeation cell.[20,21] In this technique, the hydrogen evolution reaction (HER) occurs on one side (charging side) of a thin metal membrane (see Fig. 1)

$$H^+ + e^- + M \xrightarrow{k_1} M\text{-}H_{ads} \qquad [1]$$

where $M\text{-}H_{ads}$ refers to an adsorbed hydrogen atom on the metal surface and k_1 is the rate constant of the discharge step of the HER. This adsorbed hydrogen atom combines with another adsorbed hydrogen atom to form a hydrogen molecule, *i.e.*

$$M\text{-}H_{ads} + M\text{-}H_{ads} \xrightarrow{k_2} 2M + H_2(g) \qquad [2]$$

where k_2 is the rate constant of the recombination step of the HER.

This adsorbed hydrogen on the charging surface of the membrane is also involved in the hydrogen absorption reaction (HAR) by which the adsorbed hydrogen is absorbed in the metal lattice beneath the surface, *i.e.*

$$M\text{-}H_{ads} \underset{k_{des}}{\overset{k_{abs}}{\rightleftharpoons}} H_{abs} + M \qquad [3]$$

where H_{abs} refers to the absorbed hydrogen atom within the metal lattice and k_{abs} and k_{des} refer to the rate constants of the forward and backward directions of Reaction 3, respectively (see Fig. 1). This absorbed hydrogen diffuses (permeates) within the metal lattice and is oxidized at the other (exit) side of the membrane, under the effect of an anodic potential.

The steady-state anodic current at the exit surface of the membrane is a measure of the steady-state permeation rate of hydrogen through the membrane, *i.e.*

$$i_\infty = \frac{FDC^o}{L} \qquad [4]$$

where D is the diffusion coefficient of atomic hydrogen within the metal, C^o is the concentration of the absorbed hydrogen just beneath the metal surface on the charging side where the HER takes place, and L is the thickness of the membrane. Equation 4 holds for hydrogen permeation when trapping effects are insignificant,[22] as in the case of the carefully annealed iron (steel) used here. Much work has been published on hydrogen permeation using this technique.[23-33] Analysis of the results in most of these works[8,10,24,26-33] considered the diffusion of hydrogen within the metal membrane to be the slow step and the surface reaction (Reaction 3) to be in quasi equilibrium. Within this framework, the individual rate constants of the forward and backward directions of Reaction 3 could not be evaluated. Some workers[4,23,25,30] were able to take into account the surface reaction at the entry side of the membrane (see Fig. 1) to evaluate the desorption rate constant (the reverse direction of Reaction 3). However, evaluation of the absorption rate constant (the forward direction of Reaction 3) was not possible without the use of independent methods to evaluate the hydrogen surface coverage.[23,30] Within the framework of the Iyer, Pickering, and Zamanzaden (IPZ) analysis,[28,29] which does not require that Reaction 3 be in quasi equilibri-

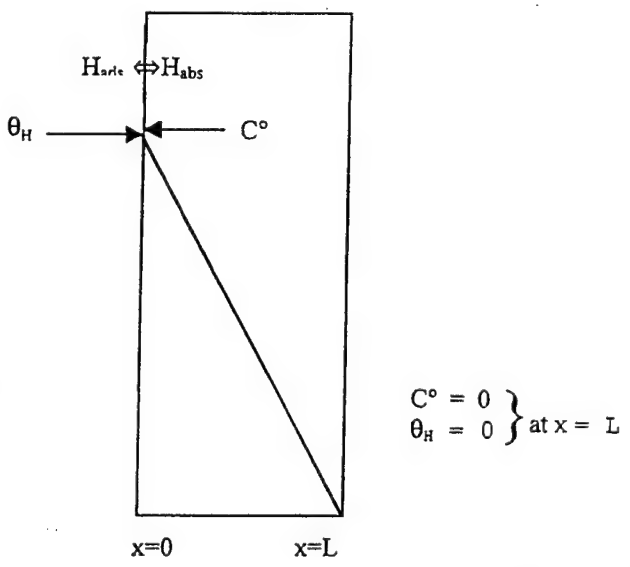

Figure 1. A schematic illustration showing the conditions on the hydrogen entry (charging) and exit sides of the iron (steel) membrane.

* Electrochemical Society Student Member.
** Electrochemical Society Active Member.
*** Electrochemical Society Fellow.
[a] Present address: General Motors, Global Alternative Propulsion Center, Warren, MI 48090, USA.
[b] Present address: Department of Chemistry, Faculty of Science, Cairo University, Egypt.
[z] E-mail: pick@ems.psu.edu

Journal of The Electrochemical Society, **147** (8) 2959-2963 (2000)
S0013-4651(99)09-067-9 CCC: $7.00 © The Electrochemical Society, Inc.

um, the fractional degree of coverage as well as both the absorption and desorption rate constants can now be determined.

This paper presents the first results of experimental measurements of the rate constants of the absorption and desorption steps of hydrogen evolution, using the IPZ analysis, on iron membranes of different thicknesses in a buffered acid medium. The analysis of the experimental results also yields the degree of hydrogen surface coverage, the concentration of hydrogen in the membrane at the input surface, and the extent of surface control during the absorption-permeation process. We also revise one of the important equations of the IPZ analysis and the conclusions thereof.

Theory

According to Reaction 1, the rate (current density) of the HER for Tafel behavior is given by

$$i_c = Fk_1C_{H^+}(1 - \theta_H)\exp\left(-\frac{F}{RT}\alpha\eta\right) \quad [5]$$

where k_1 is the rate constant for proton discharge, C_{H^+} is the hydrogen ion concentration, θ_H is the fractional hydrogen surface coverage, α is the transfer coefficient of the HER, which can be readily calculated from the measured Tafel slope, η is the hydrogen overpotential, and F, R, and T have their usual meanings. Equation 5 can be rearranged to give[28,29]

$$i_c \exp\left(\frac{F}{RT}\alpha\eta\right) = i_o'(1 - \theta_H) \quad [6]$$

where $i_o' = Fk_1C_{H^+} = i_o/(1 - \theta_H^e)$, i_o is the exchange current density of the HER, and θ_H^e is the equilibrium coverage. The left side of Eq. 6 is referred to as the charging function, which previously appeared as a key function in the IPZ analyses of the rate constants of the HER and HAR for iron and other metals which readily absorb hydrogen.[28,29]

The rate of the recombination reaction, Reaction 2, is given by

$$i_r = Fk_2\theta_H^2 \quad [7]$$

The adsorbed hydrogen resulting from Reaction 1 is distributed between Reactions 2 and 3. Hence, at steady state

$$i_c = i_r + i_\infty \quad [8]$$

A mass balance on the charging side of the membrane reveals that[3,4,21,28-30]

$$i_\infty = Fk_{abs}\theta_H - Fk_{des}C^o \quad [9]$$

Combining and rearranging Eq. 4 and 9 gives[3,4,21,30]

$$i_\infty = F\left(\frac{k_{abs}}{1 + k_{des}\dfrac{L}{D}}\right)\theta_H \quad [10]$$

To sum up the kinetics and transport properties of the system in one constant, Eq. 10 is expressed as

$$i_\infty = Fk\theta_H \quad [11]$$

where k is a kinetic-diffusion constant

$$k = \frac{k_{abs}}{1 + k_{des}\dfrac{L}{D}} \quad [12]$$

Equation 12 reveals that k (and hence i_∞, see Eq. 10) increases as L decreases and/or D increases. This equation conveys the correct physical picture of the dependence of k (and hence i_∞) on both D and L, and is a modification pointed out by Ramasubramanian *et al.*[34] of the quantity (k'') given in the original IPZ analysis, where $k'' = kL/D$.[28,29] The constant k is important in that it combines the kinetics of hydrogen absorption and desorption at the charging side of the membrane surface and the transport properties within the membrane and hence is called the kinetic-diffusion constant. Previously, we have called k'' the thickness-dependent absorption-desorption constant, but in addition to its cumbersome length, this definition ignores the dependence of k on D which is just as important as that on L. Henceforth, k is referred to as the kinetic-diffusion constant.

At the limit of large D and small L, such that $1 >> k_{des}L/D$, $k = k_{abs}$, and hence using Eq. 11, one obtains

$$i_\infty = Fk_{abs}\theta_H \quad [13]$$

This indicates that the rate of hydrogen permeation is controlled by the surface step.[4] However, at the limit of large L and/or small D, Eq. 12 gives $k = Dk_{abs}/k_{des}L$, which when substituted in Eq. 11, yields

$$i_\infty = \frac{FD}{L}\frac{k_{abs}}{k_{des}}\theta_H \quad [14]$$

Under this condition, the absorption-permeation process approaches pure diffusion control, in which case C^o is independent of L, which is a limiting case of Eq. 4 when Eq. 3 is in quasi equilibrium.

The reciprocal of k (Eq. 12) is given by

$$\frac{1}{k} = \frac{1}{k_{abs}} + \frac{k_{des}}{k_{abs}}\frac{L}{D} \quad [15]$$

which is a corrected version of that given previously.[28,29] On the right side of Eq. 15, the contribution of the first term to the sum of the two terms is a measure of the amount of surface control during the absorption-permeation process. Once k is known (see below), one can plot $1/k$ *vs.* the membrane thickness, L, to obtain a straight line with a slope of k_{des}/Dk_{abs} and an intercept of $1/k_{abs}$. The slope and intercept can be solved for k_{abs} and k_{des}.[28,29] Combining Eq. 7 and 11 gives[28,29]

$$i_\infty = k\sqrt{\frac{F}{k_2}}\sqrt{i_r} \quad [16]$$

This relation has been experimentally observed by Dafft *et al.*[35] and others in various systems. Equation 16 predicts a straight-line relation between i_∞ and $\sqrt{i_r}$ passing by the point of origin with a slope of $k\sqrt{F/k_2}$. The slope can be used to obtain k_2 once k is known.

Combining Eq. 6 and 11 gives a relation between the charging function and the steady-state hydrogen permeation current density[28,29]

$$i_c \exp\left(\frac{F}{RT}\alpha\eta\right) = i_o - \frac{i_o}{Fk}i_\infty \quad [17]$$

Equation 17 relates the charging function, $i_c \exp(\alpha\eta F/RT)$, which is solely determined by the conditions at the charging surface of the membrane to i_∞, which is determined by the transport of hydrogen through the membrane. It predicts a straight-line relation between the charging function and i_∞; from the slope and intercept, one can calculate i_o, k_1 ($= i_o/FC_{H^+}$), and k. Then, k can be used in Eq. 11 to obtain the hydrogen surface coverage, θ_H, as well as k_2 (Eq. 16). The values of k for the different membrane thicknesses can be used to yield k_{abs} and k_{des} as described above (Eq. 15).

Substituting for i_∞ from Eq. 4 in Eq. 9 and rearranging, one obtains[4,28]

$$C^o = k\theta_H L/D \quad [18]$$

Equation 18 provides for the calculation of the hydrogen concentration in the membrane at the input surface once k and θ_H are known, and is an alternative to calculating C^o from Eq. 4 using the measured i_∞ value.

Experimental

The electrochemical hydrogen permeation cell was similar to that used by Frumkin[20] and by Devanathan and Stachurski.[21] The cell was used to collect data on both the HER and HAR on iron membranes of different membrane thicknesses. This thickness range for

the permeation measurements avoided excessive surface control and short-circuit, *e.g.*, grain boundary, permeation of hydrogen while permitting the attainment of measurable steady-state permeation rates which were achieved in less than 10 min for all runs.[28,29] The iron (steel) membranes with thicknesses of 0.10, 0.25, 0.50, and 0.85 mm were obtained from Goodfellow with the following composition: Mn, 0.3%; Si, 0.1%; C, <0.08%; S <0.05%; the balance was iron. They were polished down to 0.5 μm alumina and then degreased in acetone and washed with double-distilled water. They were subsequently annealed in pure hydrogen at 900°C for 2 h in a tube furnace and furnace-cooled in the same atmosphere. The exit surface of the iron membrane was coated with electrolessly deposited palladium using Pallamerse solution before the membrane was mounted in the cell. The electrolyte in the charging (input) compartment of the cell was an acidic solution of 0.1 N H_2SO_4 + 0.9 N Na_2SO_4 of pH 1.8. It was prepared from analytical grade chemicals and double-distilled water. Before admitting the solution to the cell, it was pre-electrolyzed at 3 mA for 2 h to remove impurities that could otherwise affect the quality of the data. The solution was subsequently deaerated with hydrogen. The exit compartment of the cell contained 0.1 N NaOH, and the potential of the Pd-coated exit surface of the iron membrane was set at 0.150 mV(Hg/HgO) using a potentiostat to ensure complete oxidation of the dissolved hydrogen diffusing through the membrane.

To minimize the production of hydrogen traps in the membrane during the measurements, the cathodic current, i_c, at the charging surface was set at its highest value and then decreased stepwise after reaching within minutes the steady-state permeation current at each value of i_c. Similarly, for the polarization curve measurements in the same charging compartment of the cell, the cathodic current, i_c, was decreased stepwise after reaching in seconds the stationary electrode potential of the charging surface at each value of i_c. Further details on the experimental setup are reported elsewhere.[28,29,31,33]

Results and Discussion

The current-potential relations measured on the charging side of each membrane gave a Tafel line with a slope of 120 mV, independent of the membrane thickness. This corresponds to a value of $\alpha = 0.5$. Figure 2 shows plots of i_∞ *vs.* $\sqrt{i_r}$ for membranes of different thicknesses. These data plot well as straight lines passing through the point of origin, in accordance with Eq. 16, indicating that the mechanism of the HER is coupled Volmer discharge-Tafel recombination. The slopes of the lines in Fig. 2 decrease with increasing membrane thickness, as predicted by Eq. 12 and 16.

Figure 3 shows the straight-line relations obtained between the charging function, $i_c \exp(\alpha\eta F/RT)$, and the steady-state hydrogen permeation current density, i_∞, for different membrane thicknesses. Table I lists the values of i_o estimated from the intercept of these plots in accordance with Eq. 17, the slopes of the lines in Fig. 3, and the kinetic-diffusion constant, k, obtained from these slopes (Eq. 17) on iron membranes of different thicknesses in 0.1 N H_2SO_4 + 0.9 N Na_2SO_4. Table I shows that as the membrane thickness increases, the value of the kinetic-diffusion constant, k, decreases. It further shows

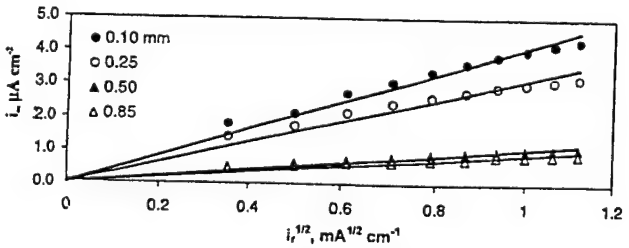

Figure 2. The relation between the steady-state hydrogen permeation current density, i_∞, and square root of the recombination current density, $\sqrt{i_r}$, obtained on iron membranes of different thicknesses in 0.1 N H_2SO_4 + 0.9 N Na_2SO_4 (pH 1.8).

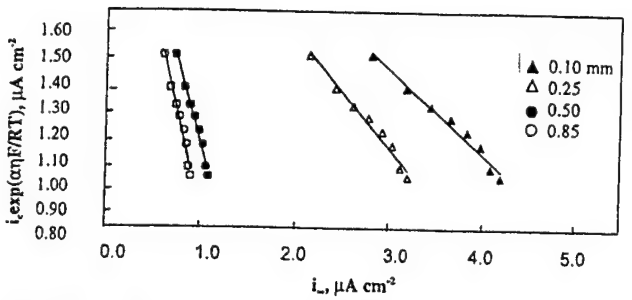

Figure 3. The relation between the charging function, $i_c \exp(\alpha\eta F/RT)$, and the steady-state hydrogen permeation current density, i_∞, for iron membranes of different thickness in 0.1 N H_2SO_4 + 0.9 N Na_2SO_4.

that the exchange current density does not change with the membrane thickness.

The reciprocal of the values of the kinetic-diffusion constant, k, was plotted in Fig. 4 *vs.* the membrane thickness, L, to evaluate k_{abs} and k_{des}, according to Eq. 15. Figure 4 shows a straight-line relation with a positive slope and positive intercept with the y axis, in accordance with Eq. 15 and the IPZ analysis. The diffusivity of hydrogen within the membranes was obtained using the breakthrough time.[21] A value of $D = 1.2 \pm 0.02 \times 10^{-5}$ cm^2 s^{-1} was found for all thicknesses. This value compares well with reported values for the diffusivity of hydrogen in iron.[2,3] It also reveals that the diffusivity was not a function of the membrane thickness.[22]

From the slope and intercept of Fig. 4, we calculated values of $k_{abs} = 2.0 \times 10^{-10}$ mol cm^{-2} s^{-1} and $k_{des} = 1.9 \times 10^{-3}$ cm s^{-1}. This value of k_{des} can be compared to the values of 1-3 $\times 10^{-2}$ cm s^{-1} measured in solutions of pH 13 on high purity iron samples ranging from 50 to 900 μm thick,[25] 10^{-2} cm s^{-1} measured in H_2SO_4 on Armco iron ranging in thickness from 0.026 to 0.129 cm,[23] and 10^{-3} cm s^{-1} measured on commercially pure iron (99.7%) in 0.2 N NaOH.[36] The value of $k_{abs} = 2.0 \times 10^{-10}$ mol cm^{-2} s^{-1} can be compared to the values reported recently by Zhang *et al.*,[36] in the form of the product θk_{abs} ranging from 10^{-11} to 10^{-13} mol cm^{-2} s^{-1}. There are also the values reported by Kim and Wilde[30] and Subramanyan.[6] Both of these works used absolute values of coverage and hence obtained k_{abs} in units of s^{-1}, namely, 3-5 and 1.5 s^{-1}, respectively. To convert these values of k_{abs} from units of s^{-1} into units of mol cm^{-2} s^{-1}, one must multiply them by the monolayer capacity of hydrogen adsorbed on iron. A value of 2×10^{-9} mol cm^{-2} was used by Kim and Wilde,[30] which is essentially an arbitrary value. Using this value, their rate constants of 3-5 and 1.5 s^{-1} give values of 6-10 $\times 10^{-9}$ and 3×10^{-9} mol cm^{-2} s^{-1}. Using $k_{abs} = 2 \times 10^{-10}$ mol cm^{-2} s^{-1} and $k_{des} = 1.9 \times 10^{-3}$ cm s^{-1}, the contribution of surface control can be estimated from Eq. 15. The magnitudes of the first term are approximately 7 and 38% of the sum of both terms on the right side of Eq. 15 for the 0.85 and 0.10 mm membranes, respectively (Table I).

The hydrogen surface coverage, θ_H, was calculated from Eq. 11 using the k values obtained for the membranes of different thicknesses. Figure 5 shows that the magnitude of θ_H increases with more

Table I. Values of i_o, $-i_o'/Fk$, and k (Eq. 17) and the % surface control for iron membranes of different thicknesses in 0.1 N H_2SO_4 + 0.9 N Na_2SO_4 (pH 1.8).

L (mm)	i_o (A cm^{-2})	$-\frac{i_o'}{Fk}$	k (mol cm^{-2} s^{-1})	% surface control
0.10	2.0×10^{-6}	0.32	6.6×10^{-11}	38
0.25	2.0×10^{-6}	0.40	5.4×10^{-11}	20
0.50	2.0×10^{-6}	1.20	2.1×10^{-11}	10
0.85	2.0×10^{-6}	1.45	1.4×10^{-11}	7

S0013-4651(99)09-067-9 CCC: $7.00 © The Electrochemical Society, Inc.

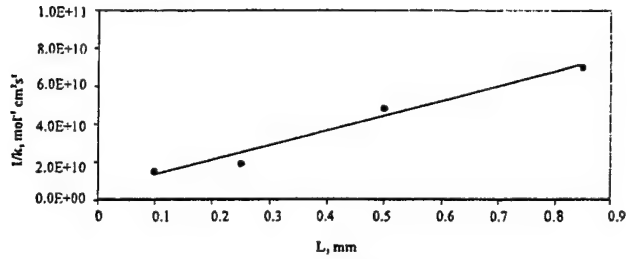

Figure 4. The relation between the reciprocal of the kinetic-diffusion constant, k, and the membrane thicknesses, L, for iron in 0.1 N H_2SO_4 + 0.9 N Na_2SO_4.

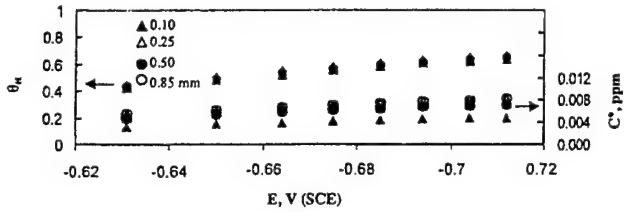

Figure 5. The relation between the hydrogen surface coverage, θ_H, and the electrode potential, E, obtained on iron membranes of different thicknesses in 0.1 N H_2SO_4 + 0.9 N Na_2SO_4, and the corresponding hydrogen concentration, C^o, in the iron membrane at the input surface.

negative E values, in accordance with its expected dependence on the overpotential η.[8,30] This trend is well documented in the literature.[37-45] It follows that θ_H is also independent of the membrane thickness, as indicated by the data in Fig. 5. These values of θ_H were obtained from the model assuming the Langmuir adsorption isotherm. Others have obtained similar values for θ_H on iron and steels also using the Langmuir adsorption isotherm.[40,46] Support for the use of the Langmuir adsorption isotherm also comes from the results using the Frumkin isotherm, which show that the interaction parameter is negligible (of the order of 0.2).[47] From the values of the hydrogen surface coverage, the hydrogen concentration in the iron at the input surface, C^o, can be obtained from Eq. 18. These values are also shown in Fig. 5 and are of the same order of magnitude as C^o values obtained from the diffusion law, Eq. 4 (using the data in Table II and the measured D values).

Conclusions

Applying the IPZ analysis to the measured steady-state hydrogen permeation data for different values of charging current and membrane thickness, the specific rate constants of hydrogen absorption and desorption were obtained for iron in an acid sulfate solution. The analysis utilized a corrected Eq. 15 from that given in the original work.[28,29] Using these results, the amount of surface control during the hydrogen absorption-permeation process could be evaluated for each membrane thickness. The analysis yielded also, as previously obtained for a single membrane thickness, the degree of hydrogen surface coverage, θ_H, exchange current density, i_o, and the rate constants of the HER. It also yielded the important kinetic-diffusion constant k derived previously[34] which is proportional to the k' constant ($k = k'D/L$) presented previously,[28,29] which combines the rate constants of absorption and desorption at the charging surface and the transport properties of the membrane. For the iron/acidic sulfate system, the IPZ analysis gives $k_{abs} = 2 \times 10^{-10}$ mol cm^{-2} s^{-1} and $k_{des} = 1.9 \times 10^{-3}$ cm s^{-1}, in fair agreement with the few values obtained by other methods in the literature. The hydrogen surface coverage was a function of the applied cathodic potential in accordance with the literature, but not of the sample thickness (Fig. 5).

Acknowledgment

Professor Konrad G. Weil and Dr. Rajan N. Iyer provided helpful comments. The authors acknowledge financial support of this work by the U.S. Steel Corporation, the Office of Naval Research (grant no. N00014-96-1-0913), and the Division of the International Programs of the NSF (grant INT-9724698).

List of Symbols

C_{H+}	hydrogen ion concentration, mol cm^{-3}
C^o	concentration of absorbed hydrogen at the input surface, mol cm^{-3}
D	hydrogen diffusion coefficient, cm^2 s^{-1}
F	Faraday's constant, C mol^{-1}
i'_o	$Fk_1C_{H+} = i_o/(1 - \theta_H^e)$, A cm^{-2}
i_o	exchange current density, A cm^{-2}
i_r	steady-state recombination current density, A cm^{-2}
i_∞	steady-state hydrogen permeation current density, A cm^{-2}
k_1	discharge rate constant, cm s^{-1}
k_2	recombination rate constant, mol cm^{-2} s^{-1}
k_{abs}	absorption rate constant, mol cm^{-2} s^{-1}
k_{des}	desorption rate constant, cm s^{-1}
k	kinetic-diffusion constant, mol cm^{-2} s^{-1}
R	gas constant, 8.314 J mol^{-1} K^{-1}
T	absolute temperature, K

Greek

α	transfer coefficient, dimensionless
η	cathodic overvoltage, V
θ_H^e	hydrogen surface coverage at equilibrium, dimensionless
θ_H	hydrogen surface coverage, dimensionless

References

1. T. Mizuno and M. Enyo, in *Modern Aspects of Electrochemistry*, R. E. White, B. E. Conway, and J. O'M. Bockris, Editors, Vol. 30, p. 415, Plenum Press, New York (1996).
2. B. G. Pound, in *Modern Aspects of Electrochemistry*, J. O'M. Bockris, B. E. Conway, and R. E. White, Editors, Vol. 25, p. 63, Plenum, New York (1993).
3. L. Nanis, in *Environment-Sensitive Fracture Engineering Materials*, Z. A. Foroulis, Editor, p. 361, The Metallurgical Society of AIME, Warrendale, PA (1983).
4. B. G. Atcya and H. E. Abd Elal, in *Corrosion-Industrial Problems, Treatment and Control Techniques*, Proceedings of the 1st Arabian Conference on Corrosion '84, Kuwait Foundation for the Advancement of Science, p. 201 (1987).
5. T. Zakroczymski, in *Symposium on Hydrogen Degradation of Ferrous Alloys*, R. Oriani, J. P. Hirth, and M. Smialowski, Editors, p. 239, Noyes Publications, Park Ridge, NJ (1985).

Table II. Values of the steady state hydrogen permeation current density obtained on iron membranes of different thickness in 0.1 N H_2SO_4 + 0.9 N Na_2SO_4 and at different values of the cathodic charging current density.

	i_∞ (μA cm^{-2})			
i_c (mA cm^{-2})	L = 0.10 mm	L = 0.25 mm	L = 0.50 mm	L = 0.85 mm
0.61	2.74	2.14	0.71	0.61
0.71	3.08	2.42	0.81	0.66
0.79	3.39	2.62	0.89	0.73
0.87	3.64	2.77	0.95	0.76
0.93	3.85	2.92	0.99	0.83
1.00	4.04	3.03	1.04	0.85
1.06	4.19	3.12	1.07	0.88
1.12	4.32	3.2	1.09	0.89

S0013-4651(99)09-067-9 CCC: $7.00

6. B. K. Subramanyan, in *Comprehensive Treatise of Electrochemistry*, J. O'M. Bockris, B. E. Conway, and R. E. White, Editors, Vol. 4, p. 411, Plenum Press, New York (1981).
7. M. Smialowski, in *Hydrogen in Steels*, Pergamon Press, New York (1962).
8. J. McBreen and M. A. Genshaw, in *Proceedings of the Conference on Fundamental Aspects of Stress Corrosion Cracking*, p. 51, NACE, Columbus (1961).
9. H. K. Birnbaum, in *Atomistics of Fracture*, R. M. Latanision and R. M. Pickens, Editors, Plenum Press, New York (1981).
10. T. Zakroczymski, V. Kleshnya, and J. Flis, *J. Electrochem. Soc.*, **145**, 1142 (1998).
11. *Papers of the 2nd National Symposium on Test Methods for Hydrogen Embrittlement: Prevention and Control*, ASTM Technical Publication no. 962, L. Raymond, Editor, ASTM, Philadelphia, PA (1988).
12. M. A. Fullenwider, in *Hydrogen Entry and Action in Metals*, Pergamon Press, New York (1983).
13. T. Akiyama, H. Isogai, and J. Yagi, *J. Alloys Compd.*, **252**, L1 (1997).
14. R. Chahine and T. K. Bose, *Int. J. Hydrogen Energy*, **19**, 161 (1994).
15. B. A. Kolachev and A. A. Ilyin, *Int. J. Hydrogen Energy*, **21**, 975 (1996).
16. K. Dutta and O. N. Srivastava, *J. Mater. Sci.*, **28**, 3457 (1993).
17. T. Kohno, S. Tsuruta, and M. Kanda, *J. Electrochem. Soc.*, **143**, L198 (1996).
18. J. K. Gross, P. Spatz, A. Zuttel, and L. Schlapbach, *J. Alloys Compd.*, **240**, 206 (1996).
19. L. M. Das, *Int. J. Hydrogen Energy*, **219**, 789 (1996).
20. A. N. Frumkin and N. Aladyalova, *Acta Physicochim. (USSR)*, **19**, 1 (1944).
21. M. A. Devanathan and Z. Stachurski, *Proc. R. Soc. Chem.*, **A270**, 90 (1962).
22. L. S. Darken and R. P. Smith, *Corrosion*, **5**, 1 (1949).
23. M. A. Devanathan and Z. Stachurski, *J. Electrochem. Soc.*, **111**, 619 (1964).
24. J. O'M. Bockris, J. McBreen, and L. Nanis, *J. Electrochem. Soc.*, **112**, 1025 (1965).
25. E. A. Maleeva, K. S. Pedan, and V. N. Kudryavtsev, *Russ. J. Electrochem.*, **30**, 1228 (1994).
26. B. E. Wilde and C. D. Kim, *Corrosion*, **42**, 243 (1986).
27. R. F. Blundy and L. L. Shreir, *Corros. Sci.*, **17**, 509 (1977).
28. R. N. Iyer, H. W. Pickering, and M. Zamanzadeh, *J. Electrochem. Soc.*, **136**, 2463 (1989); R. N. Iyer and H. W. Pickering, *J. Electrochem. Soc.*, **137**, 3512 (1990).
29. R. N. Iyer and H. W. Pickering, *Annu. Rev. Mater. Sci.*, **20**, 299 (1990).
30. C. D. Kim and B. E. Wilde, *J. Electrochem. Soc.*, **118**, 202 (1971).
31. M. H. Abd Elhamid, B. G. Ateya, and H. W. Pickering, *J. Electrochem. Soc.*, **144**, L58 (1997).
32. S. S. Chatterjee, B. G. Ateya, and H. W. Pickering, *Metall. Trans. A*, **9A**, 398 (1978); M. Zamanzadeh, A. Allam, H. W. Pickering, and G. K. Hubler, *J. Electrochem. Soc.*, **127**, 1688 (1980); M. Zamanzadeh, A. Allam, C. Kato, B. G. Ateya, and H. W. Pickering, *J. Electrochem. Soc.*, **129**, 284 (1982).
33. M. H. Abd Elhamid, B. G. Ateya, and H. W. Pickering, *J. Electrochem. Soc.*, **147**, 2258 (2000).
34. M. Ramasubramanian, B. N. Popov, and R. E. White, *J. Electrochem. Soc.*, **145**, 1907 (1998).
35. E. G. Dafft, K. Bohnenkamp, and H. J. Engell, *Corros. Sci.*, **19**, 591 (1979).
36. T. Y. Zhang, Y. P. Zheng, and Q. Y. Wu, *J. Electrochem. Soc.*, **146**, 1741 (1999).
37. M. A. Devanathan, J. O'M. Bockris, and W. Mehl, *J. Electroanal. Chem.*, **1**, 143 (1959).
38. D. H. Coleman, G. Zheng, B. N. Popov, and R. E. White, *J. Electrochem. Soc.*, **143**, 1871 (1995).
39. I. Epelboin, P. Morel, and H. Takenouti, *J. Electrochem. Soc.*, **118**, 1282 (1971).
40. H. A. Durtee, D. M. See, B. N. Popov, and R. E. White, *J. Electrochem. Soc.*, **144**, 2313 (1997).
41. R. N. Iyer, I. Takauchi, M. Zamanzadeh, and H. W. Pickering, *Corrosion*, **46**, 360 (1990).
42. J. O'M. Bockris, J. L. Carbajal, B. R. Scharifker, and K. Chandrasekaran, *J. Electrochem. Soc.*, **134**, 1957 (1987).
43. H. J. Flitt and J. O'M. Bockris, *Int. J. Hydrogen Energy*, **7**, 411 (1982).
44. M. A. Devanathan and M. Selvaratnam, *Trans. Faraday Soc.*, **56**, 1820 (1960).
45. S. Y. Qian, B. E. Conway, and G. Jerkiewicz, *J. Chem. Soc., Faraday Trans.*, **94**, 2945 (1998).
46. D. Tromans, *Acta Metall. Mater.*, **42**, 2043 (1994).
47. F. Al-Faqeer and H. W. Pickering, In preparation.

Journal of The Electrochemical Society, 148 (6) E248-E251 (2001)
0013-4651/2001/148(6)/E248/4/$7.00 © The Electrochemical Society, Inc.

An Analysis Procedure for Hydrogen Absorption under Frumkin Adsorption Conditions

F. M. Al-Faqeer* and H. W. Pickering**,z

Department of Materials Science and Engineering, The Pennsylvania State University, University Park, Pennsylvania 16802, USA

This paper communicates a more general derivation of the Iyer-Pickering-Zamenzadeh (IPZ) analysis of hydrogen absorption. It is applicable to metal/electrolyte systems under Frumkin adsorption conditions for the discharge-recombination process of hydrogen evolution, as well as to Langmuir adsorption conditions covered by the original derivation. As such, it does not require prior knowledge of the dimensionless factor f that describes the deviation from ideal Langmuir behavior. This analysis appropriately reduces to the original IPZ analysis for Langmuir adsorption conditions for which $f = 0$. It yields the value of (f) as well as the other unknowns in the system: the discharge (k_1) and recombination (k_2) rate constants, the exchange current density (i_o), the kinetic-diffusion constant (k), the hydrogen surface coverage (θ_H), and the hydrogen concentration in the metal at the charging surface (C^o).

Manuscript submitted August 18, 2000; revised manuscript received February 12, 2001.

The Frumkin adsorption isotherm assumes that the free energy of adsorption of a species decreases with coverage according to the following equation[1-4]

$$\Delta G_\theta^\circ = \Delta G_0^\circ + fRT\theta \qquad [1]$$

where f is a dimensionless factor that describes the deviation from the ideal Langmuir behavior. The fRT quantity is sometimes called the rate of change of the standard free energy of adsorption, ΔG_θ° and ΔG_0° are the standard free energy of adsorption at a certain coverage, θ, and at zero coverage, $\theta = 0$, respectively, R is the gas constant, and T is the absolute temperature.

The Langmuir adsorption isotherm assumes the standard free energy of adsorption is independent of coverage ($f = 0$). This isotherm is usually applicable at low values of coverage ($\theta < 0.1$) and at coverages close to unity ($\theta > 0.9$).[3,4] In some instances it has been found to be applicable also for intermediate coverages of hydrogen on iron surfaces.[5,6]

The Iyer-Pickering-Zamanzadeh (IPZ) analysis[7-9] developed three major relationships between the hydrogen evolution reaction (HER) and the hydrogen adsorption reaction (HAR). The first one is between the steady-state hydrogen permeation current density, i_∞, and the hydrogen recombination current density, i_r. This relation is shown in Eq. 2. Another relationship is between the charging function, $i_c \exp(a\alpha\eta)$, and i_∞ which is shown in Eq. 3. The last one is between i_∞ and the hydrogen coverage, θ_H, shown in Eq. 4

$$i_\infty = k\sqrt{\frac{F}{k_2}} \cdot \sqrt{i_r} \qquad [2]$$

$$i_c \exp(a\alpha\eta) = i_o'\left(1 - \frac{1}{Fk} i_\infty\right) \qquad [3]$$

$$i_\infty = Fk\theta_H \qquad [4]$$

where i_c is the charging current density, $i_o' = Fk_1C_{H+} = i_o/(1 - \theta_H^e)$, i_o is the exchange current density of the HER and θ_H^e is the hydrogen surface coverage at equilibrium, C_H^+ is the hydrogen ion concentration in the electrolyte, $a = F/RT$ where F, R, and T have their usual meanings, α is the transfer coefficient, and η is the overpotential of the HER. k is the kinetic-diffusion constant and is defined as

$$k = \frac{k_{abs}}{1 + k_{des}\dfrac{L}{D}} \qquad [5]$$

where k_{abs} is the rate constant for hydrogen absorption into the metal at the charging surface, k_{des} is the desorption rate constant for the hydrogen moving in the opposite direction, *i.e.*, from the absorbed to adsorbed state, D is the hydrogen diffusion coefficient within the membrane, and L is the membrane thickness.

Equation 5 is a modified version of Eq. 4a in the original IPZ analysis[7] and was recently derived by Ramasubramanian *et al.*[10] More details about the IPZ analysis can be found elsewhere.[7-9] For the local equilibrium of the intermediate absorption-desorption reaction, the concentration of hydrogen inside the metal is obtained as[5]

$$C^o = k\theta_H L/D \qquad [6]$$

Experimental

The electrochemical hydrogen permeation cell was similar to that used by Devanathan and Stachurski.[11] The cell was used to collect data on the HER and HAR on iron membranes of thickness 0.25 mm in acidic solution of 1 M Na_2SO_4, acidified to pH 2 using H_2SO_4 (blank solution) and blank solution with a small addition of thiosulfate ($S_2O_3^{2-}$). Thiosulfate is known to be a promoter for hydrogen absorption by iron which does not satisfy the requirement of the original IPZ analysis.[12,13] The membrane was coated with palladium only on its exit side. Further details about the experimental setup can be found elsewhere.[5]

Analysis Development

Using the Volmer discharge-Tafel hydrogen adatom combination process of hydrogen evolution at appreciable overpotentials (so there is negligible hydrogen oxidation), which was the basis for the original IPZ analysis,[7-9] the HER proceeds as follows

$$H^+ + M + e^- \xrightarrow{k_1} M\text{-}H_{ads} \qquad [7]$$

$$M\text{-}H_{ads} + M\text{-}H_{ads} \xrightarrow{k_2} H_2 + 2M \qquad [8]$$

Some of the adsorbed hydrogen atoms, $M\text{-}H_{ads}$, will absorb into the iron, H_{abs}, and quickly establish the back equilibria

$$M\text{-}H_{ads} \underset{k_{des}}{\overset{k_{abs}}{\rightleftharpoons}} H_{abs} + M \qquad [9]$$

The absorbed hydrogen diffuses through the iron membrane.

* Electrochemical Society Student Member.
** Electrochemical Society Fellow.
z E-mail: pick@ems.psu.edu

Table I. Summary of major relations developed by the original IPZ analysis and the generalized (Frumkin) IPZ analysis derived in this paper.

Frumkin adsorption isotherm		Langmuir adsorption isotherm
$\Delta G_\theta^\circ = \Delta G_0^\circ + fRT\theta$	[1]	$\Delta G_\theta^\circ = \Delta G_0^\circ$
Generalized IPZ analysis		Original IPZ analysis
$\ln\left(\frac{\sqrt{i_r}}{i_\infty}\right) = \ln\left(\sqrt{\frac{k_2}{F}}\cdot\frac{1}{k}\right) + \frac{\alpha f}{Fk} i_\infty$	[14]	$i_\infty = k\sqrt{\frac{F}{k_2}}\sqrt{i_r}$ [2]
$\frac{\sqrt{i_r}}{i_\infty} i_c \exp(a\alpha\eta) = \sqrt{\frac{k_2}{F}}\cdot\frac{i_0'}{k}\left(1 - \frac{1}{Fk} i_\infty\right)$	[19]	$i_c \exp(a\alpha\eta) = i_0'\left(1 - \frac{1}{Fk} i_\infty\right)$ [3]

In writing the rate equations in view of the Frumkin adsorption conditions, one has for the rate of proton discharge and hydrogen evolution[2,8,9]

$$i_c = i_0'(1 - \theta_H)\exp(-a\alpha\eta)\exp(-\alpha f\theta_H) \quad [10]$$

$$i_r = Fk_2\theta_H^2 \exp(2\alpha f\theta_H) \quad [11]$$

where i_c and i_r are the current densities of proton discharge (Eq. 7) and hydrogen adatom combination (Eq. 8), respectively.

Inserting θ_H from Eq. 4 into Eq. 11

$$i_r = Fk_2\left(\frac{i_\infty}{Fk}\right)^2 \exp\left(2\alpha f\frac{i_\infty}{Fk}\right) \quad [12]$$

Taking the square root of Eq. 12

$$\sqrt{i_r} = \sqrt{\frac{k_2}{F}}\cdot\frac{i_\infty}{k}\cdot\exp\left(\alpha f\frac{i_\infty}{Fk}\right) \quad [13]$$

Dividing both sides of Eq. 13 by i_∞ and taking the natural logarithm (ln)

$$\ln\left(\frac{\sqrt{i_r}}{i_\infty}\right) = \ln\left(\sqrt{\frac{k_2}{F}}\cdot\frac{1}{k}\right) + \frac{\alpha f}{Fk} i_\infty \quad [14]$$

This relation, which was also derived by Iyer *et al.*,[8] in a similar form but with different slope and intercept, can be used for determining the rate constants when the value of f is known or can otherwise be estimated.[8,9,14] An independent evaluation of f, however, is not an easy task. In the following derivation, we arrive at another relationship which, when applied to the steady-state permeation data, can yield the rate constants without a prior knowledge of the value of f. In fact, the value of f is a result of the analysis.

Rearranging Eq. 10 and solving for $\exp(\alpha f\theta_H)$

$$\exp(\alpha f\theta_H) = \frac{i_0'(1 - \theta_H)}{i_c \exp(a\alpha\eta)} \quad [15]$$

Taking the square root of Eq. 11

$$\sqrt{i_r} = \sqrt{Fk_2}\cdot\theta_H\cdot\exp(\alpha f\theta_H) \quad [16]$$

Substituting Eq. 15 into Eq. 16

$$\sqrt{i_r} = \sqrt{Fk_2}\cdot\theta_H\cdot\frac{i_0'(1 - \theta_H)}{i_c \exp(a\alpha\eta)} \quad [17]$$

Rearranging and inserting for θ_H from Eq. 4 into Eq. 17

$$\sqrt{i_r} i_c \exp(a\alpha\eta) = \sqrt{Fk_2}\cdot\frac{i_\infty}{Fk}\cdot i_0'\left(1 - \frac{i_\infty}{Fk}\right) \quad [18]$$

Dividing both sides of Eq. 18 by i_∞

$$\frac{\sqrt{i_r}}{i_\infty} i_c \exp(a\alpha\eta) = \sqrt{\frac{k_2}{F}}\cdot\frac{i_0'}{k}\left(1 - \frac{1}{Fk} i_\infty\right) \quad [19]$$

Equations 14 and 19 can be simplified to Eq. 2 and 3 if the Langmuir adsorption conditions are assumed instead of the Frumkin adsorption conditions. In other words, the derived IPZ analysis in this paper reduces to the original Langmuir IPZ analysis[7] if the standard free energy of adsorption is assumed to be independent of the hydrogen coverage, *i.e.*, $f = 0$. Thus, the original IPZ analysis is a special case of the IPZ analysis in this paper, in the same way the Langmuir isotherm is a special case of the Frumkin isotherm. These relations are summarized in Table I.

Plots of both $\ln(\sqrt{i_r}/i_\infty)$ and $(\sqrt{i_r}/i_\infty) i_c \exp(a\alpha\eta)$ *vs.* i_∞ should give straight lines according to Eq. 14 and 19, respectively.

The procedure of calculating the unknowns in the system is

1. From the slope and intercept of Eq. 19, k can be calculated.
2. From the slope of Eq. 14 and knowing k from step 1, f can be calculated, after using the charging (Tafel) data to obtain the value of α.
3. From the intercept of Eq. 14 and knowing k from step 1, k_2 can be calculated.
4. From the intercept of Eq. 19 and knowing k from step 1 and k_2 from step 3, i_0' can be calculated.
5. From Eq. 4 and knowing k from step 1, the hydrogen surface coverage (θ_H) can be calculated.

Results and Discussion

Figure 1 shows the relationship between the steady-state hydrogen permeation current density, i_∞, and the square root of the hydrogen recombination current density, $\sqrt{i_r}$, where i_r is obtained as the difference between the impressed i_c value and the measured i_∞ value.[7] The figure shows a straight line passing by the origin for the blank (*i.e.*, without $S_2O_3^{2-}$) solution. This agrees with Eq. 2 and indicates that the HER occurs according to the reaction sequence in

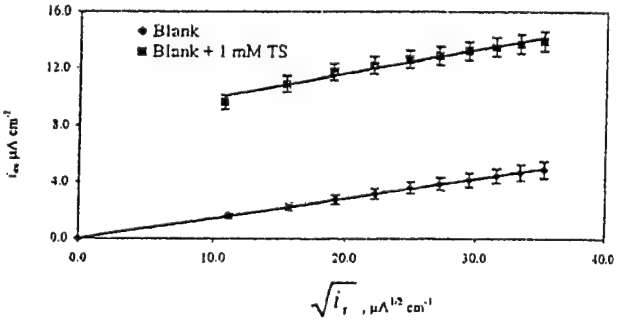

Figure 1. The relation between the measured steady-state hydrogen permeation current, i_∞, and the square root of the recombination current, $\sqrt{i_r}$. Blank = 1 M Na_2SO_4, pH 2. TS = $S_2O_3^{2-}$.

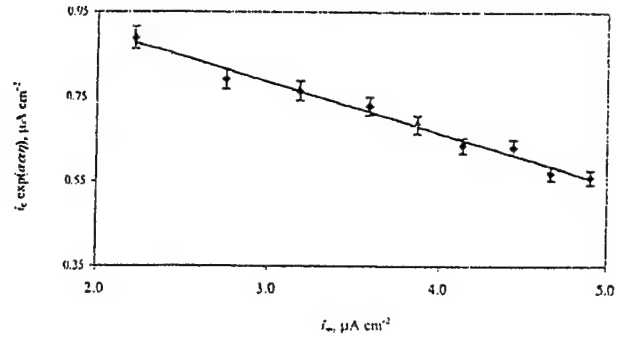

Figure 2. The relation between the charging function, $i_c \exp(a\alpha\eta)$, and the measured steady-state hydrogen permeation current, i_∞, for the blank (1 M Na_2SO_4, pH 2.) solution.

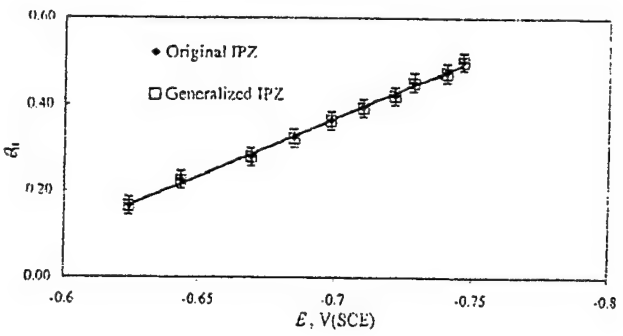

Figure 3. The variation of the hydrogen surface coverage, θ_H, with the electrode potential for the blank (1 M Na_2SO_4, pH 2.) solution.

Eq. 7 and 8, that Eq. 7 is not near equilibrium, *i.e.*, hydrogen oxidation is negligible, and that the IPZ analysis can be applied to the steady-state hydrogen permeation data.[7-9]

However, in the presence of thiosulfate, the line, although linear (Fig. 1), does not pass by the origin and has a finite intercept with the y axis. Therefore, the original IPZ analysis cannot be used to evaluate the steady-state hydrogen permeation data in the presence of thiosulfate, as discussed elsewhere[8] based on the analysis of hydrogen permeation data for H_2S additions to acidic chlorate solutions. We therefore used these results as an example to test the applicability of the analysis which is based on the Frumkin approach, in spite of the fact that there is no independent evidence that the Frumkin approach is a better description than the Langmuir approach for H adsorption under these conditions. Furthermore, we ignored any effect that the sulfur species may have had on the density of available hydrogen adsorption sites on the surface, for the sake of an approximation.

Figure 2 shows the relationship between the charging function [$i_c \exp(a\alpha\eta)$] and the measured steady-state hydrogen permeation current density, i_∞, for the blank solution. The figure shows a straight line with a negative slope and positive intercept in accord with Eq. 3. The rate constants of the HER, k_1 and k_2, the kinetic-diffusion constant of the HAR, k, the exchange current density, i_o, and the corresponding hydrogen concentration just inside the metal at the charging surface, C^o, were calculated for these data obtained in the blank (thiosulfate-free) solution using the original IPZ analysis. Results are summarized in Table II. Hydrogen coverages, θ_H, and hydrogen concentrations, C^o, at different electrode potentials (E) were calculated and the results are shown in Fig. 3 and 4, respectively. Details on these calculations can be found elsewhere.[7,8]

The steady-state hydrogen permeation data for both the blank solution and thiosulfate solution were also tested using the generalized IPZ analysis derived in this paper. Figure 5 shows a straight line relationship between $\ln(\sqrt{i_r}/i_\infty)$ and the measured steady-state hydrogen permeation current density, i_∞, in accord with Eq. 14. Figure 6 shows a linear relation between $(\sqrt{i_r}/i_\infty)i_c\sqrt{\exp(a\alpha\eta)}$ and the measured steady-state hydrogen permeation current density, i_∞, in accord with Eq. 19. The procedure summarized here was used to calculate the unknowns. The Tafel slope was 120 mV, which corresponds to a value of $\alpha = 0.5$. The results are shown in Table II. The calculated hydrogen coverage using the generalized IPZ analyses is also shown in Fig. 3. Since it is unknown to what extent the sulfur species in the solution may have affected the density of available adsorption sites for hydrogen, the values for the thiosulfate solution in Table II could be limiting ones.

Results using the two different IPZ analyses were found to be similar when the requirements of both the original and generalized IPZ analyses were fulfilled. Only the generalized IPZ analysis can be applied when the requirement of the original IPZ analysis is not fulfilled (*i.e.*, the relation between i_∞ *vs.* $\sqrt{i_r}$ is not linear and/or does not pass by the origin, *e.g.*, the blank + 1 mM TS line in Fig. 1).

The factor f was assumed to be zero in the derivation of the original IPZ analysis. The generalized IPZ analysis yields a value close to zero ($f = 0.20$) for the blank solution, whereas it yields a value of $f = 9.9$ for the blank solution containing 1 mM thiosulfate solution. The good correlation between the original and generalized IPZ analyses (Fig. 3) along with the low (essentially zero) calculated value of f support the existence of the Langmuir condition in the case of the blank solution.

Conclusions

The original IPZ analysis has been made more general so as to be applicable to steady-state hydrogen permeation data for a wide range of metal/electrolyte systems undergoing the HER. This new

Table II. Values of different constants obtained by applying the original (Langmuir) IPZ and the generalized (Frumkin) IPZ analyses to measured steady-state permeation data for iron in the blank solution (1 M Na_2SO_4, pH 2) or in the blank + 1 mM $S_2O_3^{2-}$ solution.

Variable	Original IPZ (blank)	Generalized IPZ (blank)	Generalized IPZ (blank + 1 mM $S_2O_3^{2-}$)
k, mol cm^{-2} s^{-1}	1.02×10^{-10}	1.02×10^{-10}	2.68×10^{-10}
k_2, mol cm^{-2} s^{-1}	5.02×10^{-8}	4.63×10^{-8}	2.28×10^{-10}
i_o, μA cm^{-2}	1.17	1.17	34.4
k_1, cm s^{-1}	1.21×10^{-6}	1.21×10^{-6}	3.56×10^{-5}
f	0 (assumed)	0.20	9.90

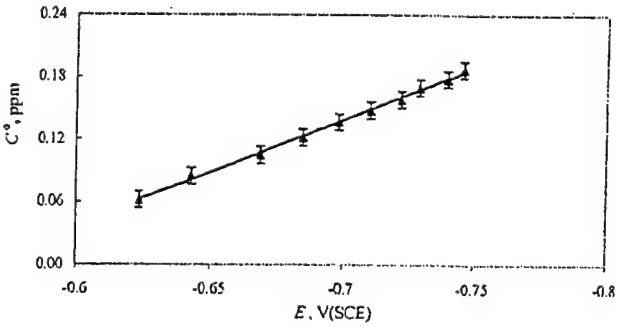

Figure 4. The variation of the hydrogen concentration just inside the charging surface, C^o, with the electrode potential for the blank (1 M Na_2SO_4, pH 2) solution.

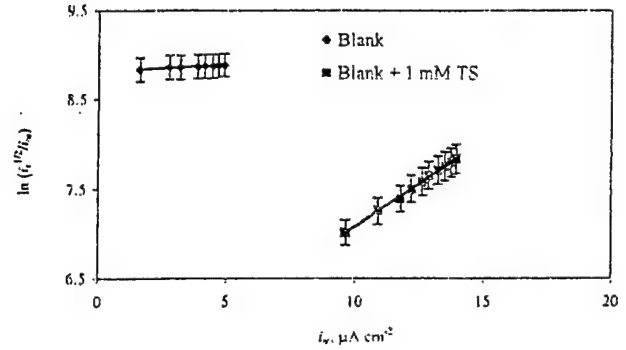

Figure 5. The relation between $\ln(\sqrt{i_r}/i_\infty)$ and the steady-state permeation current density, i_∞. Blank = 1 M Na_2SO_4, pH 2, TS = $S_2O_3^{2-}$.

IPZ analysis improves upon an earlier version derived for Frumkin adsorption conditions. It is more useful than the earlier version because it does not require a prior knowledge of f, as its predecessor did. Rather, the IPZ analysis derived in this paper yields the value of f for those metal/electrolyte systems that meet the conditions for application of the IPZ analysis given elsewhere.[5-7] In addition, it yields the rate constants (k_1 and k_2) and the exchange current density, i_o, of the HER, the kinetic-diffusion constant, k, of the HAR, hydrogen surface coverage, θ_H, and the hydrogen concentration just inside the metal surface, C^o, just as the original IPZ analysis does for Langmuir adsorption conditions.

The generalized (Frumkin) IPZ analysis can be simplified to the original (Langmuir) IPZ analysis when the standard free energy of adsorption is independent of the surface coverage, *i.e.*, $f = 0$. The results obtained for a system exhibiting the Langmuir adsorption conditions are the same using either the original or the generalized IPZ analyses. However, the generalized IPZ analysis must be used for the systems which do not meet the Langmuir conditions, *i.e.*, for systems in which the measured steady-state hydrogen permeation data do not satisfy Eq. 2 and/or Eq. 3, *e.g.*, see Fig. 4b and 6b of Ref. 8 for the HER in a pH 2 chlorate solution with small addition of H_2S. Still, the applicability of these analyses in more complicated

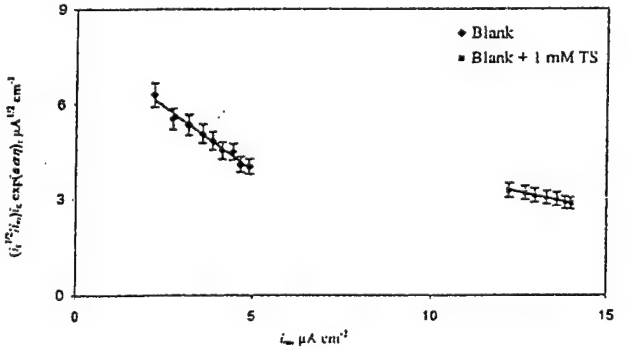

Figure 6. The relation between $(\sqrt{i_r}/i_\infty)\ i_c \exp(\alpha\alpha\eta)$ and the steady-state permeation current density, i_∞. Blank = 1 M Na_2SO_4, pH 2, TS = $S_2O_3^{2-}$.

electrolytes, in particular when the availability of hydrogen adsorption sites could be affected by other solution species, needs to be taken into consideration.

Acknowledgment

We thank K. G. Weil, B. G. Ateya, and M. Abd Elhamid for helpful discussions on the preparation of this work. The authors gratefully acknowledge financial support by the U.S. Steel Corporation, Saudi Aramco, and the Office of Naval Research.

The Pennsylvania State University assisted in meeting the publication costs of this article.

List of Symbols

a	a constant, FI/RT, V^{-1}
C_H^+	hydrogen ion concentration in the electrolyte, mol L^{-1}
C^o	hydrogen concentration in the metal at the charging surface, ppm
D	hydrogen diffusion coefficient, cm^2 s^{-1}
F	Faraday constant, 96484.6 C mol^{-1}
f	a factor that describes the deviation from the ideal Langmuir behavior, dimensionless
ΔG_θ^o	standard free energy of adsorption at certain coverage, J mol^{-1}
ΔG_0^o	standard free energy of adsorption at zero coverage, J mol^{-1}
i_c	charging current density, A cm^{-2}
i_∞	steady-state hydrogen permeation current density, A cm^{-2}
i_o	exchange current density, A cm^{-2}
i_o'	$i_o/(1 - \theta_H^e)$, A cm^{-2}
i_r	hydrogen recombination current density, A cm^{-2}
k_{abs}	absorption rate constant, mol (cm^2 s)$^{-1}$
k_{des}	desorption rate constant, cm s^{-1}
k	kinetic-diffusion constant, mol cm^{-2} s^{-1}
k_1	discharge rate constant, cm s^{-1}
k_2	recombination rate constant, mol (cm^2 s)$^{-1}$
L	membrane thickness, cm
R	gas constant, 8.314 J (mol K)$^{-1}$
T	absolute temperature, K

Greek

α	transfer coefficient, dimensionless
η	overpotential of the HER, V
θ_H	hydrogen surface coverage, dimensionless
θ_H^e	hydrogen surface coverage at equilibrium, dimensionless

References

1. M. Temkin and V. Pyzhev, *Acta Physicochim. URSS*, 12, 327 (1940).
2. A. Frumkin and N. Aladjalova, *Acta Physicochim. URSS*, 19, 1 (1944).
3. E. Gileadi and B. E. Conway, in *Modern Aspects of Electrochemistry*, Vol. 3, J. O'M. Bockris and B. E. Conway, Editors, pp. 347-442. Butterworths, Washington, DC (1964).
4. E. Gileadi, *Electrode Kinetics for Chemists, Chemical Engineers, and Materials Scientists*, Wiley-VCH, New York (1993).
5. M. H. Abd Elhamid, B. G. Ateya, and H. W. Pickering, *J. Electrochem. Soc.*, 147, 2258 (2000).
6. M. H. Abd Elhamid, B. G. Ateya, and H. W. Pickering, *J. Electrochem. Soc.*, 147, 2959 (2000).
7. R. N. Iyer, H. W. Pickering, and M. Zamanzadeh, *J. Electrochem. Soc.*, 136, 2463 (1989).
8. R. N. Iyer, I. Takeuchi, M. Zamanzadeh, and H. W. Pickering, *Corrosion (Houston)*, 46, 460 (1990).
9. R. N. Iyer and H. W. Pickering, *Mechanism and Kinetics of Electrochemical Hydrogen Entry and Degradation of Metallic Systems, Annual Review of Materials Science*, Vol. 20, Annual Reviews, Inc., Palo Alto, CA (1990).
10. M. Ramasubramanian, B. N. Popov, and R. E. White, *J. Electrochem. Soc.*, 145, 1907 (1998).
11. M. A. Devanathan and Z. Stachurski, *Proc. Roy. Soc. Chem.*, A270, 90 (1962).
12. F. M. Al-Faqeer, M.S. Thesis, The Pennsylvania State University, University Park, PA (1999).
13. M. H. Abd Elhamid, B. G. Ateya, K. G. Weil, and H. W. Pickering, *Corrosion (Houston)*, 57, (2001).
14. A. Durairajan, A. Krishnyier, B. S. Haran, R. E. White, and B. N. Popov, *Corrosion (Houston)*, 56, 283 (1998).

Effect of Thiosulfate and Sulfite on the Permeation Rate of Hydrogen Through Iron

M.H. Abd Elhamid, B.G. Ateya,** K.G. Weil,*** and H.W. Pickering*****

ABSTRACT

Effects of thiosulfate ($S_2O_3^{2-}$) and sulfite (SO_3^{2-}) on hydrogen evolution and permeation within iron have been studied in acid and neutral solutions. Results show that thiosulfate increases the hydrogen permeation rate and depolarizes the hydrogen evolution reaction at concentrations as low as 0.1 mM, in acid or neutral media. Sulfite showed similar and somewhat less pronounced effects in the acid medium and no effect on either process in the neutral medium. Results are discussed in light of the stability of the various sulfur species and their effects on the rates of both processes.

KEY WORDS: environmentally assisted corrosion, hydrogen evolution, hydrogen overvoltage, hydrogen permeation, steel, sulfide stress corrosion, thiosulfate

INTRODUCTION

The degrading effects of sulfur-containing (thio) compounds on the integrity of metals and alloys have been well recognized. Of these compounds, thiosulfate is commonly encountered in the pulp, paper, and oil and gas industries and as a product of sulfate-reducing bacteria. For this reason, extensive studies have been conducted by various authors to evaluate and understand the effects of thiosulfate on crevice corrosion,[1-2] pitting corrosion,[3-4] stress corrosion cracking,[5-6] and anodic dissolution of metals and alloys.[7-8] Furthermore, some authors have considered the electrochemistry of thiosulfate[9] and its adsorption behavior.[10]

Generally, it is accepted that thiosulfate has a strong promoting effect on the anodic dissolution of metals.[7-8] However, measurements of its effects on hydrogen absorption have been less systematic and less conclusive.[11-13]

The objective of this paper was to evaluate the effects of thiosulfate and sulfite on the permeability of electrolytic hydrogen within iron. Sulfites were included in this study since thiosulfate decomposes readily to give sulfite species and colloidal sulfur in mild acidic media similar to those media encountered in pits, crevices, and cracks.

EXPERIMENTAL PROCEDURES

An electrochemical hydrogen permeation cell[14-17] was used in this study to collect data on both hydrogen evolution and permeation within iron (steel) membranes in sulfate solutions containing different thiosulfate or sulfite concentrations. Figure 1 shows the position of the iron membrane as it was mounted between the two parts of the cell. Steel membranes

Submitted for publication February 2000; in revised form, December 2000.

* Department of Materials Science and Engineering, The Pennsylvania State University, University Park, PA 16802. Present address: Global Alternative Propulsion Center, General Motors, Warren, MI 48090.
** Department of Materials Science and Engineering, The Pennsylvania State University, University Park, PA 16802. Present address: Chemistry Department, Faculty of Science, Kuwait University, Kuwait.
*** Department of Materials Science and Engineering, The Pennsylvania State University, University Park, PA 16802.
**** Department of Materials Science and Engineering, The Pennsylvania State University, University Park, PA 16802. E-mail: pick@ems.psu.edu.

0010-9312/01/000083/$5.00+$0.50/0

with 0.25 mm thicknesses were obtained from a commercial source with the following composition: 0.3% Mn, 0.1% Si, < 0.08% C, < 0.05% S, and bal. Fe. They were polished successively to 0.05-μm alumina (Al_2O_3), degreased in acetone (CH_3COCH_3), washed with double-distilled water, and subsequently annealed in pure hydrogen at 900°C for 2 h in a tube furnace, followed by a furnace cool in the same atmosphere. Solutions of 0.05 M sulfuric acid (H_2SO_4) + 0.45 M sodium sulfate (Na_2SO_4, pH 1.8) and 0.5 M Na_2SO_4 (pH 7) were used throughout this study. All solutions were prepared from analytical grade chemicals and double-distilled water. Before admitting the solutions to the cell, they were pre-electrolyzed using platinum electrodes for 2 h under deaeration using hydrogen. These were then used as blank solutions to which different concentrations of thiosulfate or sulfite were added. The solutions were subsequently deaerated with hydrogen. One surface of the membrane was coated with palladium before the membrane was mounted in the cell. Areas of the input (charging) and exit (palladium-coated) surfaces of the membranes were 0.8 cm^2. The palladium-coated surface was held at 0.150 mV (mercury/mercuric oxide [Hg/HgO]) in 0.05 M sodium hydroxide (NaOH) to ensure complete oxidation of the atomic hydrogen diffusing through the membrane. The other (charging) surface of the membrane faced the thiosulfate contaminated solution and was subjected to hydrogen charging under cathodic polarization. Further details about the experimental arrangement are reported elsewhere.[16-17]

RESULTS AND DISCUSSION

The cathodic charging current is supported by the hydrogen evolution reaction (HER) taking place at the input surface of the membrane, i.e.:

$$H^+(aq) + e^- \rightarrow H_{ads} \quad (1)$$

$$2H_{ads} \rightarrow H_2(g) \quad (2)$$

where H_{ads} refers to a hydrogen atom adsorbed on the metal surface. Reactions (1) and (2) represent the discharge-recombination mechanism of the HER. A fraction of this adsorbed hydrogen (H_{ads}) gets absorbed into the lattice of the metal (H_{abs}) through a surface reaction:

$$H_{ads} \leftrightarrow H_{abs} \quad (3)$$

Reaction (3) (hydrogen absorption reaction [HAR]) leads to the establishment of a finite concentration (C^o) of hydrogen atoms absorbed just beneath the charging surface of the membrane. It is this absorbed hydrogen that diffuses through the membrane

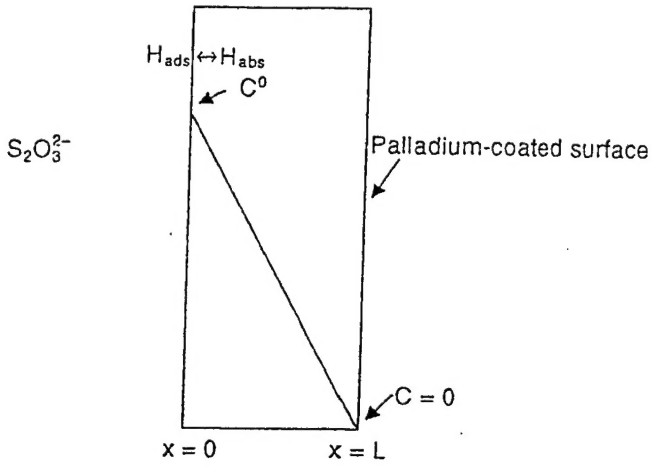

FIGURE 1. *A schematic illustration showing the conditions at the hydrogen entry (charging, x = 0) and exit sides of the iron (steel, x = L) membrane. C^o and C are the hydrogen concentrations in the membrane at x = 0 and x = L, respectively.*

toward the palladium-coated surface where it gets oxidized at a rate that is measured by the permeation current, i_p. For the present system, it has been shown that the rate of the permeation process is controlled by diffusion of atomic hydrogen within the membrane, such that:

$$i_\infty = \frac{FDC^o}{L} \quad (4)$$

where F is the Faraday constant, D is the diffusivity of hydrogen within the membrane, L is its thickness, and i is the steady-state value of i_p.

Figure 2 shows the effect of thiosulfate concentration on the hydrogen permeation transients through the steel membranes for a cathodic charging rate of 1.25 mA/cm^2 in the 0.05-M H_2SO_4 + 0.45-M Na_2SO_4 (blank) solution. Note the profound effect of the concentration of thiosulfate on i_p, particularly the i_∞. A 0.1-mM thiosulfate addition to the blank solution increases the i_∞ by about twofold, while the addition of 10 mM thiosulfate increases i_∞ by about sixfold. This demonstrates that the addition of thiosulfate increases the i_∞ of hydrogen within the steel in acidic (pH 1.8) solution. This is attributed to an increase in C^o, which results from the effects of thiosulfate (and/or its decomposition products) on the rate of hydrogen absorption within the membrane (Reaction [3]). In addition, thiosulfate enhances the HER in the pH 1.8 solution (Reactions [1] and [2]). Figure 3 shows Tafel plots of the HER obtained on steel at different thiosulfate concentrations ($\eta = E - E^{eq}$, E^{eq} = –0.349 V vs saturated calomel electrode [SCE]). This figure shows that an increase in thiosulfate concentration enhances the HER (i.e., the hydrogen overpotential decreases). The Tafel slope

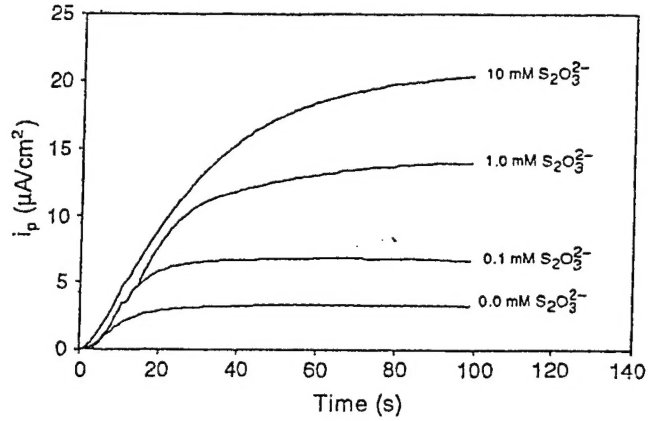

FIGURE 2. *Effect of $S_2O_3^{2-}$ concentration on the hydrogen permeation transients obtained on a steel membrane of thickness 0.25 mm in 0.05 M H_2SO_4 + 0.45 M Na_2SO_4 (pH 1.8) at a cathodic charging current density of 1.25 mA/cm².*

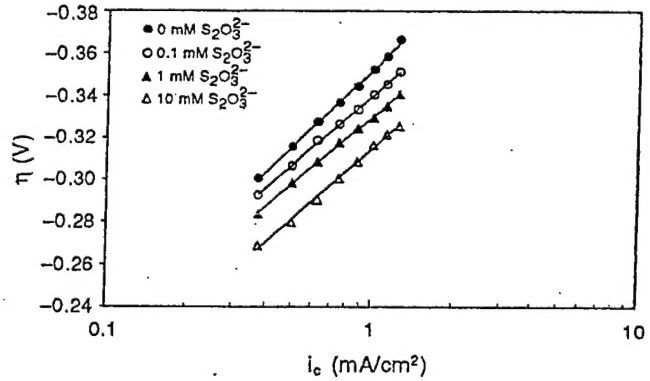

FIGURE 3. *Effect of $S_2O_3^{2-}$ concentration on the Tafel plots of the HER obtained on a steel membrane of thickness 0.25 mm in 0.05 M H_2SO_4 + 0.45 M Na_2SO_4.*

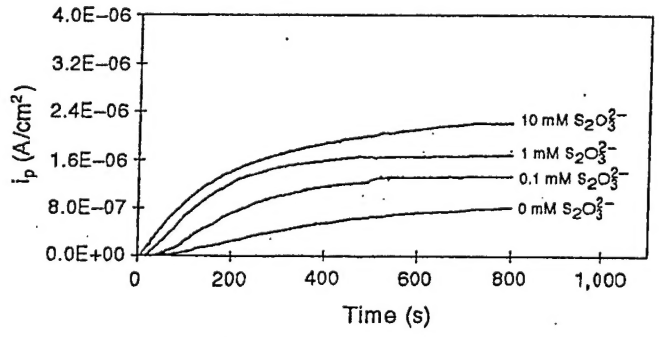

FIGURE 4. *Effect of $S_2O_3^{2-}$ concentration on the hydrogen permeation transients obtained on a steel membrane of thickness 0.25 mm in 0.5 M Na_2SO_4 (pH 7) at a charging current density of 1.25 mA/cm².*

amounts to 130 mV = 2.3RT/0.45F for the conditions in Figure 3. This compares well with a theoretical value of 2.3RT/0.5F for the coupled discharge-recombination mechanism which is to be expected when the Langmuir isotherm is applicable.

In acidic media, thiosulfate readily decomposes to give colloidal sulfur and sulfurous acid (H_2SO_3):

$$S_2O_3^{2-} + 2H^+ \rightarrow S + H_2SO_3 \qquad (5)$$

Consequently, the increase in the rates of the HER (Reactions [1] and [2]) and of the HAR (Reaction [3]) may be attributed to the remaining thiosulfate ions, colloidal sulfur, H_2SO_3, and/or the reduction products of any of the above species.

The next set of experiments were carried out on thiosulfate in a neutral medium, where Reaction (5) is not likely to occur and the predominant species in solution is the thiosulfate ion. The hydrogen permeation transients in the neutral medium are shown in Figure 4. This figure shows that thiosulfate increases the permeation rate of hydrogen within iron in the neutral medium. A concentration of 0.1 mM thiosulfate increases i_∞ by about twofold (which is comparable to that observed in the acid medium) while the 10-mM concentration increases i_∞ by about threefold (which is less than that observed in the acid medium). This increase in the hydrogen permeation rate in the neutral solution was also accompanied by an increase in the rate of hydrogen evolution. Figure 5 shows the current-overpotential plots obtained in 0.5 M Na_2SO_4 at different thiosulfate concentrations ($\eta = E - E^{eq}$, $E^{eq} = -0.661\ V_{SCE}$). Hence, thiosulfate also depolarizes the HER in the neutral medium. The Tafel slope is 200 mV, 2.3 RT/0.29F, in the blank electrolyte and in the presence of 0.1 mM and 1 mM thiosulfate. This indicates that the mechanism of the HER is no longer coupled discharge-recombination that requires a Tafel slope of 120 mV = 2.3 RT/0.50F. Note that in the 10-mM thiosulfate solution the Tafel slope is 120 mV. However, this value is affected considerably by the cathodic reduction of thiosulfate at the relatively high concentration of 10 mM.

Comparison of Figures 2 and 4 reveals that the rate of hydrogen permeation within iron is greater in an acidic than neutral medium, for both the blank solution and in the presence of a given amount of thiosulfate (or its decomposition products). The increase in i_∞ produced by the thiosulfate is also greater in the acid solution. This points to a possible enhancing effect also by the decomposition products of thiosulfate on hydrogen permeation. To test this hypothesis, experiments were run in the presence of sodium sulfite (Na_2SO_3) in the acidic medium (pH 1.8) at the same concentrations as in the thiosulfate experiments (Figure 6). It was revealed that sulfite causes an increase in the hydrogen permeation rate. This is also coupled by an increase in the rate of the HER (Figure 7). As a result of the proteolytic equilibria involving sulfite ions, which are:

$$H_2SO_3 \rightarrow H^+ + HSO_3^- \quad k_1 = 1.2\times10^{-2} \qquad (6)$$

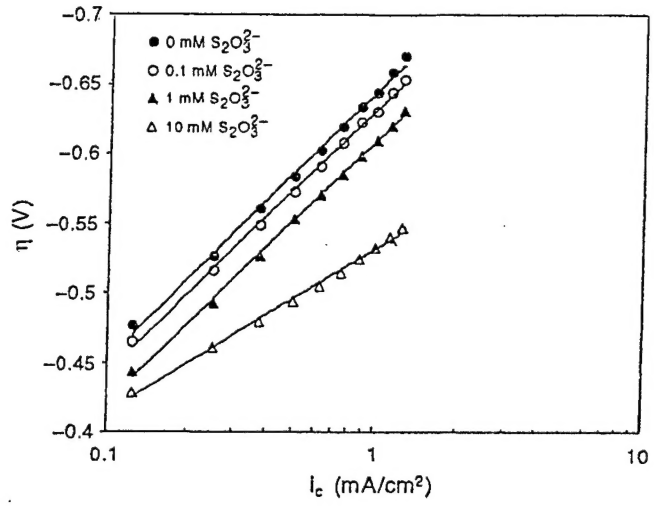

FIGURE 5. *Effect of $S_2O_3^{2-}$ concentration on the Tafel plots of the HER obtained on a steel membrane of thickness 0.25 mm in 0.5 M Na_2SO_4.*

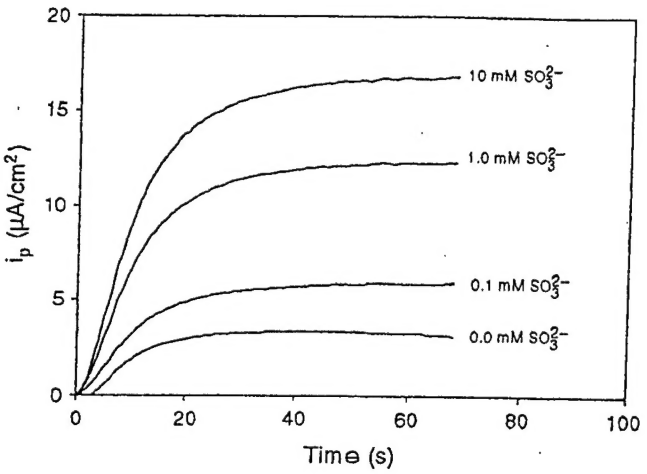

FIGURE 6. *Effect of SO_3^{2-} concentration on the hydrogen permeation transients obtained on a steel membrane of thickness 0.25 mm in 0.05 M H_2SO_4 + 0.45 M Na_2SO_4 (pH 1.8) at a charging current density of 1.25 mA/cm².*

$$HSO_3^- \rightarrow H^+ + SO_3^{2-} \qquad k_2 = 6.2\times10^{-3} \qquad (7)$$

the test solutions in the acid medium contain predominantly H_2SO_3, HSO_3^-, and to a much lesser extent, SO_3^{2-}.[18] In the neutral medium, where the predominant species is SO_3^{2-}, Na_2SO_3 had no effect on either the HER or the hydrogen permeation current within the iron.

The extent of the enhancement in the hydrogen permeation rate at different thiosulfate or sulfite concentrations may be expressed quantitatively by an enhancement factor, ε:

$$\varepsilon = \frac{i_\infty(\text{additive})}{i_\infty(\text{blank})} \qquad (8)$$

where i_∞ (additive) and i_∞ (blank) are the steady-state hydrogen permeation current densities for the solution with and without the additive, respectively. Table 1 lists values of i_∞ and ε for different concentrations of thiosulfate and Na_2SO_3 in acidic and neutral solutions. The table reveals that thiosulfate (and/or its decomposition products) in acid medium shows a higher promoting effect (larger ε) than Na_2SO_3 at the same concentration. If one assumes that 1 mol of (SO_3^{2-} + HSO_3^- + H_2SO_3) results from the decomposition of 1 mol of thiosulfate, it can be reasoned that the resulting colloidal sulfur and/or its reduction products also cause some enhancement of the hydrogen permeation. In addition, thiosulfate was found to promote hydrogen permeation within iron in the neutral medium.

In addition to their effects on hydrogen evolution and permeation within iron, $S_2O_3^{2-}$, SO_3^{2-}, and S are thermodynamically unstable at the rather negative

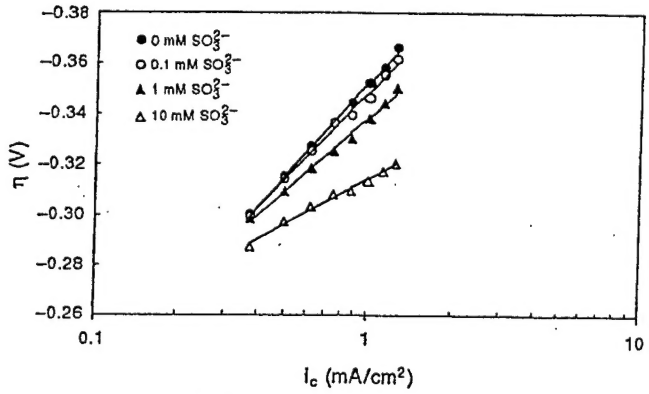

FIGURE 7. *Effect of SO_3^{2-} concentration on the Tafel plots of the HER obtained on a steel membrane of thickness 0.25 mm in 0.05 M H_2SO_4 + 0.45 M Na_2SO_4 at a charging current density of 1.25 mA/cm².*

potentials of these experiments[18] and, therefore, may be reduced on the metal surface to hydrogen sulfide (H_2S). H_2S is well known to enhance hydrogen absorption into metals and to enhance the HER.[19-23] However, as is shown in the literature, these reduction reactions do not play a significant role under the conditions of these experiments.[24] Even very small amounts of H_2S, however, could contribute to the observed enhanced hydrogen permeability.[23]

CONCLUSIONS

❖ Thiosulfate promotes hydrogen evolution and permeation within iron in acidic and neutral solutions. Its effects in the acid medium are attributed mainly to its decomposition products (i.e., H_2SO_3, HSO_3^-, SO_3^-, and colloidal sulfur) since thiosulfate is readily de-

TABLE 1

Effects of the Concentrations of $S_2O_3^{2-}$ and SO_3^{2-} on the Hydrogen Permeation Rate within Iron and the Enhancement Factor (ε) in Acidic (pH 1.8) and Neutral (pH 7) Solutions at a Charging Current of 1.25 mA/cm²

C (mM)	$S_2O_3^{2-}$ pH 1.8		SO_3^{2-} pH 1.8		$S_2O_3^{2-}$ pH 7	
	i_∞ (μA/cm²)	ε	i_∞ (μA/cm²)	ε	i_∞ (μA/cm²)	ε
0	3.2	1	3.2	1	0.8	1
0.1	6.6	2.0	5.9	1.8	1.3	1.6
1	14.0	4.3	12.4	3.8	1.7	2.1
10	20.4	6.3	16.8	5.2	2.2	2.8

composed in acidic media to give the above products, and since results with only sulfite in the same acidic solution show slightly less enhancement of hydrogen permeation. Thiosulfate in neutral solution, where it remains mainly undecomposed, also causes enhancement of the hydrogen absorption reaction but to a lesser extent. On the other hand, sulfite in the neutral medium has no effect on either process. Thus, the major effects of thiosulfate are caused by its decomposition product in acidic media and to thiosulfate, itself, in neutral media. The mechanisms involved in the enhancement processes are yet to be determined.

ACKNOWLEDGMENTS

The authors acknowledge financial support of this work by the U.S. Steel Corporation, the Office of Naval Research (grant no. N00014-96-1-0913) and the Division of International Programs of the NSF (grant INT-9724698).

REFERENCES

1. R.C. Alkire, S.E. Lott, J. Electrochem. Soc. 136 (1989): p. 3,256.
2. C.S. Brossia, R.G. Kelly, Corrosion 54 (1998): p. 145.
3. C. Duret-Thual, D. Costa, W.P. Yang, P. Marcus, Corros. Sci. 39 (1997): p. 913.
4. P.R. Roberge, S. Wang, R. Roberge, Corrosion 52 (1996): p. 733.
5. E.A. Ashour, E.A. Abd El Meguid, B.G. Ateya, Corrosion 53 (1997): p. 612.
6. W-T. Tsai, M-J. Sheu, J-T. Lee, Corros. Sci. 38 (1996): p. 33.
7. R.J. Kucernak, R. Peat, D.E. Williams, J. Electrochem. Soc. 139 (1992): p. 2,337.
8. R.C. Newman, W.P. Wong, H. Ezuber, A. Garner, Corrosion 45 (1989): p. 282.
9. P. Marcus, E. Protopopoff, Corros. Sci. 39 (1997): p. 1,741.
10. A.E. Thomas, A. Kolics, A. Wieckowski, J. Electrochem. Soc. 144 (1997): p. 586.
11. H.H. Horowitz, J. Electrochem. Soc. 132 (1985): p. 2,064.
12. R.P. Hu, P. Manolatos, M. Jerome, M. Meyer, J. Galland, Corros. Sci. 40 (1998): p. 619.
13. C.C. Juang, J.K. Wu, Corros. Sci. 36 (1994): p. 1,727.
14. A.N. Frumkin, N. Aladyalova, Acta Physicochim (USSR) 19 (1944): p. 1.
15. M.A. Devanathan, Z. Stachurski, Proc. Roy. Soc. Chem. A270 (1962): p. 90.
16. M.H. Abd Elhamid, B.G. Ateya, H.W. Pickering, J. Electrochem. Soc. 144 (1997): p. L58.
17. M.H. Abd Elhamid, B.G. Ateya, H.W. Pickering, J. Electrochem. Soc. 147 (2000): p. 2,959.
18. M. Pourbaix, ed., Atlas of Electrochemical Equilibria in Aqueous Media (Houston, TX: NACE International, 1974), p. 545.
19. P.R. Rhodes, "Corrosion Mechanism of Carbon Steel in Aqueous H_2S Solutions," in H_2S Corrosion in Oil and Gas Production, eds. R.N. Tuttle, R.D. Kane (Houston, TX: NACE, 1991), p. 843.
20. S.Y. Tsai, H.C. Shih, J. Electrochem. Soc. 145 (1998): p. 1,968.
21. F. Elshawesh, J.C. Scully, Brit. Corros. J. 33 (1998): p. 49.
22. R.N. Iyer, I. Takauchi, M. Zamanzadeh, H.W. Pickering, Corrosion 46 (1990): p. 360.
23. Y. Saio, K. Nobe, Brit. Corros. J. 30 (1995): p. 119.
24. D. Tromans, L. Frederick, Corrosion 40 (1984): p. 633.